

Reply to comments by Referee #1

Summary

This manuscript presents a review of data assimilation in atmospheric chemistry models and contains a wealth of information.

I appreciate that the authors addressed some of my comments from my “short review” before this manuscript was published in ACPD. Nonetheless, my overall opinion is nearly unchanged—I still think the manuscript is too long and unfocused and that the writing and presentation are the main shortcomings of this manuscript. However, I have little concern regarding the scientific content, as I believe the authors appropriately encapsulated most of the work to date on data assimilation in atmospheric chemistry models.

I have identified several places where I think the authors can shorten their paper. However, ultimately, I will defer to the authors’ choices. If the authors do not wish to make any substantial omissions, that is fine, but I expect that many readers will be turned-off from this article because of its size and often unfocused writing.

Reply: Since this is a review paper, we feel that it is appropriate to provide fairly comprehensive descriptions of methods, data sets, past applications, and selected case studies. Nevertheless, we eliminated some material where we felt that it was appropriate to do so and we also followed some recommendations concerning the organization of Section 3.

Bigger comments and suggestions

1. I feel you should strongly consider removing section 5 and all the figures because they add little to the paper. Section 5.2 is essentially just Pagowski and Grell (2012) restated, and section 5.3 is already-published work from P. Saide. I found section 5.4 to be the most interesting of the case studies, but even that can be safely removed, in my opinion. While it’s nice to have figures in an article, I feel that in this case, they don’t contribute to further understanding of the topics already described in the text.

I feel that section 2.4 can be omitted. A few lines about nonlinearity and non-Gaussianity can easily be slipped into other earlier material in section 2.

Is section 2.5 really necessary? The point of this paper is data assimilation, not verification approaches. If you’re going to keep section 2.5, then, within it, I suggest removing the “leave-one-out-approach” because, as you mention, this approach is very expensive, and quite frankly, I believe a bit silly and unpractical.

Can section 3.3 be omitted? I felt it added little to the text.

The first paragraph of section 4.2 can be safely omitted. Further, I feel that the text in section 4.2 beginning “Most retrieval products” through the end of the section can be removed.

I feel that section 4.3 can be safely omitted too—of course observations are used in chemical data assimilation. Most of this content has been said somehow earlier.

Reply: We feel that it is important to show some examples of data assimilation in atmospheric chemistry models, as those illustrate some of the associated advantages and limitations. We debated whether the case studies could be incorporated into Section 3. However, we decided to keep them as a separate section because they not only provide illustrations of the data assimilation methods, but also exemplify the use of

observational data sets (ground-level and satellite data), which have been described in Section 4.

We agree that section 2.4 is rather short. Nevertheless, we believe it deserves a subsection on its own because this issue is likely to become a major mathematical and technical hardship of CCMM, when coupling heterogeneous variables, some of them physically bounded. These assumptions often contradict mathematical axioms of standard data assimilation methods such as Gaussianity of the errors. Coupled climate models (with sea ice for instance) and coupled ocean-biogeochemical models also face the same class of issues and addressing this non-Gaussianity issue is already considered a major challenge.

We agree that the leave-one-out approach is not numerically feasible and we have modified Section 2.5 accordingly.

Section 3.3 is useful as a link between the data assimilation methods, which are described in Section 3 and the observational data sets, which are described in Section 4.

The first paragraph of Section 4.2 introduced the major agencies operating satellites. This paragraph has been removed. Acronyms have been defined in other parts of the texts where needed.

The end of Section 4.2 starting with “Most retrieval products...” is useful as a reminder of the necessary components of the retrieval products. In particular, DOAS is a popular retrieval approach, but providing kernels with the DOAS approach has become common practice only very recently.

Section 4.3 is important as it exemplifies the methods to use observations for data assimilation in an optimal manner. Therefore, it is complementary, rather than redundant, of the earlier section and it provides a bridge with the case studies section.

2. Section 3.1 should be broken into subsections to make it easier to read. Perhaps one subsection could contain studies looking at inverse modeling and another those that examined modifying initial conditions.

Similarly, section 3.2 should also be broken into subsections. I'd suggest one subsection for gaseous chemistry data assimilation and another for aerosol data assimilation.

Reply: We have reorganized Section 3.1 along the suggested lines. However, it was not possible to break it down into only two sub-sections and it has been organized into four sub-sections.

It was not possible to break down Section 3.2 into sub-sections along the same lines as Section 3.1 since inverse modeling has not been performed with CCMM yet. To break it down into assimilation of gaseous and aerosol data was not feasible either, because some applications have assimilated both gaseous and aerosol data. Furthermore, it appears that data assimilation into CCMM tends to differ at the moment by their data assimilation techniques (4D-Var, 3D-Var, Kalman filter) as mentioned in the

introductory paragraph. Therefore, we kept the current organization. Since Section 3.2 is shorter than Section 3.1, it seems appropriate not to break it down into sub-sections.

3. In general, I strongly urge you to remove all unnecessary text, primarily in section 3. The details of the various studies do not have to be mentioned here. For example, in the paragraph about Schutgens et al. (2010), beginning on page 32253, the sentences starting with "To obtain" and "In addition" can probably be safely removed without detracting from the main point of this study. If readers want more information, they can consult the reference.

Reply: We feel that some summary description of the cited studies is needed in order to provide sufficient information regarding those applications. Therefore, only minimal text removal was performed.

Smaller comments and suggestions

1. *P 32236, L 24: Clarify how this paper differs from Zhang et al. (2012b)*

Reply: We added the following text: "..., however, only data assimilation in CTM was addressed".

2. *I feel the paragraph beginning on line 17 on page 32237 can be shortened.*

Reply: This paragraph was slightly reduced.

3. *Suggest rewriting the first sentence of section 2.1*

Reply: This sentence was rewritten as follows: "Data assimilation in geosciences has been initially applied to meteorology where methods...".

4. *P 32238, L 14: 90's should be "1990s"*

Reply: This has been corrected.

5. *P 32238, L 18-20: What errors? Please be precise.*

Reply: We meant all errors (background, observation, posterior). This has been rewritten as: "...on all errors...".

6. *P 32239, L 27: "of" not "in", specify it's the background error covariances*

Reply: "in" is correct; "of" is appropriate only when several elements are listed after "consist of...", meaning "composed of...".

The definition of inflation is valid for any type of errors. In practice, inflation could be (and often is) applied to any type of error covariance: background, posterior but also observation.

7. P 32240, L 20: *This sentence can probably be omitted.*

Reply: We feel that this sentence is a crucial remark backed up by recent numerical experiments: It tells that 4D-Var has an advantage over EnKF. Because of the popularity of EnKF, it is often forgotten that 4D-Var should outperform EnKF in strongly nonlinear conditions if it were not for the flow dependence. Therefore, this remark is quite relevant for CTM and perhaps also for CCMM.

8. P 32241, L 5-10: *How are the "hybrid ensemble/variational" and "ensemble variational schemes" different? I believe you're referring to the same thing.*

Reply: Hybrid methods consist in coupling two different data assimilation schemes such as an ensemble scheme (EnKF), and a variational scheme (3D-Var and 4D-Var). Because of the use of 3D-Var and 4D-Var, it usually entails using climatological information. Ensemble variational schemes are not always the result of the coupling of two data assimilation schemes, and/or do not necessarily use climatological information (for instance, the iterative ensemble Kalman smoother). There is a very smart account on the issue by Andrew Lorenc (however, it is meteorology-oriented): http://www.wcrp-climate.org/WGNE/BlueBook/2013/individual-articles/01_Lorenc_Andrew_EnVar_nomenclature.pdf. We changed "hybrid ensemble/variational" into "hybrid" to avoid any confusion.

9. *In section 2.3, it might be appropriate to mention the NMC method as a way of obtaining background errors.*

Reply: Yes, we agree.

"Algorithms relying on consistency check, cross validation and statistical likelihood have been used in meteorology (Hollingsworth and Lönnberg, 1986; Desroziers and Ivanov, 2001; Chapnik et al., 2004; Desroziers et al., 2005) to better assess those pivotal statistics."

was modified as follows:

"Algorithms relying on consistency check, cross validation, statistical likelihood (Hollingsworth and Lönnberg, 1986; Desroziers and Ivanov, 2001; Chapnik et al., 2004; Desroziers et al., 2005) or the empirical but efficient National Meteorological Center (NMC) technique (Parrish and Derber, 1992) have been used in meteorology to better assess those pivotal statistics."

10. P 32250: *Suggest omitting the paragraph beginning in line 14.*

Reply: The first sentence has been deleted.

11. P 32252, L 12: *"led" not "lead"*

Reply: This has been corrected.

12. P 32255: Please rewrite the sentence beginning in line 11. I suggest omitting lines 13-17.

Reply: This sentence has been rewritten as follows: "The authors showed that data assimilation of a combination of different observations (including multiple species) is a very effective way to remove systematic model errors."

We preferred to keep the end of that paragraph. Although it sounds intuitive, it is nevertheless relevant to future prospects of data assimilation in CCMM as data from different sources are more and more likely to be used.

13. I suggest omitting the text beginning in line 18 on page 32255 through the end of the section. Seems out of place to me.

Reply: This paragraph and the following one have been deleted, along with the associated figures.

14. I believe lines 4-15 on page 32265 could be removed, since IMPROVE and STN network observations are not suitable for data assimilation purposes.

Reply: Such data, which are not available in near real-time, are not suitable for air quality forecasting; however, they can be used for re-analyses of air pollutant concentrations.

15. Suggest omitting the paragraph beginning "MPLNET is a global lidar" on page 32266.

Reply: Assimilation of lidar data has recently been shown to improve air quality forecasts; therefore, it seems appropriate to keep this paragraph on lidar networks unchanged.

16. P 32271, L 18, "past" not "passed"

Reply: This has been corrected.

17. P 32284, L 18: Please rewrite this sentence.

Reply: This sentence has been rewritten as follows: "Assimilating distinct data sets that influence the same model variable could lead to some contradictory information concerning that model variable when the error statistics are misspecified (e.g., unknown bias in semi-volatile PM components); therefore, it will be essential to properly specify those measurement error statistics."

18. P 32287, Lines 1-9: This material was just said nearly verbatim in section 6. Please consider removing.

Reply: It is not uncommon for the main conclusions of an article to appear in the main text, the conclusion, and the abstract. Some journals accordingly do not accept

conclusion sections. However, since *Atmos. Chem. Phys.* articles typically include a conclusion section, we prefer to keep this part of the conclusion unchanged.

Reply to comments of Referee #2

This paper presents a large review of data assimilation in atmospheric chemistry models with a special focus on coupled chemistry meteorology models (CCMM). First the author proposes a review of assimilation methods used/developed for chemical data applications. A very complete review of chemical data assimilation studies is presented. Also a very interesting review of available chemical observations is given by the authors. Moreover, authors present specific case studies to illustrate the state of data assimilation science for atmospheric chemistry. The paper is in general clear and well written and it is probably a review that will serve the community of atmospheric chemistry and more specifically the community of chemical weather prediction. I m then favorable to the publication of this paper but i have the feeling that the paper could be more “efficient” and clear with some minor modifications. Hereafter, i make few remarks that, I hope, could help to improve the paper.

Page 32255 – Line 18: At the end of the section 3.1, you are presenting the results of a study where SCHIAMACHY observations have been assimilated. This study is probably very interesting but it seems that, contrary to the other examples of the section, the results are not related to a publication. The consequence is that the readers do not have the possibility to understand/evaluate the results. Maybe, the corresponding publication is missing but under this form it is like you were presenting results almost without description of the model, the assimilation, the case study, the set-up of the assimilation experiment, the nature of the observation used. In this state, i would recommend you to skip this section and the corresponding figure.

Reply: The two paragraphs referring to this data assimilation study and the associated figures have been deleted.

Page 32275 – Line 9: The case studies presented within section 5 are more documented than the case study mentioned above. Nevertheless, the interest to have such examples in the paper is not obvious. Maybe these case studies (at least one or two) should be used to illustrate a paragraph more focused on CCMM. Indeed, It is not clear from the paper what are the applications/processes that could be targeted with the use of data assimilation in CCMM. The example of the use of CCN to improve aerosol is relatively unexpected but very interesting and I think we would like to have a more exhaustive list of the domain that could benefit assimilation in CCMM. Which of these potential applications could be expected in a very near future when considering current available observations ?

Reply: We feel that it is important to show some examples of data assimilation in atmospheric chemistry models, as those illustrate some of the associated advantages and limitations. We debated whether the case studies could be incorporated into Section 3. However, we decided to keep them as a separate section because they not only provide illustrations of the data assimilation methods, but also exemplify the use of observational data sets (ground-level and satellite data), which have been described in Section 4.

It is difficult to anticipate which indirect effects of data assimilation would benefit various model variables via meteorology/chemistry interactions and, therefore, it does not seem feasible to develop an exhaustive list of such potential benefits at this point. Nevertheless, we added a sentence in the conclusion pointing out such potential benefits and giving as examples the improvement in aerosol concentrations following CCN data assimilation and the potential improvement in meteorology (thermal structure and circulation) following AOD data assimilation during dust storms.

A last remark, you mention that CCMM are costly in term of time calculation which combined with assimilation is even more critical. Is there a tendency to have simplified chemistry compared to off-line CTM ?

Reply: CCMM typically use the same gas-phase chemical kinetic mechanisms as CTM. There are some versions of CCMM that use simplified representations of aerosol processes (in terms of particle size resolution and/or chemical composition); however, some CCMM use fairly detailed representations of both particle size resolution and chemical composition.

1 **Data Assimilation in Atmospheric Chemistry Models: Current Status and Future**
2 **Prospects for Coupled Chemistry Meteorology Models**

3
4
5
6 **M. Bocquet^{1,2}, H. Elbern³, H. Eskes⁴, M. Hirtl⁵, R. Žabkar⁶, G.R. Carmichael⁷, J.**
7 **Flemming⁸, A. Inness⁸, M. Pagowski⁹, J.L. Pérez Camaño¹⁰, P.E. Saide⁷, R. San**
8 **Jose¹⁰, M. Sofiev¹¹, J. Vira¹¹, A. Baklanov¹², C. Carnevale¹³, G. Grell⁹, C.**
9 **Seigneur¹.**

10
11 ¹CEREA, Joint Laboratory École des Ponts ParisTech/EDF R&D, Université Paris-Est,
12 Marne-la-Vallée, France

13 ²INRIA, Paris Rocquencourt Research Center, France

14 ³Institute for Physics and Meteorology, University of Cologne, Germany

15 ⁴KNMI, De Bilt, The Netherlands

16 ⁵Central Institute for Meteorology and Geodynamics, Vienna, Austria

17 ⁶Faculty of Mathematics and Physics, University of Ljubljana, Slovenia

18 ⁷Center for Global and Regional Environmental Research, University of Iowa, USA

19 ⁸European Centre for Medium-range Weather Forecasts, Reading, UK

20 ⁹NOAA/ESRL, Boulder, Colorado, USA

21 ¹⁰Technical University of Madrid (UPM), Madrid, Spain

22 ¹¹Finnish Meteorological Institute, Helsinki, Finland

23 ¹²World Meteorological Organization (WMO), Geneva, Switzerland and Danish
24 Meteorological Institute (DMI), Copenhagen, Denmark

25 ¹³Department of Mechanical and Industrial Engineering, University of Brescia, Italy

26
27
28 Correspondence to: C. Seigneur (seigneur@cerea.enpc.fr)

29
30 **Abstract**

31
32
33 Data assimilation is used in atmospheric chemistry models to improve air quality forecasts,
34 construct re-analyses of three-dimensional chemical (including aerosol) concentrations and
35 perform inverse modeling of input variables or model parameters (e.g., emissions). Coupled
36 chemistry meteorology models (CCMM) are atmospheric chemistry models that simulate
37 meteorological processes and chemical transformations jointly. They offer the possibility to
38 assimilate both meteorological and chemical data; however, because CCMM are fairly
39 recent, data assimilation in CCMM has been limited to date. We review here the current
40 status of data assimilation in atmospheric chemistry models with a particular focus on future
41 prospects for data assimilation in CCMM. We first review the methods available for data
42 assimilation in atmospheric models, including variational methods, ensemble Kalman filters,
43 and hybrid methods. Next, we review past applications that have included chemical data
44 assimilation in chemical transport models (CTM) and in CCMM. Observational data sets
45 available for chemical data assimilation are described, including surface data, surface-based
46 remote sensing, airborne data, and satellite data. Several case studies of chemical data
47 assimilation in CCMM are presented to highlight the benefits obtained by assimilating
48 chemical data in CCMM. A case study of data assimilation to constrain emissions is also
49 presented. There are few examples to date of joint meteorological and chemical data
50 assimilation in CCMM and potential difficulties associated with data assimilation in CCMM

51 are discussed. As the number of variables being assimilated increases, it is essential to
52 characterize correctly the errors; in particular, the specification of error cross-correlations
53 may be problematic. In some cases, offline diagnostics are necessary to ensure that data
54 assimilation can truly improve model performance. However, the main challenge is likely to
55 be the paucity of chemical data available for assimilation in CCMM.

56 **1. Introduction**

57
58 Data assimilation pertains to the combination of modeling with observational data to produce
59 a most probable representation of the state of the variables considered. For atmospheric
60 applications, the objective of data assimilation is to obtain a better representation of the
61 atmosphere in terms of meteorological and atmospheric chemistry variables (particulate
62 matter (PM) is included here as part of atmospheric chemistry).

63
64 Data assimilation has been used for many decades in dynamic meteorology to improve
65 weather forecasts and construct re-analyses of past weather. Several recent reviews of data
66 assimilation methods used routinely in meteorology are available (e.g., Kalnay, 2003; Navon,
67 2009; Lahoz et al., 2010). The use of data assimilation in atmospheric chemistry is more
68 recent, because numerical deterministic models of atmospheric chemistry have been used
69 routinely for air quality forecasting only since the mid 1990's; previously, most air quality
70 forecasts were conducted with statistical approaches (Zhang et al., 2012a). Data assimilation
71 is also used in air quality since the 1990's for re-analysis to produce air pollutant
72 concentration maps (e.g., Elbern and Schmidt, 2001), inverse modeling to improve (or
73 identify errors in) emission rates (e.g., Elbern et al., 2007; Vira and Sofiev, 2012; Yumimoto
74 et al., 2012), boundary conditions (e.g., Roustan and Bocquet, 2006) and model parameters
75 (e.g., Barbu et al., 2009; Bocquet, 2012). Regarding air quality re-analyses, the 2008/50
76 European Union (EU) Air Quality Directive (AQD) suggests the use of modeling in
77 combination with fixed measurements "to provide adequate information on the spatial
78 distribution of the ambient air quality" (Borrego, in press; OJEU, 2008). An overview of data
79 assimilation of atmospheric species concentrations for air quality forecasting was recently
80 provided by Zhang et al. (2012b); however, only data assimilation in CTM was addressed.
81 We address here data assimilation in atmospheric chemistry models, which we define to
82 include both atmospheric chemical transport models (CTM), which use meteorological fields
83 as inputs (e.g., Seinfeld and Pandis, 2006), and coupled chemistry meteorology models
84 (CCMM), which simulate meteorology and atmospheric chemistry jointly (Zhang, 2008;
85 Baklanov et al., 2014). In particular, we are interested in the future prospects and potential
86 difficulties associated with data assimilation in CCMM.

87
88 In spite of available previous experience in data assimilation for meteorological modeling on
89 one hand and chemical transport modeling on the other hand, conducting data assimilation in
90 CCMM can be challenging because of interactions among meteorological and chemical
91 variables. Assimilating large bodies of various meteorological and air quality data may lead
92 to a point of diminishing return. The objective of this review is to present the current state of
93 the science in data assimilation in atmospheric chemistry models. Because of the limited
94 experience available with CCMM, our review covers primarily data assimilation in CTM
95 and, to a lesser extent, in CCMM. The emphasis for future prospects is placed on the
96 preferred approaches for CCMM and the challenges associated with the combined
97 assimilation of data for meteorology and atmospheric chemistry. Potential difficulties are
98 identified based on currently available experience and recommendations are provided on the
99 most appropriate approaches (methods and data sets) for data assimilation in CCMM.
100 Recommendations for method development are also provided since current efforts are
101 ongoing in this area of geosciences.

102
103 We present in Section 2 an overview of the data assimilation techniques that are used in
104 atmospheric modeling. Next, their applications to atmospheric chemistry are presented in
105 Section 3; most applications to date pertain to meteorology and atmospheric chemistry

Supprimé : including techniques that are currently used operationally as well as techniques that have been developed recently (or are under development) and may be used operationally in the next few years

106 separately, nevertheless a few recent applications pertaining to CCMM are described. Data
107 assimilation in the context of optimal network design is also discussed because it may be
108 used to improve the representativeness of observational monitoring networks. The
109 observational data sets available for data assimilation are described in Section 4. Selected
110 case studies of data assimilation in CCMM are presented in Section 5 to illustrate the current
111 state of the science. A case study of data assimilation performed in the context of inverse
112 modeling of the emissions is also presented. Potential difficulties associated with data
113 assimilation in CCMM are discussed in Section 6. Finally, recommendations for future
114 method development, method applications and pertinent data sets are provided in Section 7,
115 along with a discussion of future prospects for data assimilation in CCMM.

Supprimé : Those include mainly satellite data, ground-based remote sensing data (e.g., lidar data) and in situ observations; data gaps are identified and recommendations are made to improve the completeness of the observational networks in the context of CCMM. The use of data indirectly related to model variables (e.g., satellite data on biomass fire intensity) is also discussed.

118 2. Methods of data assimilation in meteorology and atmospheric chemistry

120 2.1 Overview of the methods

122 Data assimilation in geosciences has been initially applied to meteorology where methods
123 have been very soon operationally implemented (Lorenc, 1986; Daley, 1991; Ghil and
124 Malanotte-Rizzoli, 1991; Kalnay, 2003; Evensen, 2009; Lahoz et al., 2010). Building on
125 established data assimilation methodology, assimilation of observations in offline CTM has
126 emerged in the late 1990's (Carmichael et al., 2008; Zhang et al., 2012a). Here, we briefly
127 describe the most common techniques used in both fields and comment on their differences
128 when appropriate.

Supprimé : D

Supprimé : natural playground

Supprimé : always

130 As far as spatial analysis is concerned, most common data assimilation methods hardly differ.
131 They are mainly based on statistical Gaussian assumptions on all errors and the analysis
132 relies on the simple but efficient Best Linear Unbiased Estimator (BLUE). At a given time,
133 BLUE strikes the optimal compromise between the observations and a background estimate
134 of the system state, often given by a previous forecast. Such BLUE analysis can be
135 performed solving for the gain matrix (that balances the observations and the background)
136 using linear algebra, a procedure called Optimal/Statistical Interpolation (OI) (Fedorov,
137 1989; Daley, 1991), or it can be obtained through a three-dimensional (3D) variational spatial
138 analysis, usually called 3D-Var. Within BLUE, it is mandatory to provide a priori statistics
139 for both the observation errors and the errors of the background.

Supprimé : the

141 When time is accounted for, these methods need to be generalized. In particular, errors (or
142 their statistics) attached to the best estimate must be propagated in time, which leads to
143 substantial hardships in both statistical interpolation and variational approaches. The OI
144 approach may be generalized to the (extended) Kalman filter (Ghil and Malanotte-Rizzoli,
145 1991), while 3D-Var is generalized to 4D-Var (Penenko and Obraztsov, 1976; Le Dimet and
146 Talagrand, 1986; Talagrand and Courtier, 1987; Rabier et al., 2000). Kalman filters and
147 3D/4D-Var can be combined to address deficiencies of both methods: divergence of the filter
148 and static covariance in variational methods (at least initially for 4D-Var) (Lorenc, 2003).

150 2.1.1 Filtering approaches

152 The extended Kalman filter requires the propagation of the error covariance matrix of rank
153 the dimension of state-space, which can become unaffordable beyond a few hundred. Yet,
154 when the analysis happens to be strongly localized, the method becomes affordable such as
155 in land surface data assimilation. For higher dimensional applications, it has been replaced by

156 the reduced-rank Kalman filter and the ensemble Kalman filter, and many variants thereof
157 (Evensen, 1994; Verlaan and Heemink, 1997). In both cases, the uncertainty is propagated
158 through a limited number of modes that are forecast by the model. This makes these methods
159 affordable even with large dimensional models, especially because of the natural parallel
160 architecture of such ensemble filtering. Unfortunately, the fact that the ensemble is of finite
161 size entails a deficient estimation of the errors mostly due to undersampling, which may lead
162 to divergence of the filter. This needs to be fixed and has been so through the use of inflation
163 (Pham et al., 1998; Anderson and Anderson, 1999) and localization (Houtekamer and
164 Mitchell, 2001; Hamill et al., 2001).

165
166 Inflation consists in additively or multiplicatively inflating the error covariance matrices so
167 as to compensate for an underestimation of the error magnitude. The inflation can be fixed or
168 adaptive, or it can be rendered by physically-driven stochastic perturbations of the ensemble
169 members. Localization is made necessary when the finite size of the ensemble whose
170 variability is too small in high-dimensional systems makes the analysis inoperative.

171 Localization can be performed by either filtering the ensemble empirical error covariance
172 matrix and making it full-rank using a Schur product with a short-range correlation function
173 (Houtekamer and Mitchell, 2001) or performing parallel spatially local analyzes (Ott et al.,
174 2004). Those methodological advances have been later tested and weighted with offline
175 CTM (Hanea et al., 2004; Constantinescu et al., 2007a,b; Wu et al., 2008).

176 177 **2.1.2 Variational approaches**

178
179 Four-dimensional (4D) variational data assimilation (4D-Var) that minimizes a cost function
180 defined in space and in time, requires the use of the adjoint of the forward and observation
181 models, which may be costly to derive and maintain. It also requires the often complex
182 modeling of the background error covariance matrix. Since linear algebra operations on this
183 huge matrix are prohibitive, the background error covariance matrix is usually modeled as a
184 series of operators, whose correlation part can for instance be approximated as a diffusion
185 operator (Weaver and Courtier, 2001). This modeling is even more so pregnant in air quality
186 data assimilation when the statistics of the errors on the parameters also need prior statistical
187 assumptions (Elbern et al., 2007). However, as a smoother, 4D-Var could theoretically
188 outperform ensemble Kalman filtering in nonlinear enough systems, if it was not for the
189 absence of flow-dependence in the background statistics (Bocquet and Sakov, 2013). It also
190 easily accounts for asynchronous observations that are surely met in an operational context.

191
192 Most operational 4D-Var are strong-constraint 4D-Var, which implies that the model is
193 assumed to be perfect. Accounting for model error and/or extending the length of the data
194 assimilation window would require generalizing it to weak-constraint 4D-Var (Penenko,
195 1996; Fisher et al., 2005, Penenko, 2009). However, several difficulties arise, such as the
196 necessity to characterize model error and to significantly extend control space. On the
197 contrary, filtering approaches quite easily incorporate model errors that nevertheless still
198 need to be assessed. 4DVar has been rapidly evaluated and promoted in the context of air
199 quality forecasting (Fisher and Lary, 1995; Elbern and Schmidt, 1999, 2001; Quélo et al.,
200 2006; Chai et al., 2006; Elbern et al., 2007; Wu et al., 2008).

201
202 New data assimilation methods that have been recently developed are currently being tested
203 in meteorological data assimilation such as hybrid schemes (Lorenc, 2003; Wang et al.,
204 2007), particle filters (van Leeuwen, 2009; Bocquet et al., 2010) and ensemble variational
205 schemes (Buehner et al., 2010a, 2010b). However, the flow dependence of the methods in air

Supprimé : ensemble/variational

206 quality is not as strong as in meteorology, and it remains to be seen whether those methods
207 have a potential in offline atmospheric chemistry modeling and, in the long term, in online
208 CCMM (Bocquet and Sakov, 2013).

209

210 **2.2 From state estimation to physical parameter estimation**

211

212 As soon as time is introduced, differences appear between meteorological models and
213 offline CTM. For instance, the dynamics of a synoptic scale meteorological model is chaotic
214 while the non-chaotic dynamics of offline CTM, even though possibly very non-linear, is
215 mainly driven by forcings, such as emissions and insolation. As a consequence, a combined
216 estimation of state and parameters might be an advantage in CTM data assimilation. A
217 possible difference is also in the proven benefit of model error schemes where stochastic
218 parameterizations offer variability that most CTM lack. More generally, one should
219 determine which parameters have a strong influence on the forecasts and, at the same time,
220 are not sufficiently known. Whereas pure initial value estimation might be a satisfying
221 answer for synoptic meteorological models, emission, deposition, and transformation rates as
222 well as boundary conditions are in competition with initial values for CTM for medium- to
223 long-range forecasts.

224

225 With model parameter estimation, which is desirable in offline atmospheric data assimilation,
226 the filtering and variational methods come with two types of solution. The (ensemble)
227 filtering approach requires the augmentation of the state variables with the parameters (Ruiz
228 et al., 2013). 4D-Var easily lends itself to data assimilation since the parameter variables can
229 often be accounted for in the cost function (Penenko et al., 2002; Elbern et al., 2007; Bocquet,
230 2012; Penenko et al., 2012). However, it is often required to derive new adjoint operators
231 corresponding to the gradient of the cost function with respect to these parameters if the
232 driving mechanisms are not external forcings. Often, adjoint models and operators can
233 nonetheless be obtained through a simplifying approximation (Issartel and Baverel, 2003;
234 Krysta and Bocquet, 2007; Bocquet, 2012; Singh and Sandu, 2012).

235

236 **2.3 Accounting for errors and diagnosing their statistics**

237

238 All the above schemes rely on the knowledge of the error statistics for the observations and
239 the background (state or parameters). Yet, in a realistic context, it is always imperfect. The
240 performance of the data assimilation schemes is quite sensitive to the specification of these
241 errors. Algorithms relying on consistency check, cross validation and statistical likelihood
242 (Hollingsworth and Lönnberg, 1986; Desroziers and Ivanov, 2001; Chapnik et al., 2004;
243 Desroziers et al., 2005) or the empirical but efficient National Meteorological Center (NMC)
244 technique (Parrish and Derber, 1992) have been used in meteorology to better assess those
245 pivotal statistics. Paradoxically, they have slowly percolated in air quality data assimilation
246 where they should be crucial given the uncertainty on most forcings or the sparsity of
247 observations for in situ concentration measurements.

248

249 The error covariance matrices can be parameterized with a restricted set of hyper-parameters,
250 and those hyper-parameters can be estimated through maximum-likelihood or L-curve tests
251 (Ménard et al., 2000; Davoine and Bocquet, 2007; Elbern et al., 2007). Alternatively, with
252 sufficient data, the whole structure of the error covariance matrices in the observation space
253 can be diagnosed using consistency matrix identities; see for example Schwinger and Elbern
254 (2010) who applied the approach of Desroziers et al. (2005) to a stratospheric chemistry 4D-
255 Var system.

Supprimé : have been used in meteorology

Mis en forme : Police :(Par défaut) Times New Roman, 12 pt, Police de script complexe :Times New Roman, 12 pt, Anglais Royaume-Uni

Mis en forme : Police :(Par défaut) Times New Roman, 12 pt, Police de script complexe :Times New Roman, 12 pt, Anglais États-Unis

Mis en forme : Police de script complexe :Times New Roman, 12 pt

256
257
258
259
260
261
262
263
264
265
266
267
268
269
270
271
272
273
274
275
276
277
278
279
280
281
282
283
284
285
286
287
288
289
290
291
292
293
294
295
296
297
298
299
300
301
302
303
304
305

As mentioned above, stochastic perturbations, as well as multi-physics parameterizations (within ensemble methods) can be implemented to offer more variability and counteract model error. More dedicated parameterizations of model error are possible and occasionally bring in substantial improvement. Kinetic energy backscatter (Shutts, 2005) or physical tendency perturbations at the ECMWF (Buizza et al., 1999) are used in numerical weather predictions. In air quality, a subgrid statistical method has been successful in quantitatively estimating and removing representativeness errors (Koohkan and Bocquet, 2012).

2.4 Nonlinearity and non-Gaussianity and the need for advanced methods

The aforementioned methods that are essentially derived from the BLUE paradigm may be far from optimal when dealing with significant nonlinearities or significantly non-Gaussian statistics. This surely happens when accounting for the convective scale or for the hydrometeors in meteorology. It also occurs when modeling aerosols and assimilating aerosols/optical observations. It is also bound to happen whenever positive variables are dealt with (which is the case for most of the variables in air quality). It could become important when error estimates of species concentrations are commensurate with those concentrations. It will happen with online coupling of meteorology and atmospheric chemistry. Possible solutions are a change of variables, the (related) Gaussian anamorphosis, maximum entropy on the mean inference, particles filters or the use of variational schemes that account for nonlinearity well within the data assimilation window (Bocquet et al., 2010).

2.5 Verification of the data assimilation process

Clearly, one would expect that model performance would improve with data assimilation. However, comparing model simulation results against the observations that have been assimilated is only a test of internal consistency of the data assimilation process and it cannot be construed as a verification of the improvement due to the data assimilation. Verification must involve testing the model against observations that have not been used in the data assimilation process. One may distinguish two broad categories of verification.

One approach is to test the result of a model simulation for a different time window than that used for the data assimilation. Since data assimilation is used routinely in meteorology to improve weather forecast, a large amount of work has been conducted to develop procedures to assess the improvement in the forecast resulting from the data assimilation. The model forecast with and without data assimilation may be tested in the forecast range (i.e., following the data assimilation window) either against observations or against reanalyses. Numerical weather forecast centers perform such verification procedures routinely and various performance parameters have been developed to that end. See for example Table 6 in Yang et al. (2012a) for a non-exhaustive list of such parameters. Ongoing research continuously adds to such procedures (e.g., Rodwell et al., 2010; Ferro and Stevenson, 2011). Similar procedures may be used with CCMM to evaluate the improvement provided by data assimilation in a forecasting mode (e.g., see case studies in Sections 5.2 and 5.3).

Another approach to evaluate the improvement of model performance due to data assimilation consists in comparing model performance for the data assimilation time window, but using a set of data that was not used in the assimilation process. The Leave-one-out approach, where data from only n-1 stations are assimilated and the left-out station is used for evaluation is computationally expensive and, therefore, typically unfeasible. Consequently, the Group

Mise en forme : Puces et numéros

Supprimé : One may mention the following approaches:

Supprimé : ¶

Supprimé :

Supprimé : Starting from n stations where observations are available,

Supprimé : . The procedure is iterated n times, using a different station for evaluation each time. This approach

Supprimé :

Supprimé : however,

Supprimé : in some cases simply

Supprimé : It may be used without the iteration process to limit the computational burden, but the procedure is then sensitive to the selection of the station used for evaluation.¶

306 | selection approach is more commonly used. A subset of the stations where observations are
307 available (usually 15% to 25% of the total number of stations) is selected at the beginning of
308 the verification process; those stations are not used in the data assimilation process and are
309 used only for model performance evaluation with and without data assimilation. Clearly, the
310 group selection approach is sensitive to the selection of that subset of stations.
311

Supprimé :

312 The methods mentioned above can be applied in the case of different observational sources
313 (e.g., ground based observations, satellite data, lidar data). They can also be applied in cases
314 where data assimilation is used to conduct inverse modeling to estimate emissions or model
315 parameters. For example, Koohkan et al. (2013) used both an evaluation in a forecast mode
316 and a leave-one-out approach to evaluate the improvement in model performance resulting
317 from a revised emission inventory obtained via inverse modeling.
318

319 One must note that the availability of chemical data is significantly less than that of
320 meteorological data and, for all approaches, this paucity of chemical data will place some
321 limits on the depth of the verification of the improvement due to data assimilation that can be
322 conducted.
323

323

324

325 3. Applications

326

327 3.1 Data assimilation in CTM

328

329 Many successful applications have demonstrated the benefits of data assimilation applied in
330 CTM either with the purpose to produce re-analysis fields or with the focus on improvement
331 of accuracy of model inputs (IC, BC, and emissions) and forecasts. To represent the current
332 status and to illustrate the performance of data assimilation for these purposes, we provide
333 examples from regional and global studies, using different types of observational data,
334 including in-situ, airborne, and satellite data.
335

336 3.1.1 Initial conditions and re-analysis fields

337

338 A range of techniques have been used for estimating the best known estimate for the state
339 space variables, such as ozone (O₃), nitrogen dioxide (NO₂), carbon monoxide (CO) or
340 aerosols (particulate matter, PM), with the purpose either to conduct air quality assessments
341 or to improve the initial conditions for forecast applications. Elbern and Schmidt (2001) in
342 one of the pioneer studies providing a chemical state analysis for the real case O₃ episode
343 with the use of a 4D-Var based optimal analysis, EURAD CTM model, with surface O₃
344 observations and radiosonde measurements. Analyses of the chemical state of the atmosphere
345 obtained on the basis of a 6 hour data assimilation interval were validated with observational
346 data withheld from the variational DA algorithm. The authors showed that the initial value
347 optimization by 4D-Var provides a considerable improvement for the 6 to 12 hour O₃
348 forecast including the afternoon peak values, but vanishing improvements afterwards. A
349 similar conclusion was later reached in other studies (e.g., Wu et al., 2008; Tombette et al.
350 2009; Wang et al. 2011; Curier et al. 2012). Chai et al (2006), with the STEM-2K1 model
351 and 4D-Var technique applied to assimilate aircraft measurements during the TRACE-P
352 experiment showed not only that adjusting initial fields after assimilating O₃ measurements
353 improves O₃ predictions, but also that assimilation of NO_y measurements improves
354 predictions of nitric oxide (NO), NO₂, and peroxy acetyl nitrate (PAN). In this study, the
355 concentration upper bounds were enforced using a constrained limited memory Broyden-

Supprimé : the

Supprimé : -

356 | Fletcher-Goldfarb-Shanno ~~minimizer~~ to speed up the optimization process in the 4D-Var and
357 the same approach was later used also by Chai et al. (2007) for assimilating O₃ measurements
358 from various platforms (aircraft, surface, and ozone sondes) during the International
359 Consortium for Atmospheric Research on Transport and Transformation (ICARTT)
360 operations in the summer of 2004. Here, the ability to improve the predictions against the
361 withheld data was shown for every single type of observations. A final analysis where all the
362 observations were simultaneously assimilated resulted in a reduction in model bias for O₃
363 from 11.3 ppbv (the case without assimilation) to 1.5 ppbv, and in a reduction of 10.3 ppbv
364 in RMSE. It was also demonstrated that the positive effect in air quality forecast for the near
365 ground O₃ was seen even out to 48 hours after assimilation.
366

Supprimé : -B

Supprimé : (L-BFGS-B)

367 In addition to the variational data assimilation work, a number of atmospheric chemistry data
368 assimilation applications used sequential approaches, including various Kalman filter
369 methods. Coman et al. (2012) in their study used an Ensemble Square Root Kalman Filter
370 (EnSRF) to assimilate partial lower tropospheric ozone columns (0 - 6 km) provided by the
371 IASI (Infrared Atmospheric Sounding Interferometer) instrument into a continental-scale
372 CTM, CHIMERE, for July 2007. In spite of the fact that IASI shows higher sensitivity for O₃
373 in the free troposphere and lower sensitivity at the ground, validations of analyses with
374 assimilated O₃ observations from ozone sondes, MOZAIC aircraft and AIRBASE ground
375 based measurements, showed 19% reduction of the RMSE and 33 % reduction of the bias at
376 the surface. The more pronounced reduction of the errors in the afternoon than in the
377 morning was attributed to the fact that the O₃ information introduced into the system needs
378 some time to be transported downward.
379

Supprimé : K

380 The limitations and potentials of different data assimilation algorithms with the aim of
381 designing suitable assimilation algorithms for short-range O₃ forecasts in realistic
382 applications have been demonstrated by Wu et al. (2008). Four assimilation methods were
383 considered and compared under the same experimental settings: optimal interpolation (OI),
384 reduced-rank square root Kalman filter (RRSQRT), ensemble Kalman filter (EnKF), and
385 strong-constraint 4D-Var. The comparison results revealed the limitations and the potentials
386 of each assimilation algorithm. The 4D-Var approach due to low dependency of model
387 simulations on initial conditions leads to moderate performances. The best performance
388 during assimilation periods was obtained by the OI algorithm, while ~~the~~ EnKF had better
389 forecasts than OI during the prediction periods. The authors concluded that serious
390 investigations on error modeling are needed for the design of better DA algorithms.
391

392 Data assimilation approaches have been used also with the purpose of combining the
393 measurements and model results in the context of air quality assessments. Candiani et al.
394 (2013) formalized and applied two types of offline data assimilation approaches (OI and
395 EnKF) to integrate the results of the TCAM CTM (Carnevale et al., 2008) and ground-level
396 measurements and produce PM₁₀ re-analysis fields for a regional domain located in northern
397 Italy. The EnKF delivered slightly better results and more model consistent fields, which was
398 due to the fact that, for ~~the~~ EnKF, an ensemble of simulations randomly perturbing only
399 PM₁₀ precursor emissions highlighted the importance of a consistent emission inventory in
400 the modeling. EnKF approaches along with surface measurements have also been used for
401 other models such as CUACE/dust (Lin et al., 2008). The use of such air quality re-analyses
402 in the context of air quality regulations (e.g., assessment of air quality exceedances over
403 specific areas, estimation of human exposure to air pollution) has been discussed by Borrego
404 et al. (in press).
405

406 Kumar et al. (2012) used a bias-aware optimal interpolation method (OI) in combination with
407 the Hollingsworth-Lönnerberg method to estimate error covariance matrices to perform re-
408 analyses of O₃ and NO₂ surface concentration fields over Belgium with the regional-scale
409 CTM AURORA for summer (June) and winter (December) months. Re-analysis results were
410 evaluated objectively by comparison with a set of surface observations that were not
411 assimilated. Significant improvements were obtained in terms of correlation and error for
412 both months and both pollutants.

413
414 Satellite data have also been assimilated into CTM to improve performance in terms of
415 surface air pollutant concentrations. For example, Wang et al. (2011) assimilated NO₂
416 column data from OMI of the AURA satellite into the Polyphemus/Polair3D CTM to
417 improve air quality forecasts. Better improvements were obtained in winter than in summer
418 due to the longer lifetime of NO₂ in winter. Several studies have used aerosol optical depth
419 (AOD, also referred to as aerosol optical thickness or AOT) observations along with CTM to
420 obtain better air quality re-analyses. Some of these studies used the OI technique along with
421 models such as STEM (Adhikary et al., 2008; Carmichael et al., 2009), CMAQ (Park et al.,
422 2011; Park et al., 2014), MATCH (Collins et al., 2001), and GOCART (Yu et al., 2003).
423 Other studies used variational approaches with models such as EURAD (Schroeder-
424 Homscheidt et al., 2010; Nieradzic and Elbern, 2006) and LMDz-INCA (Generoso et al.,
425 2007).

426
427 The question whether assimilation of lidar measurements instead of ground-level
428 measurements has a longer lasting impact on PM₁₀ forecast, was investigated by Wang et al.
429 (2013). They compared the efficiency of assimilating lidar network measurements or
430 AirBase ground network over Europe using an Observing System Simulation Experiment
431 (OSSE) framework and an OI assimilation algorithm with the POLAIR3D CTM (Sartelet et
432 al., 2007) of the air quality platform POLYPHEMUS (Mallet et al., 2007). Compared to the
433 RMSE for one-day forecasts without DA, the RMSE between one-day forecasts and the truth
434 states was improved on average by 54% by the DA with data from 12 lidars and by 59% by
435 the DA with AirBase measurements. Optimizing the locations of 12 lidars, the RMSE was
436 improved by 57 %, while with 76 lidars the improvement of the RMSE became as high as
437 65%. For the second forecast days the RMSE was improved on average by 57% by the lidar
438 data assimilation and by 56% by the AirBase data assimilation, compared to the RMSE for
439 second forecast days without data assimilation. The authors concluded that assimilation of
440 lidar data corrected PM₁₀ concentrations at higher levels more accurately than AirBase data,
441 which caused the spatial and temporal influence of the assimilation of lidar observations to
442 be larger and longer. Kahnert (2008) is another example of assimilation of lidar data by using
443 the MATCH model on a 3D-Var framework.

444 [3.1.2 Initial conditions versus other model input fields](#)

445
446
447 Pollutant transport and transformations in CTM are strongly driven by uncertain external
448 parameters, such as emissions, deposition, boundary conditions, and meteorological fields,
449 which explains why the impact of initial state adjustment is generally limited to the first day
450 of the forecast. To address this issue, i.e., to improve the analysis capabilities and prolong the
451 impact of DA on AQ forecasts, Elbern et al. (2007) extended the 4D-Var assimilation for
452 adjusting emissions fluxes for 19 emitted species with the EURAD mesoscale model in
453 addition to chemical state estimates as usual objective of DA. Surface in-situ observations of
454 sulfur dioxide (SO₂), O₃, NO, NO₂, and CO from the EEA AirBase database were assimilated
455 and forecast performances were compared for pure initial value optimization and joint

456 emission rate/initial value optimization for an August 1997 O₃ episode. For SO₂, the
457 emission rate optimization nearly perfectly reduced the emission induced bias of 10 ppb after
458 two days of simulation with pure initial values optimization, and reduced RMS errors by
459 about 60%, which demonstrated the importance of emission rate rather than initial value
460 optimization. In the case of photolytically active species, the optimization of emission rates
461 was shown to be considerably more challenging; for O₃, it was attributed mostly to the coarse
462 model horizontal resolution of 54 km. The authors concluded that grid refinement with 4D-
463 Var applied after introducing nesting techniques should enable more efficient use of NO_x
464 observations and decrease bias and RMSE for a forecast longer than 48 h.

466 In limited area modeling, experiments concerning the relative importance of the initial model
467 state and emissions of primary pollutants have been carried out with the SILAM chemistry
468 transport model (<http://silam.fmi.fi>), which includes a subsystem for variational data
469 assimilation. Both 4D- and 3D-Var methods are implemented and share the common
470 observation operators, covariance models and minimization algorithms. The main features of
471 the assimilation system are described by Vira and Sofiev (2012, 2015). In addition to model
472 initialization, the 4D-Var mode can be set to optimize emission rates either via a location-
473 dependent scaling factor or an arbitrary emission forcing restricted to a single point source.
474 The former can be used for optimizing emission inventories of anthropogenic or natural
475 pollutants (see case study 5.4), while the latter has been developed especially for source term
476 inversion in volcanic eruptions. European-wide in-situ observations are assimilated routinely
477 to produce daily analysis fields of gas-phase pollutants, while satellite observations have been
478 used mainly for emission-related case studies. The assimilation of sulfur oxide observations
479 from the Airbase database showed that for such compounds the effect of initial state
480 determination, whether with 3D- or 4D-Var, tends to disappear within 10-12 hours, whereas
481 the effect of emission correction rather starts after a few hours following the assimilation. The
482 3D-Var assimilation mode, while less versatile than 4D-Var, benefits from very low
483 computational overhead. The adjoint code, required by 4D-Var, is available for all processes
484 except aerosol chemistry.

486 3.1.3 Inverse modeling

488 The possibility to use data assimilation for establishing the initial state of the model as well
489 as for improving the emission input data connects data assimilation to the source
490 identification problem, either in the context of accidental releases or for evaluating and
491 improving emission inventories. Numerous studies used data assimilation approaches for
492 estimating or improving emission inventories. Mijling and van der A (2012) presented a new
493 algorithm (DECSO) specifically designed to use daily satellite observations of column
494 concentrations for fast updates of emission estimates of short-lived atmospheric constituents.
495 The algorithm was applied for NO_x emission estimates of East China, using the CHIMERE
496 model on a 0.25 degree resolution together with tropospheric NO₂ column retrievals of the
497 OMI and GOME-2 satellite instruments (see Table 1). The important advantage of this
498 algorithm over techniques using 4D-Var or the EnKF is the calculation speed of the
499 algorithm, which facilitates for example its operational application for NO₂ concentration
500 forecasting at mesoscale resolution. The DECSO algorithm needs only one forward model
501 run from a CTM to calculate the sensitivity of concentration to emission, using trajectory
502 analysis to account for transport away from the source. By using a Kalman filter in the
503 inverse step, optimal use of the a priori (background) knowledge and the newly observed
504 data is made. Tests showed that the algorithm is capable of reconstructing new NO_x emission
505 scenarios from tropospheric NO₂ column concentrations and detecting new emission sources

Supprimé : 4

Supprimé : ¶

¶ The data assimilation system has been run with both satellite and in-situ measurements.

Supprimé : Boundary conditions are also one of the crucial parameters. Roustan and Bocquet (2006) used inverse modeling for optimizing boundary conditions for gaseous elemental mercury (GEM) dispersion modeling. They applied the adjoint techniques using the POLAIR3D CTM with Petersen et al. (1995) mercury (Hg) chemistry model and available GEM observations at 4 EMEP stations. They showed that using assimilated boundary conditions improved GEM forecasts over Europe for all monitoring stations, whereas improvement for the two EMEP stations that provided the assimilated data was significant. The authors also extended the inverse modeling approach to cope with a more complex Hg chemistry. The generalization of the adjoint analysis performed with the Petersen model, showed no significant improvement for the simulation with the complex scheme model as compared to the complex scheme model without assimilated boundary conditions. The authors ascribed this result to the absence of well-known boundary conditions for the oxidized Hg species. They also concluded that due to the insufficient Hg observation network it was not possible to take the full benefit of the approach used in the study, for example, they were not able to use the inverse modeling of GEM to improve the sinks and emissions inventories. ¶

¶

506 such as power plants and ship tracks. Using OMI and GOME-2 data, the algorithm was able
507 to detect emission trends on a monthly resolution, such as during the 2008 Beijing Olympic
508 Games. Furthermore, the tropospheric NO₂ concentrations calculated with the new emission
509 estimates showed better agreement with the observed concentrations over the period of data
510 assimilation, both in space and time, as expected, facilitating the use of the algorithm in
511 operational air quality forecasting.

512
513 Koohkan et al. (2013) have focused on the estimation of emission inventories for different
514 VOC species via inverse modeling. For the year 2005, they estimated 15 VOC species over
515 western Europe: five aromatics, six alkanes, two alkenes, one alkyne and one biogenic diene.
516 For that purpose, the Jacobian matrix was built using the POLAIR3D CTM. In-situ ground-
517 based measurements of 14 VOC species at 11 EMEP stations were assimilated, and for most
518 species the retrieved emissions led to a significant reduction of the bias. The corrected
519 emissions were partly validated with a forecast conducted for the year 2006 using
520 independent observations. The simulations using the corrected emissions often led to
521 significant improvements in CTM forecasts according to several statistical indicators.

Supprimé : a

522
523 Barbu et al. (2009) applied a sequential data assimilation scheme to a sulfur cycle version of
524 the LOTOS-EUROS model using ground-based observations derived from the EMEP
525 database for 2003 for estimating the concentrations of two closely related chemical
526 components, SO₂ and sulfate (SO₄⁻), and to gain insight into the behavior of the assimilation
527 system for a multicomponent setup in contrast to a single component experiment. They
528 performed extensive simulations with the EnKF in which solely emissions (single or multi
529 component), or a combination of emissions and the conversion rates of SO₂ to SO₄⁻ were
530 considered uncertain. They showed that two issues are crucial for the assimilation
531 performance: the available observation data and the choice of stochastic parameters for this
532 method. The modeling of the conversion rate as a noisy process helped the filter to reduce the
533 bias because it provides a more accurate description of the model error and enlarges the
534 ensemble spread, which allows the SO₄⁻ measurements to have more impact. They concluded
535 that one should move from single component applications of data assimilation to multi-
536 component applications, but the increased complexity associated with this move requires a
537 very careful specification of the multi-component experiment, which will be a main
538 challenge for the future.

539 Boundary conditions are also one of the crucial parameters. Roustan and Bocquet (2006)
540 used inverse modeling for optimizing boundary conditions for gaseous elemental mercury
541 (GEM) dispersion modeling. They applied the adjoint techniques using the POLAIR3D CTM
542 with Petersen et al. (1995) mercury (Hg) chemistry model and available GEM observations at
543 4 EMEP stations. They showed that using assimilated boundary conditions improved GEM
544 forecasts over Europe for all monitoring stations, whereas improvement for the two EMEP
545 stations that provided the assimilated data was significant. The authors also extended the
546 inverse modeling approach to cope with a more complex Hg chemistry. The generalization of
547 the adjoint analysis performed with the Petersen model, showed no significant improvement
548 for the simulation with the complex scheme model as compared to the complex scheme
549 model without assimilated boundary conditions. The authors ascribed this result to the
550 absence of well-known boundary conditions for the oxidized Hg species. They also
551 concluded that due to the insufficient Hg observation network it was not possible to take the
552 full benefit of the approach used in the study, for example, they were not able to use the
553 inverse modeling of GEM to improve the sinks and emissions inventories.
554
555

556 Regarding other model input parameters, [the work of Storch et al. \(2007\)](#) is a rare example
557 [that used the inverse analysis techniques for the estimation of micro-meteorological](#)
558 parameters required for the characterization of atmospheric boundary layers. Bocquet (2012)
559 focused on the retrieval of single parameters, such as horizontal diffusivity, uniform dry
560 deposition velocity, and wet-scavenging scaling factor, as well as on joint optimization of
561 removal-process parameters and source parameters, and on optimization of larger parameter
562 fields such as horizontal and vertical diffusivities and the dry-deposition velocity field. In
563 that study, the Polair3D CTM of the Polyphemus platform was used and a fast 4D-Var
564 scheme was developed. The inverse modeling system was tested on the Chernobyl accident
565 dispersion event with measurements of activity concentrations in the air performed in
566 Western Europe with the REM database following Brandt et al. (2002). Results showed that
567 the physical parameters used so far in the literature for the Chernobyl dispersion simulation
568 are partly supported by that study. The question of deciding whether such an inversion
569 modeling is merely a tuning of parameters or a retrieval of physically meaningful quantities
570 was also discussed. From that study, it appears that the reconstruction of the physical
571 parameters is a desirable objective, but it seems reasonable only for the most sensitive fields
572 or a few scalars, while for large fields of parameters, regularization (background) is needed
573 to [avoid overfitting the observations](#).

Supprimé : who

Supprimé : consider

Supprimé : ing

Supprimé : tuning

574 [3.1.4 Global studies](#)

577 The benefit of data assimilation is also significant for global applications. Schutgens et al.
578 (2010) presented the impact of the assimilation of Aerosol Robotic Network (AERONET)
579 AOD and the Angström exponent (AE) using a global assimilation system for the aerosol
580 model SPRINTARS (Takemura et al., 2000, 2002, 2005). The application was based on a
581 Local EnKF approach. To obtain the ensemble of the model simulations different emission
582 scenarios, which were computed randomly for sulfate, carbon, and desert dust (i.e., the
583 aerosol species that are considered by SPRINTARS), were used. Simulated fields of AOD
584 and AE from these experiments were compared to a standard simulation with SPRINTARS
585 (no assimilation) and independent observations at various geographic locations. In addition to
586 the AERONET sites, data from SKYNET observations (South-East Asia) and MODIS Aqua
587 observations of Northern America, Europe and Northern Africa were used for the validation.
588 The authors show the benefit of the assimilation of AOD compared to the simulation without
589 considering the measurement data. It was also pointed out that the usefulness of the
590 assimilation of AE is only limited to high AOD (>0.4) and low AE cases.

591 Yumimoto et al. (2013) also used SPRINTARS but presented a different data assimilation
592 system based on 4D-Var. The aim of that study was to optimize emission estimates, improve
593 4D descriptions, and obtain the best estimate of the climate effect of airborne aerosols in
594 conjunction with various observations. The simulations were conducted using an offline and
595 adjoint model version that was developed in order to save computation time (about 30%).
596 Comparing the results with the online approach for a 1 year simulation led to a correlation
597 coefficient of $r > 0.97$ and an absolute value of normalized mean bias $NMB < 7\%$ for the
598 natural aerosol emissions and AOD of individual aerosol species. The capability of the
599 assimilation system for inverse modeling applications based on the OSSE framework was
600 also investigated in that study. The authors showed that the addition of observations over
601 land improves the impact of the inversion more than the addition of observations over the
602 ocean (where there are fewer major aerosol sources), which indicates the importance of
603 reliable observations over land for inverse modeling applications. Observation data over land
604 provide information from around the source regions. The authors also showed that, for the
605

606 inversion experiments, the aerosol classification is very important over regions where
607 different aerosol species originate from different sources and that the fine- and coarse-mode
608 AODs are inadequate for identifying sulfate and carbonaceous aerosols, which are among the
609 major tropospheric aerosol species.

611 In general, the assimilation of different species has a strong influence on both assimilated and
612 non-assimilated species through the use of interspecies error correlations and through the
613 chemical model. Over the past few years, numerous measurements of different chemical
614 species have been made available from satellite instruments. Miyazaki et al. (2012) combined
615 observations of chemical compounds from multiple satellites through an advanced EnKF
616 chemical data assimilation system. NO₂, O₃, CO, and HNO₃ measurements from the OMI,
617 TES, MOPITT, and MLS satellite instruments (see Table 1) were assimilated into the global
618 CTM CHASER (Sudo et al., 2002). The authors demonstrated a strong improvement by
619 assimilating multiple species as the data assimilation provides valuable information on
620 various chemical fields. The analysis (OmF; Observation minus Forecast) showed a
621 significant reduction of both bias (by 85 %) and RMSE (by 50 %) against independent data
622 sets when data assimilation was used. The authors showed that [data assimilation of a](#)
623 [combination of different observations \(including multiple species\)](#) is a very effective way to
624 remove systematic model errors. It was pointed out that the chemical data assimilation
625 requires observations with sufficient spatial and temporal resolution to capture the
626 heterogeneous distribution of tropospheric composition. This can be achieved through the
627 combined use of satellite and surface in-situ data. Surface data may provide strong
628 constraints on the near-surface analysis at high resolution in both space and time.

630 3.2 Data assimilation in coupled chemistry meteorology models

631
632 Since CCMM are more recent than CTM, there are fewer applications of data assimilation
633 using the former. Nevertheless, there has been a growing number of applications with
634 CCMM over the past few years and several of those are summarized below. In addition, three
635 case studies are presented in greater detail in Section 5. Past applications of data assimilation
636 in CCMM may be grouped into two major categories: applications that used the 4D-Var data
637 assimilation system of the original meteorological model and applications that used a variety
638 of techniques (3DVar, Kalman filters) with the CCMM. Examples of the former approach
639 include applications using the Integrated Forecast System (IFS) of the European Centre for
640 Medium-range Weather Forecasts (ECMWF), whereas examples of the latter approach
641 include applications using WRF-Chem. One may also distinguish the assimilation of
642 chemical data in CCMM with and without feedbacks between the chemical and
643 meteorological variables. Clearly, data assimilation in a CCMM with chemistry/meteorology
644 feedbacks is more interesting; it may, however, be more challenging, as discussed in Section
645 6.

647 One of the first applications of data assimilation with a CCMM is the assimilation of vertical
648 profiles of ozone (O₃) concentrations obtained with the AURA/MLS into the
649 ARPEGE/MOCAGE integrated system (Semane et al., 2009). ARPEGE is a mesoscale
650 meteorological model and MOCAGE is the CTM that was coupled to ARPEGE for that
651 application; both models are developed and used by Meteo France. ARPEGE simulated O₃
652 transport and the O₃ concentrations were subsequently modified at prescribed time steps with
653 MOCAGE to account for O₃ chemistry. Data assimilation is performed routinely with
654 ARPEGE using 4D-Var and that approach was used to assimilate the O₃ data into ARPEGE.
655 The data assimilation resulted in better forecasting of wind fields in the lower stratosphere.

Supprimé : the

Supprimé : using

Supprimé : also

Supprimé : via data assimilation

Supprimé : ¶

San Jose and Pérez Carmaño of the Technical University of Madrid (UPM) also performed a multi-species data assimilation with a CTM. In their work, NO₂ and O₃ data from SCanning Imaging Absorption SpectroMeter for Atmospheric CHartography (SCIAMACHY) were assimilated into a simulation conducted with the Community Multiscale Air Quality CTM (CMAQ) of the U.S. Environmental Protection Agency. SCIAMACHY makes measurements in both nadir and limb modes, which allows the subtraction of stratospheric O₃ from the total O₃ column measurements to obtain tropospheric O₃ column estimates. Figure 1a shows an example of O₃ SCIAMACHY data for 01/08/2007. CMAQ was used here in combination with MM5 for the meteorological fields and applied to two domains covering the Iberian Peninsula with a grid spacing of 27 km and the central region of Spain including the Madrid metropolitan area with a grid spacing of 9 km. A vertical resolution with 23 layers was used in both MM5 and CMAQ. Results are presented here for the episode of 1 to 8 August 2007 (see Figure 1b). ¶

¶ The vertical profiles of NO₂ and O₃ were assimilated into the CMAQ simulation for each grid cell using the Cressman (1959) method. A comparison of model simulation results with and without data assimilation showed a slight improvement from 0.751 to 0.754 in the correlation between the hourly model simulation results and O₃ concentrations available from the surface monitoring network. The results show important differences in the Madrid region with the most important ones (up to 22 µg/m³) being located ov{... [1]

656
657 This general approach is also used in the chemical data assimilation conducted at ECMWF
658 with IFS with coupled chemistry since a 4D-Var data assimilation system is operational in
659 IFS. A presentation of this data assimilation system and its application for re-analyses at
660 ECMWF is presented in Section 5.1.
661

662 Flemming and Innes (2013) have assimilated SO₂ data from GOME2 using 4D-Var into a
663 version of IFS adapted for SO₂ fate and transport. SO₂ oxidation was treated with a first-
664 order gas-phase reaction with hydroxyl (OH) radicals and its atmospheric removal was
665 treated with a first-order scavenging rate. The approach was applied to the SO₂ plume of
666 volcanic eruptions. The simulation results showed improvements following data assimilation
667 for the plume maximum concentrations but there was a tendency to overestimate the plume
668 spread, which may be due to predefined horizontal background error correlations.
669

670 Innes et al. (2013) used data assimilation into IFS coupled to the MOZART3 CTM to
671 produce reanalysis of atmospheric concentrations of four chemical species, CO, NO_x, O₃, and
672 formaldehyde (HCHO), over an 8-year period. The 4D-Var system of IFS was used for the
673 assimilation of data obtained from 8 satellite-borne sensors for CO, NO₂ and O₃. HCHO
674 satellite data were not assimilated because retrievals were considered insufficient. In this
675 application, the influence of those chemical species on meteorological variables was not
676 taken into account, which is a major difference with the previous application of Semane et al.
677 (2009). The data assimilation results showed notable improvements for CO and O₃, but little
678 effect for NO₂, because of its shorter lifetime compared to those of CO and O₃.
679

680 Flemming et al. (2011) used IFS coupled with three distinct O₃ chemistry mechanisms,
681 including a linear chemistry, the MOZART3 chemistry (see above), and the TM5 chemistry.
682 Using the IFS 4D-Var system, they assimilated O₃ data from four satellite-borne sensors
683 (OMI, SCIAMACHY, MLS, and SBUV2) to improve the simulation of the 2008
684 stratospheric O₃ hole. Notable improvements were obtained with all three O₃ chemistry
685 mechanisms.
686

687 An earlier application was conducted by Engelen and Bauer (2011) with the Radiative
688 Transfer for the Television Infrared Observation Satellite Operational Vertical Sounder
689 (RRTOV) model of IFS, where CO₂ was treated as a tracer. A variational bias correction was
690 performed with radiance data from AIRS and IASI. The improvement in the radiative
691 transfer led to improved temperature values.
692

693 Several applications using data assimilation have been conducted with WRF-Chem.
694 Scientists at the National Center for Atmospheric Research (NCAR) have assimilated data
695 into WRF-Chem. The Goddard Aerosol Radiation and Transport (GOCART) module was
696 used; it includes several PM species, but does not treat gas-phase PM interactions. Liu et al.
697 (2011) assimilated AOD from MODIS to simulate a 2010 dust episode in Asia using
698 gridpoint statistical interpolation (GSI) (Wu et al., 2002; a 3D-Var method). The results of
699 the re-analyses showed improvement in AOD, when compared to MODIS (as expected) and
700 CALIOP (as a cross-validation), and in surface PM₁₀ concentrations when compared to
701 AERONET measurements. Chen et al. (2014) used a similar approach to improve
702 simulations of surface PM_{2.5} and organic carbon (OC) concentrations during a wild biomass
703 fire event in the United States. Meteorological data (surface pressure, 3D wind, temperature
704 and moisture) were assimilated in one simulation, whereas AOD MODIS data were in
705 addition assimilated in another simulation, both using 6-hour intervals. The AOD

706 assimilation significantly improved OC and PM_{2.5} surface concentrations when compared to
707 measurements from the Interagency Monitoring of PROtected Visual Environments
708 (IMPROVE) network. Jiang et al. (2013) also used GSI 3D-Var with WRF-Chem, but
709 assimilated surface PM₁₀ concentrations instead of satellite data. Their application over
710 China showed improvement in PM₁₀ concentrations; however, the benefit of the data
711 assimilation diminished within 12 hours because of the effect of atmospheric transport
712 (vertical mixing and horizontal advection), thereby suggesting the importance of assimilating
713 PM data aloft (e.g., AOD) and/or correcting emissions, which are the forcing function for PM
714 concentrations. Accordingly, Schwartz et al. (2012) used GSI 3D-Var to assimilate both
715 AOD from MODIS and PM_{2.5} surface concentrations into WRF-Chem to improve simulated
716 PM_{2.5} concentrations over North America. The use of 6-hour re-analyses for initialization led
717 to notable improvements when both satellite and surface data were assimilated. More
718 recently, Schwartz et al. (2014) assimilated the same AOD and PM_{2.5} surface concentration
719 data using two additional methods: the EnSRF and a hybrid ensemble 3D-Var method. All
720 three methods led to mostly improved forecasts, with the hybrid method showing the best
721 performance and 3D-Var generally showing better performance than the EnSRF. However,
722 the ensemble spread was considered insufficient and it was anticipated that a larger spread
723 would lead to better results for the ensemble and hybrid methods.

Supprimé : an ensemble square-root Kalman filter (

Supprimé :)

724
725 Scientists at the National Oceanic and Atmospheric Administration (NOAA) also used the
726 GSI 3D-Var method to assimilate data into WRF-Chem. Their version of WRF-Chem
727 offered a full treatment of gas-phase chemistry and PM. Pagowski et al. (2010) assimilated
728 both O₃ and PM_{2.5} surface concentrations over North America. Model performance improved,
729 but the benefits of data assimilation lasted only for a few hours. Pagowski and Grell (2012)
730 subsequently compared 3D-Var and the EnKF to assimilate PM_{2.5} surface concentrations into
731 WRF-Chem. They concluded that better performance was obtained with the EnKF. A WRF-
732 Chem case study with assimilation of surface data is presented in Section 5.2.

733
734 Saide et al. (2012a) developed the adjoint of the mixing/activation parameterization for the
735 activation of aerosols into cloud droplets of WRF-Chem and, using 3D-Var data assimilation
736 of MODIS data, they improved aerosol simulated concentrations. The important result in that
737 work was the ability to improve aerosol simulations using the assimilation of cloud droplet
738 number concentration data, which is only possible due to the coupled nature of WRF-Chem
739 that integrates aerosol indirect effects into the forecasts. Saide et al. (2013) also used a
740 modified GSI 3DVar to assimilate MODIS AOD data into WRF-Chem for a sectional
741 aerosol treatment and using the adjoint of the Mie computation for the AOD from aerosol
742 concentrations. Improvements in aerosol concentrations were obtained at most locations
743 when compared to measurements at surface monitoring sites in California and Nevada. The
744 study found that observationally constrained AOD retrievals resulted in improved
745 performance compared to the raw retrievals and that the use of multiwavelength AOD
746 satellite data led to improvements in the simulated aerosol size distribution. This assimilation
747 tool was further used in two studies. First, AOD from the GOCI sensor on board of COMS (a
748 geostationary satellite observing northeastern Asia) was combined with MODIS AOD
749 assimilation to show that future geostationary missions are expected to improve air quality
750 forecasts considerably when included into current systems that assimilate MODIS retrievals
751 (Saide et al., 2014). Second, AOD assimilation improved forecasts of Central America
752 biomass burning smoke and was further used to assess smoke impacts on a historical severe
753 weather outbreak in the southeastern U.S. (Saide et al., 2015). The smoke impacts were
754 related to aerosol-cloud-radiation interactions, thus this study was only possible via data
755 assimilation in a CCMM, highlighting the importance of further research and applications in

756 | [this area](#). Satellite data assimilation into WRF-Chem is presented as a case study in Section
757 5.3.

758
759 Data assimilation has been conducted with other CCMM. For example, Messina et al. (2011)
760 used OI to assimilate O₃ and NO₂ data into BOLCHEM, a one-way CCMM, applied over the
761 Po Valley. They used an OSSE approach and showed that NO₂ data assimilation was
762 successful in correcting errors due to NO_x emission biases. Furthermore, the benefit of the
763 data assimilation could exceed one day. However, the assimilation of NO₂ data increased the
764 O₃ bias at night because of the nocturnal O₃/NO₂ chemistry. The combination of O₃ and NO₂
765 assimilation helped resolve that night-time issue; however, the benefit disappeared after a
766 few hours due to the short lifetime of those air pollutants as discussed in Section 3.1.

767
768 [The treatment of interactions between aerosols and meteorology in the NASA Goddard Earth](#)
769 [Observing System \(GEOS-5\) model was shown to improve the simulations of the](#)
770 [atmospheric thermal structure and general circulation during Saharan dust events \(Reale et](#)
771 [al., 2011\) and the assimilation of MODIS-derived AOD was conducted in GEOS-5 with this](#)
772 [interactive aerosol/meteorology treatment \(Reale et al., 2014\).](#)

773 774 **3.3 Optimal monitoring network design**

775
776 Atmospheric chemistry (including PM) monitoring networks should ideally be designed
777 according to a rational criterion. Such a criterion (called the science criterion) would assess
778 the ability of the network to provide information in order to optimally estimate physical
779 quantities. The overall design criterion could also account for the investment and
780 maintenance costs of the network or for the technical sustainability and reliability of stations
781 (Munn, 1981). This overall design criterion that mixes all of these aspects can be devised in
782 the form of an objective scalar function evaluating network configuration.

783
784 The science criterion often judges the ability of the network to estimate instantaneous or
785 average concentrations, or the threshold exceedance of any relevant regulated species. The
786 estimation could rely on basic interpolation, more advanced kriging, or data assimilation
787 techniques (Müller, 2007). The latter would come with a very high numerical cost, since one
788 would have to perform a double (nested) optimization on the data assimilation control
789 variables, as well as on the potential station locations.

790
791 These ideas have been used in air quality to reduce an already existing ozone monitoring
792 network (Nychka and Saltzman, 1998; Wu et al., 2010) or to extend this network (Wu and
793 Bocquet, 2011). Ab nihilo station deployment, extension and reduction of networks lead to
794 problems of different nature. For instance, when extending a network one is forced to guess
795 physical quantities and their statistics on the new stations to be gauged, requiring a costly
796 observation campaign or a clever extrapolation from existing sites to tentative sites. The
797 mathematical criterion to evaluate the skills of the modeling system for a given network,
798 beyond the choice of the observed physical quantities, also calls for a choice of performance
799 metrics. Many attractive criteria have been proposed: root mean square errors of network-
800 based estimation of the field, information-theoretical based criteria, etc. Such criteria have
801 been investigated in atmospheric chemistry in many studies conducted by environmental
802 statisticians, more recently for instance by Fuentes et al. (2007) and Osses et al. (2013).
803 Nowadays, the network design issue also concerns the sparse ground networks of greenhouse
804 gases monitoring at meso and global scales (Rayner, 2004; Lauvaux et al., 2012), which in
805 our context can be seen mostly as tracers of atmospheric transport.

806
807 In meteorology, optimal network design is often studied in an Observing System Simulation
808 Experiment context, where the impacts of new predefined observations (e.g., data retrieval
809 from a future satellite) are evaluated rather than the optimal locations of future stations.
810 Nevertheless, the dynamic placement of new and informative observations (targeting) has
811 been investigated theoretically (Berliner et al. 1999; and many since then) and experimentally
812 in field campaigns such as the Fronts and Atlantic Storm-Track Experiment (FASTEX) of
813 Meteo France (<http://www.cnr.meteo.fr/dbfastex/ftxinfo/>) and the Observing System
814 Research and Predictability Experiment of the World Meteorological Organization
815 (THORPEX;
816 <http://www.wmo.int/pages/prog/arep/wwrp/new/THORPEXProjectsActivities.html>).
817 Although these adaptive observations were shown to be very informative in the case of severe
818 events, they are based on monitoring flights and hence are very costly, whereas other
819 observations are much more abundant and cheaper.

820
821 Targeting has been little investigated in atmospheric chemistry, but recent studies have
822 demonstrated its potential, especially in an accidental context (Abida and Bocquet, 2009). It
823 would certainly be interesting to use a coupled chemical/meteorological targeting system
824 since targeting of concentration observations could also require meteorological observations
825 at the same location for a proper assimilation of chemical concentrations into a CCMM.

826
827

828 **4. Observational data sets**

829

830 Observational data sets available for data assimilation and model performance evaluation
831 include mainly in situ observations, satellite data, and ground-based remote sensing data
832 (e.g., lidar data). Air quality observation systems include routine surface-based ambient air
833 and deposition networks, satellites, field campaigns, and programs for monitoring
834 background concentrations and long-range transport of pollutants.

835 **4.1 Non-satellite observations**

836 **4.1.1 Routine air quality monitoring in North America, Europe, and worldwide**

837 Dense networks of air quality monitors are available in North America and Europe. They
838 provide measurements with near real-time availability and a short one-hourly averaging
839 period. These aspects, together with the link to health policy, make these network
840 observations especially suitable for chemical data assimilation applications.

841 In Europe, air quality observations are made available through the Air Quality Database
842 (AirBase) of the European Environmental Agency (EEA). Access is provided to validated
843 surface data, with a delay of one to two years. These validated datasets are used primarily for
844 assessments (e.g., EEA, 2013). The delivery of (unvalidated) data in near-real time through
845 EEA for data assimilation purposes is receiving much attention recently and is under
846 development, stimulated by the development of the EU Copernicus Atmosphere Service. Key
847 species provided by AirBase (<http://www.eea.europa.eu/themes/air/air-quality/map/airbase>)
848 are PM₁₀, O₃, NO₂, NO, CO, and SO₂. Apart from these, measurements are available for
849 ammonium, heavy metals (lead), benzene, and others. Related to more recent EC directives
850 (e.g. Directive 2008/50/EC), member states are developing networks to measure PM_{2.5}, but
851 the number of sites with PM_{2.5} capability is presently significantly smaller (slightly more

852 than half) than those for PM₁₀.

853 It should be noted that PM measurements are often provided on a daily-mean basis, in
854 contrast to O₃ and NO₂, for which hourly values are reported. This is not ideal for data
855 assimilation purposes, where instantaneous observations are preferred. The classification of
856 the surface observations and representativeness of measurements for larger areas is
857 important, in order to allow meaningful comparisons of the observations with air quality
858 models (e.g., Joly and Peuch, 2012). For the measurements of NO₂ it should be realized that
859 in particular sensors with molybdenum converters make the measurement also sensitive to
860 other oxidized nitrogen compounds such as PAN and nitric acid (HNO₃) (e.g., Steinbacher et
861 al., 2007).

862 In the context of the Convention of Long-Range Transboundary Air Pollution, the European
863 Monitoring and Evaluation Programme (EMEP) provides data
864 (<http://www.nilu.no/projects/ccc/emepdata.html>) on a selection of sites in Europe, for O₃,
865 NO_x, VOC, SO₂, Hg, and aerosol (PM₁₀), including additional information on carbonaceous
866 PM and secondary inorganic aerosol, which is of use for model evaluation in Europe (e.g.
867 EMEP, 2012 ; Tørseth et al., 2012). Atmospheric deposition is measured for several chemical
868 species in the EMEP network.

869 In North America, surface measurements of O₃ and PM_{2.5} are accessible through the U.S.
870 EPA's AIRNow gateway (<http://www.airnowgateway.org>). For a comprehensive description
871 of air quality observation systems over North America, we refer the reader to a report
872 (NSTC, 2013), which is available at
873 <http://www.esrl.noaa.gov/csd/AQRS/reports/aqmonitoring.pdf>. This report focuses on
874 observations in the United States, but also provides succinct information on observations in
875 Canada and Mexico.

876 Over 1300 surface stations measure hourly concentrations of O₃ using a UV absorption
877 instrument (Williams et al., 2006). The instrument error is bounded by ±2% of the
878 concentration. The majority of the measurement sites are located in urban and suburban
879 settings. The highest density of monitors is found in the eastern U.S., followed by California
880 and eastern Texas, while observations are relatively sparse in the center of the continent.
881 Hourly PM_{2.5} concentrations are measured at over 600 locations using Tapered Element
882 Oscillating Microbalance instruments (TEOM, Thermo Fisher, Continuous particulate
883 TEOM monitor, Series 1400ab, product detail, 2007, available at
884 <http://www.thermo.com/com/cda/product/detail/1,10122682,00.html>). The uncertainty of
885 PM_{2.5} measurements is calculated as 1.5 μg m⁻³ plus an inaccuracy of 0.75% times the
886 species concentration. We caution that much larger measurement errors can occur, depending
887 on meteorological conditions, because of the volatility of some aerosol species (Hitzenberger
888 et al., 2004). Geographic distribution of PM_{2.5} measuring sites is similar to that of the O₃
889 sites.

890 Concentrations of the remaining criteria pollutants (NO₂, CO, SO₂, Pb, and PM₁₀) are
891 measured at several hundred locations across the continent at varying frequencies and
892 averaging periods.

893 The IMPROVE network measures major components of PM_{2.5} (sulfate, nitrate, organic and
894 elemental carbon fractions, and trace metals) at over 100 locations in national parks and in
895 rural settings. Complementary aerosol measurements in urban and suburban locations are
896 available at more than 300 EPA's STN speciation sites. IMPROVE and STN sites typically

897 collect 24-hour samples every three days. Since those PM_{2.5} samples are collected on filters
898 and need to be sent to analytical laboratories for analysis, data are not available in near real-
899 time. Continuous aerosol species concentrations are only occasionally measured by the
900 industry-funded SEARCH network, which operates eight sites in the southeastern U.S.
901 In addition, toxics are monitored by the NATTS network sampling at 27 locations for 24
902 hours every six days. The NADP, IADN, and CASTNET networks track atmospheric wet
903 and dry deposition.

904
905 At the global scale, monitoring of atmospheric chemical composition was organized by the
906 World Meteorological Organization (WMO) Global Atmospheric Watch (GAW) program
907 about 25 years ago. The GAW program currently addresses six classes of variables (O₃, UV
908 radiation, greenhouse gases, aerosols, selected reactive gases, and precipitation chemistry).
909 The surface-based GAW observational network comprises global and regional stations,
910 which are operated by WMO members. These stations are complemented by various
911 contributing networks. Currently, the GAW program coordinates activities and data from 29
912 global stations, more than 400 regional stations, and about 100 stations operated by
913 contributing networks. All observations are linked to common references and the
914 observational data are available in the designated World Data Centers. Information about the
915 GAW stations and contributing networks is summarized in the GAW Station Information
916 System (GAWSIS; <http://gaw.empa.ch/gawsis/>).

917 **4.1.2 Other surface-based, balloon, and aircraft observations**

918 Other types of observations that can be assimilated into atmospheric models include surface-
919 based remote sensing data, such as lidar data, balloon-borne sounding systems (sondes), and
920 aircraft observations.

921 Lidar data

922 The GAW Aerosol Lidar Observation Network (GALION) provides information on the
923 vertical distribution of aerosols through advanced laser remote sensing in a network of
924 ground-based stations. Several regional lidar networks, such as the Asian Dust and Aerosol
925 Lidar Observation Network (AD-Net), the Latin America Lidar Network (ALINE), the
926 Commonwealth of Independent States (Belarus, Russia and Kyrgyz Republic) Lidar
927 NETWORK (CIS-LINET, the Canadian Operational Research Aerosol Lidar Network
928 (CORALNet), CREST funded by NOAA and run by the City University of New York
929 covering eastern North America, the MicroPulse Lidar NETWORK (MPLNET) operated by
930 NASA, the European Aerosol Research Lidar Network (EARLINET), and the Network for
931 the Detection of Atmospheric Composition Change (NDACC), Global Stratosphere are
932 participants in GALION. Some of these regional lidar networks are described in greater
933 detail below.

934
935 MPLNET is a global lidar network of 22 stations operated by NASA with lidars collocated
936 with the photometers of the NASA AERONET. The Network for the Detection of
937 Atmospheric Composition Change (NDACC) is operated by NOAA. It includes a network of
938 about 30 lidars located world-wide. AD-Net gathers 13 research lidars that cover East Asia
939 and operate continuously. The National Institute for Environmental Studies (NIES) operates
940 a lidar network in Japan (<http://www-lidar.nies.go.jp>). Initiated in 2000, EARLINET now
941 operates a set of 27 research lidar stations over Europe and is part of the Europe-funded
942 ACTRIS network (<http://actris.nilu.no>). Following the eruption of the Eyjafjallajökull

943 volcano in 2010 (Chazette et al., 2012), weather operational centers such as Meteo France
944 and the UK MetOffice are planning to deploy automatic operational lidar networks over
945 France and the United Kingdom, with the objective to deliver continuous measurements and
946 to use them in aerosol forecasting systems.

947
948 In order to be assimilated into an aerosol model, the raw aerosol signal can either be
949 converted into aerosol concentrations using assumptions on their distribution (Raut et al.,
950 2009a, 2009b, Wang et al., 2013), or it can be assimilated directly into the model solving the
951 lidar equation within the observation operator (Wang et al., 2014). Note that even in the latter
952 case, the redistribution over the aerosol size bins is carried out following the size
953 distributions of the first guess used in the analysis. It is expected that the benefit of
954 assimilating lidar signals is to last longer (up to a few days) and should propagate farther than
955 ground-based in situ measurements, owing to this height-resolved information but also owing
956 to the smaller representativeness error in elevated layers. This has recently been
957 demonstrated using lidar data from three days of intensive observations over the western
958 Mediterranean Basin in July 2012 (Wang et al., 2014b).

959 Aerosol optical properties

961 A world-wide routine monitoring of aerosol optical depth and other properties like the
962 Ångström component is provided by the photometers of the Aerosol Robotic Network
963 (AERONET, <http://aeronet.gsfc.nasa.gov>) coordinated by NASA (e.g., Holben et al. 1998).

964 The GAW aerosol network also provides measurements of aerosol properties over the globe.
965 The GAW in-situ aerosol network contains now more than 34 regional stations and 54
966 contributing stations, in addition to 21 global stations, reporting data – some of them in near-
967 real-time – to the World Data Center for Aerosols (WDCA) hosted by the Norwegian Center
968 for Air Research (NILU) and available freely to all. The GAW-PFR network for aerosol
969 optical depth (AOD), coordinated by the World Optical Depth Research and Calibration
970 Center (WORCC), includes 21 stations currently providing daily data to WORCC (GAW,
971 2014).

972 SKYNET is a network of radiometers mainly based in Eastern Asia and the database is
973 hosted by Chiba University in Japan (<http://atmos.cr.chiba-u.ac.jp>).

974 Aircraft measurements

975 In Europe, routine monitoring of the atmosphere is provided by the IAGOS (In-service
976 Aircraft for a Global Observing System) program (<http://www.iagos.org>). An increasing
977 number of aircraft is equipped to measure O₃, water vapor, and CO and instruments are
978 developed to measure NO_x, NO_y and CO₂. This initiative evolved from the successful
979 MOZAIC (Measurements of OZone, water vapor, CO, NO_x by in-service AIRbus airCraft,
980 <http://www.iagos.fr/web/rubrique2.html>) project with links to the CARIBIC
981 (<http://www.caribic-atmospheric.com>) project. In North America, NOAA-ESRL has a
982 Tropospheric Aircraft Ozone Measurement Program consisting of O₃ measurements
983 (<http://www.esrl.noaa.gov/gmd/ozwv/>) and a flask sampling program, measuring greenhouse
984 gases including CO (<http://www.esrl.noaa.gov/gmd/ccgg/aircraft/>).

985 Despite the limited coverage, aircraft chemical observations have the potential to provide
986 important improvements to models when assimilated (Cathala et al., 2003).

987 Ozone sondes

988 Balloon-borne measurements of O₃ are performed on a global scale and the data are collected
989 by the World Ozone and Ultraviolet Radiation Data Centre (WOUDC,
990 http://www.woudc.org/index_e.html). The sondes provide very detailed vertical profiles from
991 the surface to about 30-35 km altitude, with an accuracy of 5-10% (Smit et al., 2007). Apart
992 from monitoring the stratospheric O₃ layer, the data are extensively used to validate global
993 tropospheric models as well as regional air quality models.

994 Other sources of tropospheric composition information

995 Surface-based Multi-AXis Differential Optical Absorption Spectroscopy (MaxDOAS)
996 measurements are very interesting for atmospheric chemistry applications, because of their
997 ability to deliver approximately boundary-layer mean concentrations of O₃, NO₂, HCHO,
998 glyoxal (CHOCHO), SO₂, halogens and aerosols. Measurements are provided at several sites,
999 but a large-scale network is still missing.

1000 Some regional networks of ceilometer observations exist (e.g., UK Met Office, Deutscher
1001 Wetterdienst, Météo France). They provide mostly cloud base and cloud layer data. They
1002 may in some cases (e.g., volcanic plumes) provide useful information on atmospheric
1003 aerosols.

1004 The Network for the Detection of Atmospheric Composition Change (NDACC,
1005 <http://www.ndacc.org>) provides measurements relevant to evaluate tropospheric composition
1006 models, such as lidar data, O₃ sondes and MaxDOAS.

1007 Apart from ozone sondes, WMO Global Atmospheric Watch (GAW,
1008 http://www.wmo.int/pages/prog/arep/gaw/gaw_home_en.html) coordinates a variety of
1009 atmospheric observations and the data are provided through the World Data Centres. The
1010 Earth System Research Laboratory (ESRL) of NOAA provides access to a host of routine
1011 observations and links to field campaigns.

1012 For greenhouse gases, the WMO-GAW World Data Centre for Greenhouse Gases (WDCGG,
1013 <http://ds.data.jma.go.jp/gmd/wdogg/>) provides access to data with a global coverage. The
1014 Global Greenhouse Gas Reference Network (<http://www.esrl.noaa.gov/gmd/ccgg/ggrn.php>)
1015 of NOAA provides a backbone of world-wide observations. Data from the Total Carbon
1016 Column Observing Network (TCCON, <http://www.tcon.caltech.edu>) is used extensively to
1017 validate greenhouse gas assimilation and inversion systems as well as satellite data.

1018 Dedicated measurement campaigns are essential additions to the more routine capabilities
1019 discussed above. Such campaigns provide dense observations of a larger number of species
1020 and/or aerosol components with profiling capabilities and often in combination with surface
1021 in-situ and remote sensing. This provides excellent tests for multiple aspects of the models.
1022 Examples are the TRACE-P (Talbot et al., 2003; Eisele et al., 2003) and ICARTT
1023 (Fehsenfeld et al., 2006), the data of which have been used in assimilation studies.

1024 **4.2 Satellite observations**

1025 For atmospheric chemistry modeling and assimilation, the relevant species measured from
1026 space are NO₂, CO, SO₂, HCHO, CHOCHO, O₃, and aerosol optical properties (optical depth

Supprimé : The primary agencies/organizations in North America and Europe that launch and operate satellites used in the remote sensing of air quality include the National Aeronautics and Space Administration (NASA), the National Oceanic and Atmospheric Administration (NOAA), the Canadian Space Agency (CSA), the European Space Agency (ESA), the French Centre National d'Études Spatiales (CNES), and the Swedish Space Corporation (SSC). In Asia, the Japanese Aerospace Exploration Agency (JAXA) and the Korean Aerospace Research Institute (KARI) contribute to the global observing system, with recent contributions from the China National Space Administration (CNSA). ¶

1027 and other properties, aerosol backscatter profiles). The main tropospheric satellite products
1028 are listed in Table 1 and the acronyms are expanded in Table 2.

1029
1030 The satellite instruments listed in Table 1 are all on polar-orbiting satellites with a fixed
1031 overpass time. The huge benefit of satellite instruments is the large volume of data. For
1032 instance, an instrument like OMI provides a full global coverage each day with a mean
1033 resolution of about 20 km, see Figure 1. The fact that area-averages are observed, as opposed
1034 to the point measurements of the surface networks, has the advantage that the retrieved
1035 quantities can be more easily compared to model grid cell value, and the representation error
1036 is often smaller than for point observations. Another advantage of the satellite data is the
1037 sensitivity to concentrations in the free troposphere, although retrieving the vertical
1038 distribution of the concentrations may in some cases be challenging. Air quality models are
1039 typically evaluated against surface measurements and their performance inside and above the
1040 planetary boundary layer is generally not well known.

Supprimé : 2

1041
1042 On the other hand, satellite data have limitations. Currently, only one observation per day or
1043 less is available, as compared to the hourly data from the routine surface networks and there
1044 is only limited information on the diurnal cycle. Most instruments provide about one piece of
1045 vertical information in the troposphere and this information is averaged over an extended
1046 vertical range: typically a total column or average free tropospheric value is retrieved.
1047 Furthermore, there are error correlations among nearby pixels, which typically requires the
1048 application of thinning methods.

1049
1050 The retrieval of trace gases in the troposphere is far from trivial, because of the dependence
1051 on clouds, aerosols, surface albedo, thermal contrast, and other trace gases. Errors in the
1052 characterization of these interfering aspects will result in sometimes substantial systematic or
1053 quasi random errors. Furthermore, the detection limit of minor trace gases may exceed
1054 typical atmospheric concentrations (e.g., SO₂ and HCHO over Europe). More work is needed
1055 to continuously improve existing retrieval algorithms concerning the systematic errors and
1056 detection limits.

1057
1058 Many of the satellites listed in Table 1 are already past their nominal lifetime. Future follow-
1059 up missions are discussed and coordinated internationally (IGACO 2004; CEOS-ACC, 2011;
1060 GEOS, 2014; GCOS, 2010 & 2011). In Europe, the EU Copernicus program will facilitate
1061 the launch of a series of satellite missions, the Sentinels. Sentinels number 4 and 5 will
1062 provide observations of atmospheric composition. The sentinel 5 precursor mission with the
1063 TROPOMI instrument (Veefkind et al., 2012), a successor of OMI with 7 km resolution, will
1064 fill a possible gap between the present generation of instruments (see Table 1) and the next
1065 generation of satellite instruments.

Supprimé : sed

1066
1067 An international geostationary constellation of satellites to observe air quality is in
1068 preparation. This will consist of the [European Space Agency \(ESA\)](#) Sentinel 4 over Europe
1069 (Ingmann et al., 2012), the [Korean Aerospace Research Institute \(KARI\)](#) GEMS satellite
1070 over Asia (http://eng.kari.re.kr/sub01_01_02_09), and the [National Aeronautics and Space](#)
1071 [Administration \(NASA\)](#) TEMPO mission over America (Chance et al., 2013). These
1072 missions will provide unprecedented high-resolution measurement of air pollution with
1073 hourly observations from space (e.g. Fishman, 2008).

1074
1075 Most retrieval products for the satellite sensors listed in Table 1 are based on the general
1076 retrieval theory detailed by Rodgers (2000). Retrievals of atmospheric trace gas profiles are

1077 fully specified by providing the retrieved profile, the averaging kernel, the covariance matrix
1078 and the a priori profile. The assimilation observation operator, which relates the model
1079 profile x_{model} to the retrieved profile, is then:

$$x_{r,model} \approx x_{a-priori} + \mathbf{A}(x_{model} - x_{a-priori})$$

1083 The retrieval covariance describes the observation errors. The kernel and covariance together
1084 describe the altitude dependence of the sensitivity of the measurement to the concentrations,
1085 the degree of freedom of the signal and the intrinsic vertical resolution of the observation.
1086 Kernels and covariances are not always provided by the retrieval teams, which will result in a
1087 loss of information. Even the popular Differential Optical Absorption Spectroscopy (DOAS)
1088 retrieval approach for total columns may be reformulated in Rodgers' terminology and
1089 averaging kernels can be defined (Eskes and Boersma, 2003).
1090

1091 **4.3 Use of observations in chemical data assimilation**

1092 Combining satellite datasets through data assimilation is a powerful approach to put multiple
1093 constraints on the chemistry/aerosol model. An example is MACC-II, where most of the
1094 satellite datasets on O₃, CO, NO₂, AOD/backscatter, CO₂ and CH₄, as listed in Table 1, are
1095 used (e.g. Inness et al., 2013). Another example is a recent study (Miyazaki et al., 2014),
1096 where satellite observations of NO₂, O₃, HNO₃, and CO from OMI, MLS, TES and MOPITT
1097 are combined to constrain the production of NO_x by lightning. The use of satellite retrievals
1098 in assimilation applications focused on top-down emission estimates was recently reviewed
1099 (Streets et al., 2013).
1100

1102 For the use of satellite and surface/in-situ/remote sensing data in operational applications
1103 such as MACC-II, the availability of data in near-real time is an important requirement.
1104

1105 For regional air quality, the major source of information is provided by the routine surface
1106 observations, which have been put in place to monitor air quality regulations. In the USA,
1107 Europe and in parts of Asia (Japan), dense observations networks are in place. For
1108 concentrations above the surface, the monitoring network is very sparse, with a limited
1109 amount of aircraft, sonde and surface remote sensing data points. Several groups have started
1110 to incorporate satellite data to constrain tropospheric concentrations. One major aspect here
1111 is the lack of diurnal sampling, which is addressed by future geostationary missions, as
1112 discussed above. Furthermore, the number of species observed routinely from space, or from
1113 the ground, is limited, and dedicated campaigns (e.g. with aircraft) are crucial to test more
1114 model aspects. A more systematic approach to this sparseness of above-surface information
1115 would be important to improve the regional air quality models and to bridge the gap between
1116 global and regional scale modeling.
1117

1118 Recommendations for global observing systems are discussed internationally. The WMO-
1119 GAW IGACO report provides a useful overview of existing and planned satellite missions
1120 and the complementary surface, balloon and aircraft observations (IGACO, 2004). GCOS
1121 discusses the observations needed to monitor the essential climate variables (GCOS,
1122 2010+2011). The Group on Earth Observations (GEO) is coordinating efforts to build a
1123 Global Earth Observation System of Systems, or GEOSS
1124 (<http://www.earthobservations.org/geoss.shtml>), on the basis of a 10-year implementation
1125 plan. The Committee on Earth Observation Satellites (CEOS) supports GEO and has an
1126 activity on Atmospheric Composition Constellation (ACC). The CEOS ACC White Paper

1127 (CEOS-ACC, 2011) discusses the Geostationary Satellite Constellation for Observing Global
1128 Air Quality. Gaps in observing atmospheric composition are discussed in these international
1129 activities.

1130
1131 In many parts of the world, pollutant emissions are dominated by the smoke from fires. The
1132 occurrence and strength of the fires is intrinsically unpredictable, which makes these a major
1133 source of errors in the models. Recently, satellite observations of fire radiative power and
1134 burned area have been used to estimate emissions of aerosols, organic and inorganic trace
1135 gases (Giglio et al., 2013). For instance, within the MACC-II project a near-real time global
1136 fire product was developed with a resolution of 0.1 degree, which is used for reanalyses,
1137 nowcasting and even forecasting (Kaiser et al., 2012). Given the importance of fires, the use
1138 of such fire emission estimates based on observations is recommended.

1139
1140 Sand and dust storms may contribute significantly to PM (mostly PM₁₀) ambient
1141 concentrations at long distances from their source region. Because the emission source terms
1142 of sand and dust storm events are difficult to quantify, aerosol data assimilation is a
1143 promising area for sand and dust storm modeling and forecasting (SDS-WAS, 2014). The
1144 main efforts have focused on the assimilation of retrieval products (i.e. atmospheric
1145 parameters inferred from raw measurements), such as AOD retrieved from satellite
1146 reflectance or from ground-based sun photometer measurements. However, the difficulties
1147 associated with the operational use of lidar (and potentially ceilometer) observations as well
1148 as satellite aerosol vertical profiles, is the most limiting aspect in data assimilation to
1149 improve sand/dust forecasts. Although there are some initial promising non-operational
1150 experiments to assimilate aerosol vertical profiles (e.g., at the Japan Meteorological Agency),
1151 more efforts are needed to better represent the initial vertical dust structure in the models.

1152
1153 In numerical weather prediction, a significant step in forecast skill was achieved when the
1154 assimilation of retrieval products was replaced by the assimilation of satellite radiances. In
1155 this way a loss of information or introduction of biases through the extra retrieval process is
1156 avoided. It should be noted, however, that early retrievals often did not follow the full
1157 retrieval theory (Rodgers, 2000) and it is important to use the kernels, covariances and a-
1158 priori profiles in the observation operator and error matrices. Because of this success it has
1159 been debated whether to apply similar radiance assimilation approaches to the atmospheric
1160 chemistry satellite observations. We do not in general recommend such radiance assimilation
1161 approach for atmospheric composition applications for the following reasons. First, a
1162 successful radiance assimilation depends crucially on knowledge of the possible systematic
1163 biases of the instruments, a clever choice of microwindows, and state-of-the-art radiative
1164 transfer modelling. Secondly, a careful implementation of Rodgers formalism preserves the
1165 information of the satellite data, and there is a theoretical equivalence between the
1166 assimilation of retrievals and the assimilation of radiances (Migliorini, 2012). Third,
1167 retrievals can be stored in an efficient way, which avoids dealing with the large volumes of
1168 radiance data provided by the satellite instruments (Migliorini, 2012).

1169 1170 1171 **5. Case Studies**

1172
1173 In this section, four case studies are presented. The first three pertain to the
1174 assimilation of chemical concentrations for forecasting or re-analysis. The fourth one
1175 highlights inverse modeling to improve emission inventories; although it is performed
1176 with a CTM, it is relevant to CCMM as well.

1177
1178
1179
1180
1181
1182
1183
1184
1185
1186
1187
1188
1189
1190
1191
1192
1193
1194
1195
1196
1197
1198
1199
1200
1201
1202
1203
1204
1205
1206
1207
1208
1209
1210
1211
1212
1213
1214
1215
1216
1217
1218
1219
1220
1221
1222
1223
1224
1225
1226

5.1 Case Study from ECMWF: MACC re-analysis of atmospheric composition

An important application of data assimilation techniques is to produce consistent 3D gridded data sets of the atmospheric state over long periods. These meteorological re-analyses are widely used for climatological studies and more specifically to drive offline CTM. Meteorological re-analyses have been produced by several centres such as the National Centers for Environmental Prediction (NCEP; Kalnay et al. 1996), ECMWF (Gibson et al., 1997; Uppala et al., 2005, Dee et al., 2011), the Japan Meteorological Agency (JMA; Onogi et al., 2007) and the Global Modeling and Assimilation Office (Schubert et al., 1993).

Atmospheric composition, apart from water vapor, is typically not covered in these re-analysis data sets. Only stratospheric O₃ has been included in ECMWFs ERA-40 (Dethof and Hól m, 2004) and ERA-Interim (Dragani, 2011).

The availability of global satellite retrievals of reactive traces gases and aerosols from satellites such as ENVISAT, Aura, MLS, Metop, Terra and Aqua over the last two decades made it possible to produce a re-analysis data set with emphasis on atmospheric composition. Within the Monitoring Atmospheric Composition and Climate (MACC) and the Global and regional Earth-system Monitoring using Satellite and in-situ data (GEMS) project (Hollingsworth et al., 2008), the Integrated Forecasting System (IFS) of ECW MF, which had been used to produce the ERA40 and ERA-Intrim meteorological re-analysis, was extended to simulate chemically reactive gases (Flemming et al. 2009), aerosols (Morcrette et al. 2009; Benedetti et al. 2008) and greenhouse gases (Engelen et al. 2009), so that ECMWF's 4D-Var system (Courtier et al. 1994; Rabier et al., 2000) could be used to assimilate satellite observations of atmospheric composition together with meteorological observations at the global scale.

The description of the MACC model and data assimilation system and an evaluation of the MACC re-analysis for reactive gases are given by Inness et al. (2013) in full detail. The MACC system follows closely the configuration of the ERA-Interim re-analysis (Dee et al., 2011). Meteorological observations from the surface and sonde networks as well as meteorological satellite observations were assimilated together with satellite retrievals of total column and O₃ profiles, CO total columns, AOD and tropospheric columns of NO₂. The MACC re-analysis has a horizontal resolution of about 80 km (T255) for the troposphere and the stratosphere and covers the period 2003-2012.

The MACC system assimilated more than one observation data set per species if multiple data were available. For example, O₃ profile retrievals from MLS were assimilated together with O₃ total column retrievals from OMI, SBUV-2 and SCIAMACHY to exploit synergies of different instruments (Flemming et al. 2011). To reduce detrimental effects of inter-instrument biases, the variational bias correction scheme (Dee and Uppala, 2009) developed for the meteorological assimilation was adapted to correct multiple atmospheric composition retrievals.

In the context of the 4D-Var approach, it would have been possible to use the information content of the atmospheric composition retrievals to correct the dynamic fields as demonstrated by Semane et al. (2009). However, earlier experiments (Morcrette, 2003) with IFS did not show a robust benefit for the quality of the meteorological fields. Therefore, this feedback was disabled in the MACC re-analysis. A major issue in this respect would be the

1227 correct specification of the complex error covariance between meteorological fields and
1228 atmospheric composition. Also, no error correlation between different chemical species and
1229 between chemical and meteorological variables was considered.

1230
1231 While the assimilation of radiance observations was the preferred choice for the
1232 meteorological satellite observations, only retrievals of atmospheric composition total
1233 columns or profile or AOD were assimilated. Ground-based and profile in-situ observations
1234 of atmospheric composition were not assimilated but used to evaluate the MACC re-analysis.
1235 The National Meteorological Center (NMC) method (Parrish and Derber 1992) was used to
1236 estimate initial background error statistics for the atmospheric constituents apart from O₃ for
1237 which an ensemble method was applied (Fisher and Anderson, 2001).

1238
1239 A key issue for chemical data assimilation with the MACC system is the limited vertical
1240 signal of the retrievals from the troposphere, in particular from near the surface where the
1241 highest concentrations of air pollutants occur. Further, the assimilation of AOD does only
1242 constrain the optical properties of total aerosols but not of individual aerosol components. It
1243 is therefore important that the assimilating model, i.e., IFS, can simulate the source and sink
1244 terms in a realistic way. As shown by Huijnen et al. (2012), the chemical data assimilation of
1245 total column CO and AOD greatly improved the realism of the vertically integrated fields
1246 during a period of intensive biomass burning in Western Russia in 2010. However, the
1247 biggest improvement with respect to surface measurements was achieved by using a more
1248 realistic biomass burning emissions data set (GFAS, Kaiser et al. 2012).

1249
1250 The MACC re-analysis is a widely used data set which is freely available at
1251 <http://www.copernicus-atmosphere.eu>. It has been used to provide realistic boundary
1252 conditions for regional air quality models (e.g. Schere et al., 2012; Zyryanov et al., 2012).
1253 To demonstrate the long-range transport, Figure 2 shows a cross section of the zonal CO flux
1254 at 180 E averaged over the 2003-2012 period in the top panel. The bottom panel shows the
1255 time series of the monthly averaged meridional CO transported over the Northern Pacific
1256 (20N-70N, 180 E, up to 300 hPa) for the whole period. The MACC re-analysis was used to
1257 diagnose the anomalies of the inter-annual variability of global aerosols (e.g. Benedetti et al.
1258 2013) and CO (Flemming and Inness, 2014). Finally, the MACC AOD re-analysis was
1259 instrumental to estimate aerosol radiative forcing (Bellouin et al. 2013) and was presented in
1260 the Fifth Assessment Report of the Intergovernmental Panel on Climate Change (IPCC,
1261 2013). As pointed out by Inness et al. (2013), the changes in the assimilated retrieval
1262 products from different instruments, namely CO and O₃, during the 2003-2012 period as well
1263 as the rather short period of 10 years requires caution if the MACC-re-analysis is used to
1264 estimate long-term trends.

Supprimé : 3

1265 5.2 Ground-level PM_{2.5} data assimilation into WRF-Chem

1267
1268 In the following, we demonstrate an application of the EnKF (Whitaker and Hamill, 2002) to
1269 assimilate surface fine particulate matter (PM_{2.5}) observations with the WRF-Chem model
1270 (Grell et al., 2005) over the eastern part of North America. The modeling period began on 23
1271 June 2012, ended on 06 July 2012, and included a five-day spin-up period. During this
1272 modeling period, weather over the area of interest was influenced by a Bermuda high
1273 pressure system that contributed to the elevated concentrations of PM_{2.5}. For an illustration of
1274 such conditions, Figure 3 shows 24-hour average PM_{2.5} concentrations at AIRNow sites for
1275 June 29 and July 05 obtained by hourly assimilation of AIRNow observations.

Supprimé : 4

1277 PM_{2.5} observations used in the assimilation come from the U.S. EPA AIRNow data exchange
1278 program (see Section 4). Standard meteorological upper air and surface observations were
1279 also assimilated.

1280 The grid resolution of the simulations is equal to 20 km. Initial and lateral boundary
1281 conditions for meteorology were obtained from the global GFS ensemble that has been
1282 operational at NCEP since May 2012. The length of ensemble forecasts limited the extent of
1283 our forecasts to nine hours. Lateral boundary conditions for chemical species were obtained
1284 from a global CTM (MOZART) simulation (Emmons et al., 2010). Pollution by forest fires
1285 was derived from the Fire emission INventory from NCAR (FINN, Wiedinmyer et al., 2011).
1286 Parameterization choices for physical and chemical processes and specification of
1287 anthropogenic emissions follow those described by Pagowski and Grell (2012) (except for
1288 emissions of SO₂ for 2012 reduced by 40% as recommended by Fioletov et al., 2011). The
1289 reader is referred to previous work for details given therein (Pagowski and Grell, 2012).

1290 The six-hour assimilation cycle at 00z, 06z, 12z, and 18z used a one-hour assimilation
1291 window for PM_{2.5} and a three-hour assimilation window for meteorological observations.

1292 Two numerical experiments were performed:

1293 - NoDA – that included assimilation of meteorological observations only; and

1294 - EnKF –that included assimilation of both AIRNow PM_{2.5} and meteorological observations.
1295 The increments to individual PM_{2.5} species were distributed according to their a
1296 priori contributions to the total PM_{2.5} mass. For the GOCART aerosol module (Chin
1297 et al., 2000, 2002; Ginoux et al., 2001) employed in the simulations, this approach
1298 yields better results compared to using individual aerosol species as state variables
1299 in the EnKF procedure.

1300 Verification statistics presented below were calculated over the period starting at 00Z June
1301 28 and ending at 00Z July 07, 2012.

1302 In Figure 4, bias and temporal correlation of forecasts interpolated to measurement locations
1303 are shown for the two experiments. In calculating these verification statistics, all available
1304 forecasts were matched with corresponding observations. We note that the data assimilation
1305 significantly reduces negative model bias observed over most of the area of interest. A
1306 marked improvement in temporal correlation due to the assimilation, in places negative for
1307 NoDA, is also apparent.

Supprimé : 5

1308 In Figure 5, time series of bias and spatial correlation of forecasts are shown. It is noteworthy
1309 that the effect of meteorological observation assimilation on PM_{2.5} statistics is rather minor.
1310 That is both a result of the scarcity of PBL profiles available for the assimilation and
1311 difficulties in assimilating surface observations. A large positive impact of PM_{2.5} data
1312 assimilation on PM_{2.5} concentrations is confirmed in Figure 4, but forecast quality
1313 deteriorates quickly. Causes for such deterioration include deficiencies of the initial state
1314 resulting from the lack of observations of the individual PM_{2.5} species and their vertical
1315 distribution, and errors due to inaccuracies in chemical and physical parameterizations and
1316 inaccuracies of emission sources. The application of the GOCART aerosol parameterization
1317 was only dictated by computational requirements of ensemble simulations. Investigation on
1318 whether more sophisticated parameterizations of aerosol chemistry maintain the quality of
1319 forecasts for a longer period is on-going. Fast deterioration of forecasts suggests that, short of
1320 improving the model formulation and/or the emissions inventory, parameterization of model
1321 errors within the ensemble and post-processing of forecasts might provide an avenue for
1322 better PM_{2.5} prediction.

Supprimé : 6

Supprimé : observed

Supprimé : 5

Supprimé : is further confirmed

Mis en forme : Indice

Supprimé : it is apparent that

1323
1324
1325
1326
1327
1328
1329
1330
1331
1332
1333

5.3 Satellite data assimilation into WRF-Chem

The Gridpoint Statistical Interpolation (GSI) system (Kleist *et al.*, 2009), which uses a 3D-Var approach, is applied here to perform data assimilation experiments using satellite data to improve the initial aerosol state for the WRF-Chem (Grell *et al.*, 2005) model when utilizing the MOSAIC aerosol model (Zaveri *et al.*, 2008). We present two case studies, which correspond to the use of AOD (Saide *et al.*, 2013) and cloud number droplet satellite retrievals (N_d) (Saide *et al.*, 2012a). The WRF-Chem configuration is based on Saide *et al.* (2012b).

Assimilating AOD retrievals. In this case study, simulations were performed over California, USA, and its surroundings assimilating AOD retrievals. Figure 6 shows results when assimilating two 550 nm AOD retrievals, the MODIS dark target (Remer *et al.*, 2005), and the NASA neural network retrieval (<http://gmao.gsfc.nasa.gov/forecasts/>), which corrects biases with respect to AERONET (Holben *et al.*, 2001) and filters odd retrievals. The experiment shows that the AOD assimilation is able to correct the biases in the forward model providing a better agreement to AQS $PM_{2.5}$ observations and AERONET AOD measurements. $PM_{2.5}$ concentrations show low bias one hour after assimilation and then the assimilation gradually returns towards concentrations and errors found when no assimilation is performed getting close to it after 48 hours. Figure 6 also shows that the observationally constrained retrieval generally provides better results than the non-corrected AOD. An extreme case is where the dark target retrieval has problems due to the bright surfaces (Figure 6, bottom-right panel) deteriorating model performance and the corrected retrieval is able to partially fix the problem.

Supprimé : 7

Supprimé : 7

Supprimé : 7

1347
1348
1349
1350
1351
1352
1353
1354
1355
1356

Figure 7 illustrates the effects of assimilating multiple-wavelength AOD retrievals comparing its performance against just assimilating AOD at 550 nm, which is what is commonly done. Error reductions with respect to non-assimilated AOD observations are similar for both cases, but notable differences are found when comparing error reductions for the Ångström exponent (AE), a proxy for the aerosol size distribution. The simulation assimilating only 550 nm AOD does not significantly change the AE, while assimilating multiple-wavelength AOD improves performance of the AE.

Supprimé : 8

1357
1358
1359
1360
1361
1362

These results demonstrate that satellite AOD assimilation can be used for improving analysis and forecast, with additional improvements when using observationally constrained retrievals and multiple wavelength data. Thus, future work needs to point towards incorporating additional retrievals, which need to be observationally constrained to improve assimilation performance.

1363
1364
1365
1366
1367
1368
1369
1370
1371
1372

Assimilating cloud retrievals. Vast regions of the world are constantly covered by clouds, which limit our ability to constrain aerosol model estimates with AOD retrievals. In order to overcome this limitation, a novel data assimilation approach was developed to use cloud satellite retrievals to provide constraints on below-cloud aerosols (Saide *et al.*, 2012a). The method consists in using the online coupling and aerosol-cloud interactions within WRF-Chem to provide cloud droplet number (N_d) estimates, which are compared to satellite retrievals through the data assimilation framework. Figure 8 presents results for the southeastern Pacific stratocumulus deck, where the MODIS retrieval (Painemal and Zuidema, 2011) is assimilated and compared against independent GOES retrievals (Painemal *et al.*, 2012). The assimilation is able to correct the low and high biases in N_d found in the

Supprimé : 9

1373 guess with these corrections persisting even throughout the second day after assimilation.
1374 Furthermore, Saide *et al.* (2012a) show that the corrections made to the below-cloud aerosols
1375 are in better agreement with in-situ measurements of aerosol mass and number. Future steps
1376 should try to show the value of this assimilation method on other regions and find potential
1377 synergies between AOD and N_d assimilation in order to provide better aerosol forecasts and
1378 analyses.

1379
1380
1381

5.4 Satellite data assimilation for constraining anthropogenic emissions

1382 The case studies performed with the SILAM dispersion model (<http://silam.fmi.fi>) have
1383 demonstrated the possibility and efficiency of extension of the data assimilation towards
1384 source apportionment. The goal of the numerical experiment was to improve the emission
1385 estimates of $PM_{2.5}$ via assimilating the MODIS-retrieved column-integrated AOD fields. The
1386 4D-Var assimilation method generally followed the approach of Vira & Sofiev (2012) with
1387 several updates:

- 1388 - three domains were considered: Europe, Southern Africa, and Southeast Asia
- 1389 - the aerosol species included:
 - 1390 o primary OC, BC (MACCITY emission inventory, non-European domains) or
 - 1391 o primary $PM_{2.5}/PM_{10}$ (TNO-MACC emission, European domain)
 - 1392 o sulfate from SO_2 oxidation
 - 1393 o nitrate from NO_x oxidation (not adjusted during the assimilation)
 - 1394 o sea salt (embedded module in SILAM, adjusted by the assimilation)
 - 1395 o desert dust (embedded module in SILAM, adjusted by the assimilation)
 - 1396 o $PM_{2.5}$ from wildfires (IS4FIRES emission inventory, adjusted by the
 - 1397 o assimilation)
- 1398 - the assimilation window was 1 month to reduce the noise and random fluctuations of
- 1399 the emission corrections
- 1400 - the boundary conditions were taken from a global SILAM simulation
- 1401 - a complete year, 2008, was analyzed with 0.5° spatial resolution and vertical
- 1402 coverage up to the tropopause; the model was driven by ERA-Interim meteorological
- 1403 information

1404

1405 An example of SILAM a-priori AOD pattern for Asia, fully collocated with MODIS
1406 observations (Figure 9) shows the significant initial disagreement between the SILAM and
1407 MODIS AOD. In particular, the model shows almost no aerosol in northwestern India and
1408 much too low values over eastern China. Assimilation improves the distribution and reduces
1409 the negative bias (Figure 9, bottom panel). Since the amount of dust emitted by the
1410 experimental version of SILAM was quite low, the northern part of China and Mongolia are
1411 practically not corrected. But the Indian and Chinese industrial and agriculture regions were
1412 improved very efficiently. A comparison with independent data (AATSR AOD retrievals)
1413 confirmed the trends: both substantial bias reduction and increase of the correlation
1414 coefficient (Table 3).

1415 The resulting emission estimates had substantial seasonal variation, different from the a-
1416 priori estimates (Figure 10). Apart from almost doubling the annual OC emissions (from 7.8

Supprimé : 10

Supprimé : 10

Supprimé : 11

1417 Mt to 15 Mt of PM), the inversion also altered the seasonality, clearly suggesting spring and
1418 autumn as the two periods with strong emission.

1419
1420 The efficiency of the emission inversion varied between the regions and strongly depended
1421 on quality of the a-priori information. Thus, in Africa strong contribution from wild land fires
1422 might have affected the final results for other PM species.

1423
1424 The other potential issue in assimilation of total PM is the need to distribute the information
1425 among individual components that are either emitted or created by chemical transformations.
1426 In particular, there is a risk of artificial changes in SO₂ sources because in many cases the
1427 total AOD is more sensitive to changing sulfate production than to variations of the primary
1428 PM emission. A possible way out is to perform simultaneous inversion for several species,
1429 e.g., for SO₂ and PM emissions.

1430
1431

1432 6. Potential difficulties for data assimilation in CCMM

1433

1434 Data assimilation in CCMM is recent and has typically been limited to chemical (including
1435 PM) data assimilation to improve chemical and, in a few cases, meteorological predictions.
1436 The effect of assimilating jointly meteorological and chemical variables on meteorological
1437 and chemical predictions has been limited to date and it is worthwhile to discuss the potential
1438 difficulties that may be associated with such future applications, particularly in the case of
1439 CCMM with feedbacks between chemistry and meteorology.

1440

1441 The effect of chemical data assimilation on meteorological variables has been investigated in
1442 a few specific cases, for example the effect of stratospheric O₃ assimilation on winds
1443 (Semane et al., 2009) and that of AOD assimilation on the radiative budget and winds
1444 (Jacobson and Kaufman, 2006; Reale et al., 2014). It has also been shown to be potentially
1445 important using a low-order model (Bocquet and Sakov, 2013) However, joint data
1446 assimilation of both meteorological (e.g. winds or temperature) and chemical data has not
1447 been conducted to a large extent and it is not clear how much interactions could occur among
1448 meteorological and chemical state variables when assimilating both chemical and
1449 meteorological data. Assimilating distinct data sets that influence the same model variable
1450 could lead to some contradictory information concerning that model variable when the error
1451 statistics are misspecified (e.g., unknown bias in semi-volatile PM components); therefore, it
1452 will be essential to properly specify those measurement error statistics. Most likely, one of
1453 the influential data sources may dominate as being less uncertain and/or more influential.
1454 Then, either an offline sensitivity analysis could be used to diagnose which input variable to
1455 retain for data assimilation or the data assimilation process would automatically give more
1456 weight to the less uncertain/more influential variable.

1457

1458 Another potential difficulty concerns the assimilation of aggregated variables such as PM
1459 mass concentration or AOD. The effect on the model individual variables (i.e., PM individual
1460 components) is currently typically performed by modifying all PM components
1461 proportionally to the model component fractions. This approach may lead to erroneous
1462 results if the prior chemical composition differs significantly from the one in the model, for
1463 example, if one component of the aggregated variable (total PM mass) is dominating in the
1464 model, but is not the one that needs to be corrected. One example is the assimilation of AOD
1465 in the presence of a volcanic ash plume over the ocean, which may lead to a corrective
1466 increase in sea salt instead of the addition of volcanic ash in the model.

Supprimé : In the worst case,

Supprimé : due to measurement error could be assimilated

Supprimé : some

Supprimé : s

1467
1468 An approach to circumvent that problem is to assimilate individual PM component mass
1469 concentrations. However, the lack of routinely available continuous measurements of PM
1470 component concentrations has so far prevented the operational use of such information.
1471 Furthermore, this process could potentially lead to difficulties, when both total mass
1472 concentration and the mass concentrations of individual PM components are assimilated. The
1473 sum of individual PM component mass concentrations may not necessarily be consistent with
1474 the total PM mass concentration because of measurement artifacts (which may affect both the
1475 individual component mass measurements and the total PM mass measurement). If so, the
1476 data source with the least observation error should dominate or the forecast may remain little
1477 affected by the assimilation. This implies that the observation errors need to be correctly
1478 characterized. In that regard, assimilation of multi-wavelength AOD, single-scattering
1479 albedo, Ångström exponent, and/or absorption optical depth can place additional constraints
1480 on the aerosol composition by providing information on particle size and absorption.

1481
1482 Similar difficulties could arise when assimilating multiple gaseous species with chemical
1483 interactions (e.g., O₃, NO₂, HCHO). However, such multi-species data assimilation
1484 applications have been conducted successfully so far, which suggests that this process is not
1485 a major source of difficulties. Typically, the assimilation of additional chemical species (e.g.,
1486 NO₂ in addition to O₃) shows little improvement over the assimilation of the first species.

1487
1488 The assimilation of both satellite and surface data for chemical species has been conducted
1489 and previous applications have shown that it works well. It is likely that the satellite data
1490 correct concentrations in the free troposphere whereas surface data correct concentrations in
1491 the planetary boundary layer and that the two regions are not strongly coupled. Cases with
1492 conditions of deep convection when the coupling between those atmospheric regions
1493 becomes important should be investigated to stress the data assimilation process of distinct
1494 sources of data having greater interactions on the model variables.

1495
1496 Concerning data assimilation methods, the error cross-correlations, such as wind-chemical
1497 species or species-species, would be dynamically estimated with [the EnKF or another](#)
1498 [ensemble-based method](#); however, their specification would be complex if not problematic in
1499 an optimal interpolation, 3D-Var or 4D-Var data assimilation.

1500
1501 Finally, a major difficulty for data assimilation in CCMM is likely to be the paucity of data
1502 for chemical (including PM) data assimilation. For example, in the case of satellite data,
1503 insufficient vertical resolution and temporal resolution are a potential difficulty for chemical
1504 data assimilation.

1507 **7. Conclusion and Recommendations**

1508
1509 Data assimilation has been performed so far mostly as assimilation of meteorological
1510 observations in numerical weather prediction (NWP) models or as assimilation of chemical
1511 concentrations in CTM and, to a lesser extent, in CCMM. Improvements in meteorological
1512 fields typically benefits CTM and CCMM performance and there are some examples of the
1513 effect of chemical data assimilation on meteorological results; however, little work has been
1514 conducted so far to assimilate both meteorological and chemical data jointly into CCMM. As
1515 a result, the potential feedbacks of chemical data assimilation on meteorological forecasts
1516 have not been fully investigated yet.

1517
1518 Although most applications of chemical data assimilation have addressed the improvement of
1519 chemical concentration fields, the correction of emission biases may also be an important
1520 area of development and applications, in particular for emission terms that carry large
1521 uncertainties, such as sand/dust storms, biomass fires, allergenic pollen episodes, [volcanic](#)
1522 [eruptions](#), and accidental releases.
1523

1524 A major limitation of data assimilation in CCMM is likely to be the limited availability of
1525 data, particularly in near-real-time. For example, there has been no assimilation of PM
1526 component concentration data conducted so far and the assimilation of total PM
1527 concentrations necessarily involves assumptions that may not reflect reality and, therefore,
1528 significantly limit the benefits of assimilating those data. Joint assimilation of surface and
1529 satellite data has proven useful, but rather disconnected, the former affecting mostly the
1530 boundary layer concentrations while the latter affects the free troposphere concentrations. A
1531 more thorough investigation of the potential couplings between those tropospheric
1532 compartments appears warranted. Satellite data are very valuable because of the coverage
1533 that they can provide; the combination of using data from polar orbiting satellites that
1534 provide good spatial coverage but with limited temporal resolution and geostationary
1535 satellites that provide limited spatial coverage and resolution but continuous temporal
1536 coverage should be investigated (e.g., the future ESA sentinel-4 and sentinel-5 missions
1537 would provide such complementary information for atmospheric chemical species such as
1538 O₃, NO₂, SO₂, HCHO, and AOD).
1539

1540 As more chemical data become available in near-real-time, the assimilation of large data sets
1541 from widely different sources (e.g., surface, ground-based remote and satellite data) into
1542 CCMM may lead to new challenges to develop optimal and efficient data assimilation
1543 procedures. [However, assimilating a wide variety of data should benefit not only the model](#)
1544 [variable corresponding directly to the data being assimilated, but also other model variables](#)
1545 [influenced via meteorology/chemistry interactions, as exemplified for example by the](#)
1546 [improvement in aerosol concentrations via CCN data assimilation \(Saide et al., 2012a\) and](#)
1547 [the potential improvement in meteorological variables via AOD data assimilation during dust](#)
1548 [storms \(Reale et al., 2011, 2014\).](#)
1549

1550 Although data assimilation for CCMM is still in its infancy, results obtained so far suggest
1551 that it is likely that more work in this area will lead to improvements not only for
1552 atmospheric chemistry forecasts, but also for numerical weather forecasts. If such results are
1553 indeed confirmed in future applications, one could hope then that chemical data assimilation
1554 will become more valuable in terms of operational applications and that more resources,
1555 particularly in terms of data bases, will be allocated to it. Furthermore, as computer resources
1556 become increasingly more powerful, global CCMM are likely to become also more common
1557 and data assimilation in global CCMM could grow accordingly.
1558

1559 In terms of data assimilation methods, two major competing branches for data assimilation
1560 are likely to emerge for future operational applications: weak constraint 4D-Var with longer
1561 assimilation windows and ensemble 4D-Var in which covariances are evolved using
1562 ensembles but minimization of the cost function is obtained with a variational approach.
1563

1564 Finally, this review has focused on data assimilation. Image assimilation is also an important
1565 field in the geosciences. The assimilation of images such as clouds and large plumes (due to
1566 volcanic eruptions or large biomass fires) can also provide notable improvements for short-

1567 term forecasting (nowcasting). Furthermore, the source terms of volcanic eruptions, biomass
1568 fires, and sand/dust storms could be better determined via image assimilation. This area of
1569 research would complement nicely current ongoing work on data assimilation and lead to
1570 better capabilities for CCMM.

1571
1572

1573 **Acknowledgments**

1574

1575 This work was realized within and supported by the COST Action ES1004 EuMetChem.

1576

1577

1578 **References**

1579

1580 Abida, R. and Bocquet, M.: Targeting of observations for accidental atmospheric release
1581 monitoring, *Atmos. Env.*, 43, 6312-6327, 2009..

1582 Adhikary, B., Kulkarni, S., Dallura, A., Tang, Y., Chai, T., Leung, L. R., Qian, Y., Chung, C.
1583 E., Ramanathan, V., and Carmichael, G. R.: A regional scale chemical transport
1584 modeling of Asian aerosols with data assimilation of AOD observations using optimal
1585 interpolation technique, *Atmos. Environ.*, 42, 8600-8615,
1586 doi.org/10.1016/j.atmosenv.2008.08.031, 2008.

1587 Anderson, J. L. and Anderson, S. L.: A Monte Carlo implementation of the nonlinear
1588 filtering problem to produce ensemble assimilations and forecasts, *Mon. Wea. Rev.*
1589 127, 2741–2758, 1999.

1590 Aumann, H. H., Chahine, M. T., Gautier, C., Goldberg, M. D., Kalnay, E., McMillin, L. M.,
1591 Revercomb, H., Rosenkranz, P.W., Smith, W.L., Staelin, D.H., Strow, L.L. and
1592 Susskind, J.: AIRS/AMSU/HSB on the Aqua mission: Design, science objectives,
1593 data products, and processing systems, *IEEE Transactions on Geoscience and Remote*
1594 *Sensing*, 41(2), 253-264, 2003.

1595 Baklanov, A., Schlünzen, K. H., Suppan, P., Baldasano, J., Brunner, D., Aksoyoglu, S.,
1596 Carmichael, G., Douros, J., Flemming, J., Forkel, R., Galmarini, S., Gauss, M., Grell,
1597 G., Hirtl, M., Joffre, S., Jorba, O., Kaas, E., Kaasik, M., Kallos, G., Kong, X.,
1598 Korsholm, U., Kurganskiy, A., Kushta, J., Lohmann, U., Mahura, A., Manders-Groot,
1599 A., Maurizi, A., Moussiopoulos, N., Rao, S. T., Savage, N., Seigneur, C., Sokhi, R.S.,
1600 Solazzo, E., Solomos, S., Sørensen, B., Tsegas, G., Vignati, E., Vogel, B., and Zhang,
1601 Y.: Online coupled regional meteorology chemistry models in Europe: current status
1602 and prospects, *Atmos. Chem. Phys.*, 14, 317-398, 2014.

1603 Barbu, A.L., Segers, A.J., Schaap, M., Heemink, A.W., and Builtjes, P.J.H.: A multi-
1604 component data assimilation experiment directed to sulphur dioxide and sulphate over
1605 Europe, *Atmos. Environ.*, 43, 1622-1631, 2009.

1606 Barnes, W. L., Pagano, T. S., and Salomonson, V. V.: Prelaunch characteristics of the
1607 moderate resolution imaging spectroradiometer (MODIS) on EOS-AM1, *IEEE*
1608 *Transactions on Geoscience and Remote Sensing*, 36, 1088-1100, 1998.

1609 Beer, R., Glavich, T. A., and Rider, D. M.: Tropospheric emission spectrometer for the Earth
1610 Observing System's Aura satellite, *Applied Optics*, 40, 2356-2367, 2001.

1611 Bellouin N., Quaas, J., Morcrette, J.-J., and Boucher, O.: Estimates of aerosol radiative
1612 forcing from the MACC re-analysis, *Atmos. Chem. Phys.*, 13, 2045–2062.
1613 doi:10.5194/acp-13-2045-2013, 2013.

1614 Benedetti, A., Morcrette, J.-J., Boucher, O., Dethof, A., Engelen, R. J., Fisher, M., Flentje,
1615 H., Huneeus, N., Jones, L., Kaiser, J. W., Kinne, S., Mangold, A., Razinger, M.,
1616 Simmons, A. J., Suttie, M., and the GEMS-AER team: Aerosol analysis and forecast

1617 in the European Centre for Medium-Range Weather Forecasts Integrated Forecast
1618 System: Data Assimilation, *J. Geophys. Res.*, D13205, 114,
1619 doi:10.1020/2008JD011115, 2008.

1620 Benedetti, A., Jones, L. T., Inness, A., Kaiser, J. W., and Morcrette, J.-J.: [Global climate]
1621 Aerosols [in “State of the Climate in 2012”]. *Bull. Amer. Meteor. Soc.*, 94, S34–S36,
1622 2013.

1623 Berliner, L. M., Lu, Z. Q., and Snyder, C.: Statistical design for Adaptive Weather
1624 Observations, *J. Atmos. Sci.*, 56, 2536-2552, 1999.

1625 Bocquet, M., Pires, C. A., and Wu, L. : Beyond Gaussian statistical modeling in geophysical
1626 data assimilation, *Mon. Wea. Rev.* 138, 2997–3023, 2010.

1627 Bocquet, M.: Parameter field estimation for atmospheric dispersion: Applications to the
1628 Chernobyl accident using 4D-Var, *Q.J. R. Meteorol. Soc.*, 138, 664-681, 2012.

1629 Bocquet, M. and Sakov, P.: Joint state and parameter estimation with an iterative
1630 ensemble Kalman smoother, *Nonlin. Processes Geophys.*, 20, 803-818, 2013.

1631 Boersma, K. F., Eskes, H. J., Dirksen, R. J., van der A, R. J., Veefkind, J. P., Stammes, P.,
1632 Huijnen, V., Kleipool, Q. L., Sneep, M., Claas, J., Leitão, J., Richter, A., Zhou, Y.,
1633 and Brunner, D.: An improved tropospheric NO₂ column retrieval algorithm for the
1634 Ozone Monitoring Instrument, *Atmos. Meas. Tech.*, 4, 1905-1928, doi:10.5194/amt-
1635 4-1905-2011, 2011.

1636 Borrego, C., Coutinho, M., Costa, A.M., Ginja, J., Ribeiro, C., Monteiro, A., Ribeiro, I.,
1637 Valente, J., Amorim, J.H., Martins, H., Lopes, D., Miranda, A.I.: Challenges for a
1638 new air quality directive: the role of monitoring and modelling techniques, *Urban*
1639 *Climate*, <http://dx.doi.org/10.1016/j.uclim.2014.06.007>, in press.

1640 Bovensmann, H., Burrows, J. P., Buchwitz, M., Frerick, J., Noël, S., Rozanov, V. V.,
1641 Chance, K. V., and Goede, A. P. H.: SCIAMACHY: Mission Objectives and
1642 Measurement Modes. *J. Atmos. Sci.*, 56, 127–150, doi.org/10.1175/1520-0469, 1999.

1643 Brandt J, Christensen J.H, and Frohn M.: Modelling transport and deposition of caesium and
1644 iodine from Chernobyl accident using the DREAM model, *Atmos. Chem. Phys.*, 2,
1645 397–417, 2002.

1646 Buehner, M.P., Houtekamer, I., Charette, C., Mitchell, H.L., and He, B.: Intercomparison of
1647 variational data assimilation and the ensemble Kalman filter for global deterministic
1648 N.W.P., Part I. Description and single-observation experiments, *Mon. Wea. Rev.*, 138,
1649 1550-1566, 2010a.

1650 Buehner, M.P., Houtekamer, I., Charette, C., Mitchell, H.L., and He, B.: Intercomparison of
1651 variational data assimilation and the ensemble Kalman filter for global deterministic
1652 N.W.P., Part II. One-month experiments with real observations, *Mon. Wea. Rev.*, 138,
1653 1567-1586, 2010b.

1654 Buizza, R., Miller, M., and Palmer, T. N.: Stochastic representation of model uncertainties in
1655 the ECMWF ensemble prediction system, *Q. J. R. Meteor. Soc.*, 125, 2887-2908, 1999.

1656 Callies, J., Corpaccioli, E., Eisinger, M., Hahne, A., and Lefebvre, A.: GOME-2-Metop's
1657 second-generation sensor for operational ozone monitoring, *ESA bulletin*, 102, 28-36,
1658 2000.

1659 Candiani, G., Carnevale, C., Finzi, G., Pisoni, E., Volta, M.: A comparison of reanalysis
1660 techniques: Applying optimal interpolation and Ensemble Kalman Filtering to
1661 improve air quality monitoring at mesoscale, *Sci. Total Environ.*, 458–460, 7–14,
1662 2013.

1663 Carmichael, G. R., Sandu, A., Chai, T., Daescu, D., Constantinescu, E., and Tang, Y. :
1664 Predicting air quality: Improvements through advanced methods to integrate models
1665 and measurements, *J. Comp. Phys.*, 227, 3540–3571, 2008.

1666 Carmichael, G. R., Adhikary, B., Kulkarni, S., D'Allura, A., Tang, Y., Streets, D., Zhang, Q.,
 1667 Bond, T. C., Ramanathan, V., and Jamroensan, A.: Asian aerosols: current and year
 1668 2030 distributions and implications to human health and regional climate change,
 1669 *Environ. Sci. Technol.*, 43, 5811-5817, 2009.
 1670 Carnevale, C., Decanini, E., and Volta, M.: Design and validation of a multiphase 3D model
 1671 to simulate tropospheric pollution, *Sci. Total Environ.*, 390:166–76, 2008.
 1672 Cathala, M.-L., Pailleux, J., and Peuch, V.-H., Improving global chemical simulations of the
 1673 upper troposphere–lower stratosphere with sequential assimilation of MOZAIC data,
 1674 *Tellus B*, 55, 1–10, doi: 10.1034/j.1600-0889.2003.00002.x, 2003.
 1675 CEOS-ACC: A Geostationary Satellite Constellation for Observing Global Air Quality: An
 1676 International Path Forward, Prepared by the CEOS Atmospheric Composition
 1677 Constellation, Draft Version 4.0, April 12, 2011.
 1678 Chai, T. F., Carmichael, G. R., Sandu, A., Tang, Y. H., and Daescu, D. N. : Chemical data
 1679 assimilation of transport and chemical evolution over the Pacific (TRACE-P) aircraft
 1680 measurements, *J. Geophys. Res.*, 111, D02301, 2006..
 1681 Chai, T., Carmichael, G. R., Tang, Y., Sandu, A., Hardesty, M., Pilewskie, P., Whitlow, S.,
 1682 Browell, E. V., Avery, M. A., N'ed'elec, P., Merrill, J. T., Thompson, A. M., and
 1683 Williams, E.: Four dimensional data assimilation experiments with International
 1684 Consortium for Atmospheric Research on Transport and Transformation ozone
 1685 measurements, *J. Geophys. Res.*, 112, 20 D12S15, doi:10.1029/2006JD007763, 2007.
 1686 Chance, K., Liu, X., Suleiman, R. M., Flittner, D. E., Al-Saadi, J., and Janz, S. J.:
 1687 Tropospheric emissions: monitoring of pollution (TEMPO). In *SPIE Optical*
 1688 *Engineering+ Applications* (pp. 88660D-88660D). International Society for Optics
 1689 and Photonics, September 2013.
 1690 Chapnik, B., Desroziers, G., Rabier, F., and Talagrand, O.: Properties and first application of
 1691 an error-statistics tuning method in variational assimilation, *Q. J. Roy. Meteor. Soc.*,
 1692 130, 2253–2275, 2004.
 1693 Chazette, P., Bocquet, M., Royer, P., Winiarek, V., Raut, J.-C., Labazuy, P., Gouhier, M.,
 1694 Lardier, M., and Cariou, J.-P. Eyjafjallajökull ash concentrations derived from both
 1695 lidar and modeling, *J. Geophys. Res.* 117, D00U14, 2012.
 1696 Chen, D., Liu, Z., Schwartz, C.S., Lin, H.-C., Cetola, J.D., Gu, Y., and Xue, L.: The impact
 1697 of aerosol optical depth assimilation on aerosol forecasts and radiative effects during
 1698 a wild fire event over the United States. *Geosci. Model Dev.*, 7, 2709-2715, 2014.
 1699 Chin, M., Rood, R. B., Lin, S.-J., Muller, J.-F., and Thompson, A. M.: Atmospheric sulfur
 1700 cycle simulated in the global model GOCART: Model description and global
 1701 properties, *J. Geophys. Res.*, 105, 24,671–24,687, doi:10.1029/2000JD900384, 2000.
 1702 Chin, M., Ginoux, P., Kinne, S., Torres, O., Holben, B. N., Duncan, B. N., Martin, R. V.,
 1703 Logan, J. A., and Higurashi, A.: Tropospheric aerosol optical thickness from the
 1704 GOCART model and comparisons with satellite and Sun photometer measurements,
 1705 *J. Atmos. Sci.*, 59, 461–483, 2002.
 1706 Clerbaux, C., Boynard, A., Clarisse, L., George, M., Hadji-Lazaro, J., Herbin, H., Hurtmans,
 1707 D., Pommier, M., Razavi, A., Turquety, S., Wespes, C., and Coheur, P. F. :
 1708 Monitoring of atmospheric composition using the thermal infrared IASI/MetOp
 1709 sounder, *Atmos. Chem. Phys.*, 9, 6041-6054, 2009.
 1710 Collins, W. D., Rasch, P. J., Eaton, B. E., Khattatov, B. V., Lamarque, J.-F., and Zender, C.
 1711 S.: Simulating aerosols using a chemical transport model with assimilation of satellite
 1712 aerosol retrievals: Methodology for INDOEX, *J. Geophys. Res.*, 106, 7313-7336,
 1713 10.1029/2000jd900507, 2001.
 1714 Coman, A., Foret, G., Beekmann, M., Eremenko, M., Dufour, G., Gaubert, B., Ung, A.,
 1715 Schmechtig, C., Flaud, J.-M., and Bergametti, G.: Assimilation of IASI partial

1716 tropospheric columns with an Ensemble Kalman Filter over Europe, *Atmos. Chem.*
1717 *Phys.*, 12, 2513–2532, 2012..

1718 Constantinescu, E. M., Sandu, A., Chai, T., and Carmichael, G. R. Ensemble-based chemical
1719 data assimilation. i: General approach. *Q. J. R. Meteor. Soc.*, 133, 1229–1243, 2007a.

1720 Constantinescu, E. M., Sandu, A., Chai, T., and Carmichael, G. R. : Ensemble-based
1721 chemical data assimilation. ii: Covariance localization, *Q. J. R. Meteor. Soc.*, 133,
1722 1245–1256, 2007b.

1723 Courtier, P., Thépaut, J.-N., and Hollingsworth, A.: A strategy for operational
1724 implementation of 4D-Var, using an incremental approach, *Q. J. R. Meteorol. Soc.*,
1725 120, 1367-1388, 1994.

1726 Curier, R.L., Timmermans, R., Calabretta-Jongen, S., Eskes, H., Segers, A., Swart, D., and
1727 Schaap, M. Improving ozone forecasts over Europe by synergistic use of the LOTOS-
1728 EUROS chemical transport model and in-situ measurements. *Atmos. Environ.*, 60,
1729 217-226, 2012..

1730 Daley, R.: *Atmospheric Data Analysis*. Cambridge University Press, 1991..

1731 Davoine, X. and Bocquet, M.: Inverse modelling-based reconstruction of the Chernobyl
1732 source term available for long-range transport, *Atmos. Chem. Phys.* 7, 1549–1564,
1733 2007..

1734 Dee, D. P. and Uppala, S.: Variational bias correction of satellite radiance data in the ERA-
1735 Interim reanalysis, *Q. J. R. Meteorol. Soc.*, 135, 1830–1841, 2009.

1736 Dee, D P., Uppala, S. M., Simmons, A. J., Berrisford, P., Poli, P., Kobayashi, S., Andrae, U.,
1737 Balmaseda, M. A., Balsamo, G., Bauer, P., Bechtold, P., Beljaars, A. C. M. , van de
1738 Berg, L., Bidlot, J., Bormann, N., Delsol, C., Dragani, R., Fuentes, M., Geer, A. J.,
1739 Haimberger, L., Healy, S. B., Hersbach, H., Hólm, E. V., Isaksen, L., Kållberg, P.,
1740 Köhler, M., Matricardi, M., McNally, A. P., Monge-Sanz, B. M., Morcrette, J.-J.,
1741 Park, B.-K., Peubey, C., de Rosnay, P., Tavolato, C., Thépaut, J.-N., and Vitarta, F.:
1742 The ERA-Interim reanalysis: Configuration and performance of the data assimilation
1743 system, *Quart. J. R. Meteor. Soc.*, 137, 553-597, 2011.

1744 Desroziers, G., Berre, L., Chapnik, B., and Poli, P.: Diagnosis of observation, background
1745 and analysis error statistics in observation space, *Q. J. R. Meteor. Soc.*, 131, 3385–
1746 3396, 2005.

1747 Desroziers, G. and Ivanov, S.: Diagnosis and adaptive tuning of observation error parameters
1748 in a variational assimilation. *Q. J. R. Meteor. Soc.* 127, 1433–1452, 2001.

1749 Dethof, A. and Hólm, E.V.: Ozone assimilation in the ERA-40 reanalysis project, *Quart. J.*
1750 *Roy. Met. Soc.*, 130, 2851-2872, 2004.

1751 Diner, D. J., Abdou, W. A., Bruegge, C. J., Conel, J. E., Crean, K. A., Gaitley, B. J.,
1752 Helmlinger, M.C., Kahn, R.A., Martonchik, J.V., Pilorz, S.H., and Holben, B. N.:
1753 MISR aerosol optical depth retrievals over southern Africa during the SAFARI-2000
1754 dry season campaign, *Geophys. Res. Lett.*, 28, 3127-3130, 2001.

1755 Dragani, R.: On the quality of the ERA-Interim ozone reanalyses: comparisons with satellite
1756 data, *Quart. J. Roy. Meteor. Soc.*, 137: 1312–1326, doi: 10.1002/qj.821, 2011.

1757 Drummond, J. R. and Mand, G. S.: The Measurements of Pollution in the Troposphere
1758 (MOPITT) instrument: Overall performance and calibration requirements. *J. Atmos.*
1759 *Oceanic Technol.*, 13, 314-320, 1996.

1760 EEA; Air quality in Europe, 2013 report, EEA Report No 9/2013, 2013.

1761 Eisele, F., Mauldin, L., Cartrell, C., Zondio, M., Apel, E., Fried, A., Walega, J., Sheffer, R.,
1762 Lefer, B., Flocke, F., Weinheimer, A., Avery, M., Vay, S., Sachse, G., Podolske, J.,
1763 Diskin, G., Barrick, J.D., Singh, H.B., Brune, W., Harder, H., Martinez, M., Bandy,
1764 A., Thornton, D., Heikes, B., Kondo, Y., Riemer, D., Sandholm, S., Tan, D., Talbot,

Supprimé : Cressman G.P: An operational objective analysis system, *Mon. Weather Rev.*, 87, 367–374, 1959.¶

1765 R., and Dibb, J.: Summary of measurement intercomparisons during TRACE-P, *J.*
1766 *Geophys. Res.*, 108(D20), 8791, doi:10.1029/2002JD003167, 2003.

1767 Elbern, H., and Schmidt, H.: A four-dimensional variational chemistry data assimilation
1768 scheme for Eulerian chemistry transport modeling, *J. Geophys. Res.*, 104, 18583–
1769 18598, 1999..

1770 Elbern, H. and Schmidt, H.: Ozone episode analysis by four-dimensional variational
1771 chemistry data assimilation, *J. Geophys. Res.*, 106, 3569–3590, 2001..

1772 Elbern, H., Strunk, A., Schmidt, H., and Talagrand, O.: Emission rate and chemical state
1773 estimation by 4-dimensional variational inversion, *Atmos. Chem. Phys.*, 7, 3749–
1774 3769, 2007.

1775 EMEP: *Transboundary Particulate Matter in Europe: EMEP Status Report 2012*, edited by:
1776 Yttri, K. E. et al., European Monitoring and Evaluation Programme Status Report
1777 4/2012, 2012.

1778 Emmons, L. K., Walters, S., Hess, P. G., Lamarque, J.-F., Pfister, G. G., Fillmore, D.,
1779 Granier, C., Guenther, A., Kinnison, D., Laepple, T., Orlando, J., Tie, X.,
1780 Tyndall, G., Wiedinmyer, C., Baughcum, S. L., and Kloster, S.: Description and
1781 evaluation of the Model for Ozone and Related chemical Tracers, version 4
1782 (MOZART-4), *Geosci. Model Dev.*, 3, 43–67, doi:10.5194/gmd-3-43-2010, 2010.

1783 Engelen, R.J. and Bauer, P.: The use of variable CO₂ in the data assimilation of AIRS and
1784 IASI radiances, *Q.J.R. Meteorol. Soc.*, doi: 10.1002/qj.919, 2011.

1785 Engelen R. J., Serrar, S., and Chevallier, F.: Four-dimensional data assimilation of
1786 atmospheric CO₂ using AIRS observations, *J. Geophys. Res.*, 114, D03303,
1787 doi:10.1029/2008JD010739, 2009.

1788 Eskes, H., and Boersma, K. : Averaging kernels for DOAS total-column satellite
1789 retrievals, *Atmos. Chem. Phys.*, 3, 1285–1291, 2003.

1790 Evensen, G.: Sequential data assimilation with a nonlinear quasigeostrophic model using
1791 Monte Carlo methods to forecast error statistics, *J. Geophys. Res.* 99 (C5), 10,143–
1792 10,162, 1994.

1793 Evensen, G.: *Data Assimilation: The Ensemble Kalman Filter*, 2nd Edition. Springer-Verlag,
1794 2009.

1795 Fedorov, V. V.: Kriging and other estimators of spatial field characteristics (with special
1796 reference to environmental studies), *Atmos. Env.* 23, 175–184, 1989.

1797 Fehsenfeld, F.C., Ancellet, G., Bates, T.S., Goldstein, A.H., Hardesty, R.M., Honrath, R.,
1798 Law, K.S., Lewis, A.C., Leitch, R., McKeen, S., Meagher, J., Parrish, D.D.,
1799 Pszenny, A.A.P., Russell, P.B., Schlager, H., Seinfeld, J., Talbot, R., and Zbinden, R.:
1800 International Consortium for Atmospheric Research on Transport and Transformation
1801 (ICARTT): North America to Europe—Overview of the 2004 summer field study, *J.*
1802 *Geophys. Res.*, 111, D23S01, doi:10.1029/2006JD007829, 2006.

1803 Ferro, C. A. T., and Stephenson, D. B.: Extremal dependence indices: improved verification
1804 measures for deterministic forecasts of rare binary events, *Wea. Forecasting*, 26, 699–
1805 713, 2011.

1806 Fioletov, V. E., McLinden, C. A., Krotkov, N., Moran, M. D., and Yang, K.: Estimation of
1807 SO₂ emissions using OMI retrievals, *Geophys. Res. Lett.*, 38, 2011.

1808 Fisher, M. and Lary, D. J.: Lagrangian four-dimensional variational data assimilation of
1809 chemical species, *Q. J. Roy. Meteor. Soc.*, 121, 1681–1704, 1995..

1810 Fisher, M., Leutbecher, M., and Kelly, G. A.: On the equivalence between Kalman
1811 smoothing and weak-constraint four-dimensional variational data assimilation, *Q. J. R.*
1812 *Meteor. Soc.*, 131, 3235–3246, 2005..

1813 Fisher, M. and Andersson, E.: Developments in 4D-Var and Kalman Filtering. ECMWF
1814 Technical Memorandum 347. Available from ECMWF, Shinfield Park, Reading,
1815 Berkshire, RG2 9AX, UK, 2001.

1816 Fishman, J., Bowman, K. W., Burrows, J. P., Richter, A., Chance, K. V., Edwards, D. P.,
1817 Martin, R. V., Morris, G. A., Pierce, R. B. and Ziemke, J. R. : Remote sensing of
1818 tropospheric pollution from space, *Bullet. Amer. Meteor. Soc.*, 89(, 805–822, 2008.

1819 Flemming, J., Inness, A., Flentje, H., Huijnen, V., Moinat, P., Schultz, M.G., and Stein O.:
1820 Coupling global chemistry transport models to ECMWF's integrated forecast system,
1821 *Geosci. Model Dev.*, 2, 253-265, 2009.

1822 Flemming, J., Inness, A., Jones, L., Eskes, H. J., Huijnen, V., Schultz, M. G., Stein, O.,
1823 Cariolle, D., Kinnison, D., and Brasseur, G.: Forecasts and assimilation experiments
1824 of the Antarctic ozone hole 2008, *Atmos. Chem. Phys.*, 11, 1961-1977,
1825 doi:10.5194/acp-11-1961-2011, 2011,

1826 Flemming, J. and Inness, A: [Global climate] Carbon monoxide [in “State of the Climate in
1827 2013”], *Bull. Amer. Meteor. Soc.*, 95, S43-S44, 2014.

1828 Fuentes, M., Chaudhuri, A., and Holland, D. M. Bayesian entropy for spatial sampling design of
1829 environmental data, *Environ. Ecol. Stat.*, 14, 323-340, 2007.

1830 GAW: Global Atmosphere Watch (GAW) Programme: 25 years of global coordinated
1831 atmospheric composition observations and analysis, WMO, Geneva, Switzerland, 70
1832 pp., 2014.

1833 GCOS, Global Climate Observing System, implementation plan 2010, and satellite
1834 supplement, 2011,
1835 <http://www.wmo.int/pages/prog/gcos/documents/SatelliteSupplement2011Update.pdf>

1836 Generoso, S., Bréon, F. M., Chevallier, F., Balkanski, Y., Schulz, M., and Bey, I.:
1837 Assimilation of POLDER aerosol optical thickness into the LMDz-INCA model:
1838 Implications for the Arctic aerosol burden, *J. Geophys. Res.*, 112, D02311,
1839 10.1029/2005jd006954, 2007.

1840 GEOSS, Global Earth Observation System of Systems, 2014,
1841 <http://www.earthobservations.org/geoss.shtml>.

1842 Ghil, M. And Malanotte-Rizzoli, P.: Data assimilation in meteorological and oceanography.
1843 *Adv. Geophys.* 33, 141–266, 1991.

1844 Gibson J.K., Kallberg P., Uppala S.M., Nomura A., Hernandez A., and Serrano E.: ‘ERA
1845 description’, ERA-15 Report Series, No.1, ECMWF: Reading, UK, 1997.

1846 Giglio, L., Randerson, J.T., and van der Werf, G.R.: Analysis of daily, monthly, and annual
1847 burned area using the fourth-generation global fire emissions database (GFED4), *J.*
1848 *Geophys. Res. Biogeosciences*, 118, doi:10.1002/jgrg.20042, 2013.

1849 Ginoux, P., Chin, M., Tegen, I., Prospero, J., Holben, B., Dubovik, O., and Lin, S.-J.:
1850 Sources and distributions of dust aerosols simulated with the GOCART model, *J.*
1851 *Geophys. Res.*, 106, 20,225–20,273, doi:10.1029/2000JD000053, 2001.

1852 Grell, G., Peckham, S. E., Schmitz, R., McKeen, S. A., Frost, G., Skamarock, W. C., and
1853 Eder, B.: Fully coupled “online” chemistry within the WRF model, *Atmos. Environ.*,
1854 39, 6957-6975, 10.1016/j.atmosenv.2005.04.027, 2005.

1855 GSFC: Joint Polar Satellite System (JPSS) VIIRS Aerosol Optical Thickness (AOT) and
1856 Particle Size Parameter Algorithm Theoretical Basis Document (ATBD), 2011.

1857 Hamill, T. M., Whitaker, J. S., and Snyder, C.: Distance-dependent filtering of background
1858 error covariance estimates in an ensemble Kalman filter, *Mon. Wea. Rev.*, 129, 2776–
1859 2790, 2001.

1860 Hanea, R. G., Velders, G. J. M., and Heemink, A. W.: Data assimilation of ground-level
1861 ozone in Europe with a Kalman filter and chemistry transport model, *J. Geophys. Res.*
1862 109, D10302, 2004..

1863 Hitzenberger, R., Berner, A., Galambos, Z., Maenhaut, W., Cafmeyer, J., Schwarz, J., Müller,
 1864 K., Spindler, G., Wiedprecht, W., Acker, K., Hillamo, R., and Mäkelä, T.:
 1865 Intercomparison of methods to measure the mass concentration of the atmospheric
 1866 aerosol during INTERCOMP2000 —Influence of instrumentation and size cuts,
 1867 *Atmos. Environ.*, 38, 6467–6476, doi:10.1016/j.atmosenv.2004.08.025, 2004.,
 1868 Holben, B. N., Eck, T. F., Slutsker, I., Tanré, D., Buis, J. P., Setzer, A., Vermote, E., Reagan,
 1869 J. A., Kaufman, Y. J., Nakajima, T., Lavenu, F., Jankowiak, I., and Smirnov A.:
 1870 AERONET – a federated instrument network and data archive for aerosol
 1871 characterization, *Remote Sens. Environ.*, 66, 1–16, 5529, 5533, 5537, 5544, 1998.
 1872 Holben, B., Tanré, D., Smirnov, A., Eck, T., Slutsker, I., Abuhassan, N., Newcomb, W.,
 1873 Schafer, J., Chatenet, B., and Lavenu, F.: An emerging ground-based aerosol
 1874 climatology: Aerosol optical depth from AERONET, *J. Geophys. Res.*, 106, 12067-
 1875 12012,12097, 2001.
 1876 Hollingsworth, A. and Lönnberg, P.: The statistical structure of shortrange forecast errors as
 1877 determined from radiosonde data: Part 1. The wind field, *Tellus A*, 38, 111–136, 1986.
 1878 Hollingsworth, A., Engelen, R. J., Textor, C., Benedetti, A., Boucher, O., Chevallier, F.,
 1879 Dethof, A., Elbern, H., Eskes, H., Flemming, J., Granier, C., Kaiser, J. W., Morcrette,
 1880 J.-J., Rayner, R., Peuch, V.-H., Rouil, L., Schultz, M. G., Simmons, A. J. and The
 1881 GEMS Consortium: Toward a Monitoring and Forecasting System For Atmospheric
 1882 Composition: The GEMS Project, *Bull. Amer. Meteor. Soc.*, 89, 1147–1164,
 1883 doi:10.1175/2008BAMS2355.1, 2008.
 1884 Houtekamer, P. L. and Mitchell, H. L. A sequential ensemble Kalman filter for atmospheric
 1885 data assimilation, *Mon. Wea. Rev.*, 129, 123–137, 2001..
 1886 Huijnen, V., Flemming, J., Kaiser, J. W., Inness, A., Leitão, J., Heil, A., Eskes, H. J., Schultz,
 1887 M. G., Benedetti, A., Hadji-Lazarou, J., Dufour, G., and Eremenko, M.: Hindcast
 1888 experiments of tropospheric composition during the summer 2010 fires over western
 1889 Russia, *Atmos. Chem. Phys.*, 12, 4341-4364, doi:10.5194/acp-12-4341-2012, 2012.
 1890 IGACO 2004: An Integrated Global Atmospheric Chemistry Observation Theme for the
 1891 IGOS Partnership. GAW report No. 159. September 2004.
 1892 [<http://www.wmo.ch/web/arep/reports/gaw159.pdf>].
 1893 Ingmann, P., Veihelmann, B., Langen, J., Lamarre, D., Stark, H., and Courrèges-Lacoste, G.
 1894 B.: Requirements for the GMES Atmosphere Service and ESA's implementation
 1895 concept: Sentinels-4/-5 and-5p. *Remote Sensing of Environment*, 120, 58-69, 2012.
 1896 Inness, A., Baier, F., Benedetti, A., Bouarar, I., Chabrilat, S., Clark, H., Clerbaux, C.,
 1897 Coheur, P., Engelen, R. J., Errera, Q., Flemming, J., George, M., Granier, C., Hadji-
 1898 Lazarou, J., Huijnen, V., Hurtmans, D., Jones, L., Kaiser, J. W., Kapsomenakis, J.,
 1899 Lefever, K., Leitão, J., Razinger, M., Richter, A., Schultz, M. G., Simmons, A. J.,
 1900 Suttie, M., Stein, O., Thépaut, J.-N., Thouret, V., Vrekoussis, M., Zerefos, C., and the
 1901 MACC team: The MACC reanalysis: an 8 yr data set of atmospheric composition,
 1902 *Atmos. Chem. Phys.*, 13, 4073-4109, doi:10.5194/acp-13-4073-2013, 2013.
 1903 IPCC: Climate Change 2013: The Physical Science Basis. Contribution of Working Group I
 1904 to the Fifth Assessment Report of the Intergovernmental Panel on Climate Change,
 1905 Stocker, T.F., Qin, D., Plattner, G.-K., Tignor, M., Allen, S.K., Boschung, J., Nauels,
 1906 A., Xia, Y., Bex V., and Midgley, P.M. (eds.), Cambridge University Press,
 1907 Cambridge, United Kingdom and New York, NY, USA, 1535 pp, 2013.
 1908 Issartel, J.-P. and Baverel, J.: Inverse transport for the verification of the Comprehensive
 1909 Nuclear Test Ban Treaty, *Atmos. Chem. Phys.*, 3, 475–486, 2003.
 1910 Jacobson, M.Z. and Kaufman, Y.J.: Wind reduction by aerosol particles, *Geophys. Res. Lett.*,
 1911 33, L24814, doi:10.1029/2006GL027838, 2006.

- 1912 Jiang, Z., Liu, Z., Wang, T., Schartz, C.S., Lin, H.-C., and Jiang, F.: Probing into the impact
 1913 of 3DVAR assimilation of surface PM₁₀ observations over China using process
 1914 analysis. *J. Geophys. Res. Atmos.*, 118, 6738-6749, doi:10.1002/jgrd.50495, 2013.
- 1915 Joly, M. and Peuch, V.-H.: Objective classification of air quality monitoring sites over
 1916 Europe, *Atmos. Environ.*, 47, 111-123, doi:10.1016/j.atmosenv.2011.11.025, 2012.
- 1917 Kahnert, M.: Variational data analysis of aerosol species in a regional CTM: background
 1918 error covariance constraint and aerosol optical observation operators, *Tellus B*, 60,
 1919 753-770, 10.1111/j.1600-0889.2008.00377.x, 2008.
- 1920 Kaiser, J. W., Heil, A., Andreae, M. O., Benedetti, A., Chubarova, N., Jones, L., Morcrette,
 1921 J.-J., Razinger, M., Schultz, M. G., Suttie, M., and van der Werf, G. R.: Biomass
 1922 burning emissions estimated with a global fire assimilation system based on observed
 1923 fire radiative power, *Biogeosciences*, 9, 527-554, 2012.
- 1924 Kalnay, E., Kanamitsu, M., Kistler, R., Collins, W., Deaven, D., Gandin, L., Iredell, M.,
 1925 Saha, S., White, G., Woollen, J., Zhu, Y., Chelliah, M., Ebisuzaki, W., Higgins, W.,
 1926 Janowiak, J., Mo, K.C., Ropelewski, C., Wang, J., Leetmaa, A., Reynolds, R., Jenne,
 1927 R., Joseph, D.: The NCEP/NCAR 40-year reanalysis project, *Bull. Amer. Meteor.*
 1928 *Soc.*, 77, 437-470, 1996.
- 1929 Kalnay, E.: *Atmospheric modeling, data assimilation and predictability*, Cambridge
 1930 University Press, Cambridge, UK, 2003.
- 1931 Kleist, D. T., Parrish, D. F., Derber, J. C., Treadon, R., Wu, W.-S., and Lord, S.: Introduction
 1932 of the GSI into the NCEP global data assimilation system, *Weather and Forecasting*,
 1933 24, 1691-1705, 2009.
- 1934 Koohkan, M. R. and Bocquet, M.: Accounting for representativeness errors in the inversion
 1935 of atmospheric constituent emissions: Application to the retrieval of regional carbon
 1936 monoxide fluxes, *Tellus B*, 64, 19047, 2012..
- 1937 Koohkan, M.R., Bocquet, M., Roustan, Y., Kim, Y., and Seigneur, C.: Estimation of volatile
 1938 organic compound emissions for Europe using data assimilation, *Atmos. Chem.*
 1939 *Phys.*, 13, 5887-5905, 2013..
- 1940 Krysta, M. and Bocquet, M.: Source reconstruction of an accidental radionuclide release at
 1941 European scale, *Q. J. R. Meteor. Soc.*, 133, 529-544, 2007.
- 1942 Kumar, U., De Ridder, K., Lefebvre, W., and Janssen, S.: Data assimilation of surface air
 1943 pollutants (O₃ and NO₂) in the regional-scale air quality model AURORA, *Atmos.*
 1944 *Environ.*, 60, 99-108, 2012.
- 1945 Kuze, A., Suto, H., Nakajima, M., and Hamazaki, T.: Thermal and near infrared sensor for
 1946 carbon observation Fourier-transform spectrometer on the Greenhouse Gases
 1947 Observing Satellite for greenhouse gases monitoring, *Appl. Optics*, 48, 6716-6733,
 1948 2009.
- 1949 Lahoz, W., Khatatov, B., and Ménard, R. eds.: *Data assimilation - Making sense of*
 1950 *observations*, Spinger, 718 pp, 2010.
- 1951 Lauvaux, T., Schuh, A. E., Bocquet, M., Wu, L., Richardson, S., Miles, N., and Davies, K.
 1952 J.: Network design for mesoscale inversions of CO₂ sources and sinks, *Tellus B*, 64,
 1953 17980, 2012. .
- 1954 Le Dimet, F.-X. and Talagrand, O.: Variational algorithms for analysis and assimilation of
 1955 meteorological observations: Theoretical aspects, *Tellus A*, 38, 97-110, 1986.
- 1956 [Lee, J., Kim, J., Song, C. H., Ryu, J.-H., Ahn, Y.-H., and Song, C. K.: Algorithm for retrieval](#)
 1957 [of aerosol optical properties over the ocean from the Geostationary Ocean Color](#)
 1958 [Imager. *Remote Sensing of Environment*, 114, 1077-1088,](#)
 1959 [dx.doi.org/10.1016/j.rse.2009.12.021, 2010.](#)

Mis en forme : Retrait :
 Avant : 0 cm, Suspendu :
 1,25 cm, Ne pas ajuster le
 retrait de droite quand la
 grille est définie, Ne pas
 ajuster l'espace entre le
 texte latin et asiatique, Ne
 pas ajuster l'espace entre le
 texte et les nombres
 asiatiques

Mis en forme :
 Police :(asiatique) MS
 Mincho, (Asiatique)
 Japonais

- 1960 | Levelt, P. F., van den Oord, G. H., Dobber, M. R., Malkki, A., Visser, H., de Vries, J.,
 1961 Stamees, P., Lundell, J.O.V., and Saari, H.: The ozone monitoring instrument. IEEE
 1962 Transactions on Geoscience and Remote Sensing, 44(5), 1093-1101, 2006.
- 1963 Lier, P. and Bach, M.: PARASOL a microsatellite in the A-Train for Earth atmospheric
 1964 observations, Acta Astronautica, 62, 257-263, 2008.
- 1965 Lin, C., Z. Wang, J. Zhu. An Ensemble Kalman Filter for severe dust storm data assimilation
 1966 over China, Atmos. Chem. Phys., 8, 2975-2983, 2008.
- 1967 Liu, Z., Liu, Q., Lin, H.-C., Schwartz, C.S., Lee, Y.-H., and Wang, T.: Three-dimensional
 1968 variational assimilation of MODIS aerosol optical depth: Implementation and
 1969 application to a dust storm over East Asia. J. Geophys. Res., 116, D22306,
 1970 doi:10.1029/2011JD016159, 2011.
- 1971 Lorenc, A. C.: Analysis methods for numerical weather prediction, Q. J. R. Meteor. Soc.,
 1972 112, 1177–1194, 1986.
- 1973 Lorenc, A.C. The potential of the ensemble Kalman filter for NWP – a comparison with 4D-
 1974 Var, Q.J.R. Meteorol. Soc., 129, 3183-3203, 2003:.
- 1975 Mallet, V., Quélo, D., Sportisse, B., Ahmed de Biasi, M., Debry, E., Korsakissok, I., Wu, L.,
 1976 Roustan, Y., Sartelet, K., Tombette, M., and Foudhil, H.: Technical Note: The air
 1977 quality modeling system Polyphemus, Atmos. Chem. Phys., 7, 5479-5487, 2007.
- 1978 Ménard, R., Cohn, S. E., Chang, L.-P., Lyster, P. M.: Assimilation of stratospheric chemical
 1979 tracer observations using a Kalman filter. Part I: Formulation, Mon. Wea. Rev., 128,
 1980 2654–2671, 2000.
- 1981 Messina, P., D’Isodoro, M., Murizi, A., Fierli, F.: Impact of assimilated observations on
 1982 improving tropospheric ozone simulations, Atmos. Environ., 45, 6674-6681, 2011.
- 1983 Migliorini, S.: On the Equivalence between Radiance and Retrieval Assimilation, Monthly
 1984 Weather Review, 140, doi:10.1175/MWR-D-10-05047.1, 2012.
- 1985 Mijling, B. and van der A, R.J.: Using daily satellite observations to estimate emissions of
 1986 short-lived air pollutants on a mesoscopic scale, J. Geophys. Res., 117, D17302,
 1987 doi:10.1029/2012JD017817, 2012.
- 1988 Miyazaki, K., Eskes, H.J., Sudo, K., Takigawa, M., van Weele, M., and Boersma, K.F.:
 1989 Simultaneous assimilation of satellite NO₂, O₃, CO, and HNO₃ data for the analysis of
 1990 tropospheric chemical composition and emissions. Atmos. Chem. Phys., 12: 9545–
 1991 9579, 2012..
- 1992 Miyazaki, K., Eskes, H. J., Sudo, K., and Zhang, C.: Global lightning NO_x production
 1993 estimated by an assimilation of multiple satellite data sets, Atmos. Chem. Phys., 14,
 1994 3277-3305, doi:10.5194/acp-14-3277-2014, 2014.
- 1995 Morcrette, J.J., Boucher, O., Jones, L., Salmond, D., Bechtold, P., Beijaars, A., Benedetti, A.,
 1996 Bonet, A., Kaiser, J.W., Razinger, M., Schulz, M., Seerrar, S., Simmons, A.J., Sofiev,
 1997 M., Sutte, M., Tompkins, A.M., and Untch, A.: Aerosol analysis and forecast in the
 1998 European Centre for Medium -Range Weather Forecasts Integrated Forecast System:
 1999 Forward modeling, J. Geophys. Res., 114, D06206, doi:10.1029/2008JD011235,
 2000 2009.
- 2001 Morcrette, J-J.: Ozone-radiation interactions in the ECMWF forecast system, December,
 2002 ECMWF Technical Memorandum 375, available from
 2003 <http://www.ecmwf.int/publications/library/do/references/list/14> , 2003.
- 2004 Müller, W. G.: Collecting Spatial Data : Optimum Design of Experiments for Random
 2005 Fields, Third edition, Springer-Verlag, 2007.
- 2006 Munn, R. E.: The Design of Air Quality Monitoring Networks. MacMillan Publishers Ltd,
 2007 1981.

2008 Navon, I.M.: Data assimilation for numerical weather prediction: A review, in *Data*
2009 *Assimilation for Atmospheric, Oceanic and Hydrologic Applications*, S.K. Park, L.
2010 Xu, eds., Springer-Verlag, Berlin Heidelberg, Germany, 2009.

2011 Nieradzki, L. and Elbern, H.: Variational assimilation of combined satellite retrieved and in
2012 situ aerosol data in an advanced chemistry transport model, Proceedings of the ESA
2013 Atmospheric Science Conference, 12, 2006,

2014 NSTC: Air Quality Observations Systems in the United States, National Science and
2015 Technology Council, Committee on Environment, Natural Resources, and
2016 Sustainability, Washington, DC, USA, 2013.

2017 Nychka, D. and Saltzman, N.: Design of air quality networks, in Case Studies in
2018 Environmental Statistics, eds. D. Nychka, W. Piegorsch and L.H. Cox, Lecture Notes
2019 in Statistics number 132, Springer Verlag, New York, pp.51-76, 1998.

2020 OJEU: Directive 2008/50/EC of the European Parliament and of the Council of 21 May
2021 2008, Official Journal of the European Union, L 152/1, 11 June 2008.

2022 Onogi, K., Tsutsui, J., Koide, H., Sakamoto, M., Kobayashi, S., Hatsushika, H., Matsumoto,
2023 T., Yamazaki, N., Kamahori, H., Takahashi, K., Kadokura, S., Wada, K., Kato, K.,
2024 Oyama, R., Ose, T., Mannoji, N., and Taira, R.: The JRA-25 Reanalysis. *J. Meteor.*
2025 *Soc. Japan*, 85, 369-382, 2007.

2026 Osses, A., Gallardo, L. and Faundez, T.: Analysis and evolution of air quality monitoring
2027 networks using combined statistical information indexes, *Tellus B*, 65, 1982-1992, 2013.

2028 Ott, E., Hunt, B. R., Szunyogh, I., Zimin, A. V., Kostelich, E. J., Corazza, M., Kalnay, E.,
2029 Patil, D. J., Yorke, A.: A local ensemble Kalman filter for atmospheric data
2030 assimilation, *Tellus A* 56, 415–428, 2004.

2031 Pagowski, M., G.A. Grell, S.A. McKeen, S.E. Peckham, D. Devenyi: Three-dimensional
2032 variational data assimilation of ozone and fine particulate matter observations: some
2033 results using the Weather Research and Forecasting – Chemistry model and Grid-
2034 point Statistical Interpolation, *Q. J. R. Meteorol. Soc.*, 136, 2013-2024, 2010.

2035 Pagowski, M., and Grell, G. A.: Experiments with the assimilation of fine aerosols using an
2036 Ensemble Kalman Filter, *J. Geophys. Res.*, 117, D21302,
2037 doi:10.1029/2012JD018333, 2012.

2038 Painemal, D., and Zuidema, P.: Assessment of MODIS cloud effective radius and optical
2039 thickness retrievals over the Southeast Pacific with VOCALS-REx in situ
2040 measurements, *J. Geophys. Res.*, 116, D24206, 10.1029/2011jd016155, 2011.

2041 Painemal, D., Minnis, P., Ayers, J. K., and O'Neill, L.: GOES-10 microphysical retrievals in
2042 marine warm clouds: Multi-instrument validation and daytime cycle over the
2043 southeast Pacific, *J. Geophys. Res.*, 117, D19212, 10.1029/2012jd017822, 2012.

2044 Park, R. S., Song, C. H., Han, K. M., Park, M. E., Lee, S. S., Kim, S. B., and Shimizu, A.: A
2045 study on the aerosol optical properties over East Asia using a combination of CMAQ-
2046 simulated aerosol optical properties and remote-sensing data via a data assimilation
2047 technique, *Atmos. Chem. Phys.*, 11, 12275-12296, 10.5194/acp-11-12275-2011,
2048 2011.

2049 Park, M. E., Song, C. H., Park, R. S., Lee, J., Kim, J., Lee, S., Woo, J. H., Carmichael, G. R.,
2050 Eck, T. F., Holben, B. N., Lee, S. S., Song, C. K., and Hong, Y. D.: New approach to
2051 monitor transboundary particulate pollution over northeast Asia, *Atmos. Chem. Phys.*,
2052 14, 659-674, 10.5194/acp-14-659-2014, 2014.

2053 Parrish, D.F. and Derber, J. C.: The National Meteorological Center's spectral statistical-
2054 interpolation analysis scheme. *Mon. Weather Rev.*, 120, 1747-1763, 1992.

2055 Penenko, V.V., and Obraztsov, N.N.: A variational initialization method for the fields of
2056 meteorological elements, *Soviet Meteor. Hydrol.*, 11, 1-11, 1976.

- 2057 Penenko, V.V.: Some aspects of mathematical modelling using the models together with
 2058 observational data, *Bull. Nov. Comp. Center, Series Num. Model. in Atmosph.*, 4, 31-
 2059 52, 1996.
- 2060 Penenko V.V., Baklanov, A., and Tsvetova, E.: Methods of sensitivity theory and inverse
 2061 modeling for estimation of source term, *Future Generation Computer Systems*, 18,
 2062 661-671, 2002.
- 2063 Penenko, V. V.: Variational methods of data assimilation and inverse problems for studying
 2064 the atmosphere, ocean, and environment, *Num. Analysis & Applications*, 2, 341-351,
 2065 2009.
- 2066 Penenko, V., Baklanov, A., Tsvetova, E., and Mahura, A.: Direct and inverse problems in a
 2067 variational concept of environmental modeling, *Pure Appl. Geophys.*, 169, 447-465,
 2068 2012.
- 2069 Petersen, G, Iverfeldt, A., and Munthe, J.: Atmospheric mercury species over central and
 2070 northern Europe. Model calculations and comparison with observations from the
 2071 nordic air and precipitation network for 1987 and 1988, *Atmos. Environ.*, 29, 47-67,
 2072 1995.
- 2073 Pham, D. T., Verron, J., Roubaud, M. C.: A singular evolutive extended Kalman filter for
 2074 data assimilation in oceanography, *J. Marine Systems* 16, 323-340, 1998..
- 2075 Quélo, D., Mallet, V., Sportisse, B.: Inverse modeling of NO_x emissions at regional scale
 2076 over northern France: Preliminary investigation of the second order sensitivity, *J.*
 2077 *Geophys. Res.* 110, D24310, 2006.
- 2078 Rabier, F., Järvinen, H., Klinker, E., Mahfouf, J.-F., Simmons, A.: The ECMWF operational
 2079 implementation of four-dimensional variational assimilation. I: Experimental results
 2080 with simplified physics. *Q. J. R. Meteor. Soc.* 126, 1143-1170, 2000.
- 2081 Raut, J., Chazette, P., Fortain, A.: Link between aerosol optical, microphysical and chemical
 2082 measurements in an underground railway station in Paris. *Atmos. Environ.* 43, 860-
 2083 868, 2009a.
- 2084 Raut, J., Chazette, P., Fortain, A.: New approach using lidar measurements to characterize
 2085 spatiotemporal aerosol mass distribution in an underground railway station in Paris,
 2086 *Atmos. Environ.* 43, 575-583, 2009b.
- 2087 Rayner, P. J.: Optimizing CO₂ observing networks in the presence of model error: results
 2088 from TransCom 3, *Atmos. Chem. Phys.*, 4, 413-421, 2004.
- 2089 Reale, O., Lau, K.M., da Silva, A.: Impact of an interactive aerosol on the African easterly jet
 2090 in the NASA GEOS-5 global forecasting system. *Wea. Forecasting*, 26, 504-519,
 2091 2011.
- 2092 Reale, O., Lau, K.M., da Silva, A., Matsui, T.: Impact of assimilated and interactive aerosol
 2093 on tropical cyclogenesis. *Geophys. Res. Lett.*, 41, 3282-3288, 2014.
- 2094 Remer, L. A., Kaufman, Y., Tanré, D., Mattoo, S., Chu, D., Martins, J. V., Li, R. R., Ichoku,
 2095 C., Levy, R., and Kleidman, R.: The MODIS aerosol algorithm, products, and
 2096 validation, *J. Atmos. Sci.*, 62, 947-973, 2005.
- 2097 Rodgers, C. D.: *Inverse Methods for Atmospheric Sounding: Theory and Practice*, World
 2098 Scientific Publishing, 2000.
- 2099 Rodwell, M. J., Richardson, D. S., Hewson, T. D., and Haiden, T.: A new equitable score
 2100 suitable for verifying precipitation in numerical weather prediction, *Q. J. R. Meteorol.*
 2101 *Soc.*, 136, 1344-1363, 2010.
- 2102 Roustan, Y. and Bocquet, M.: Inverse modelling for mercury over Europe, *Atmos. Chem.*
 2103 *Phys.*, 6, 3085-3098, 2006.
- 2104 Ruiz, J. J., Pulido, M., Miyoshi, T.: Estimating model parameters with ensemble-based data
 2105 assimilation: A review. *J. Meteorol. Soc. Japan* 91, 0-0, 2013.

Supprimé :

Supprimé :

Supprimé :

Mis en forme : Anglais
Royaume-Uni

Mis en forme : Anglais
Royaume-Uni

Mis en forme : Italien Italie

Mis en forme : Anglais
Royaume-Uni

- 2106 Saide, P. E., Carmichael, G. R., Spak, S. N., Minnis, P., and Ayers, J. K.: Improving aerosol
 2107 distributions below clouds by assimilating satellite-retrieved cloud droplet number,
 2108 *Proceedings of the National Academy of Sciences*, 109, 11939-11943,
 2109 10.1073/pnas.1205877109, 2012a.
- 2110 Saide, P. E., Spak, S. N., Carmichael, G. R., Mena-Carrasco, M. A., Yang, Q., Howell, S.,
 2111 Leon, D. C., Snider, J. R., Bandy, A. R., Collett, J. L., Benedict, K. B., de Szoeko, S.
 2112 P., Hawkins, L. N., Allen, G., Crawford, I., Crosier, J., and Springston, S. R.:
 2113 Evaluating WRF-Chem aerosol indirect effects in Southeast Pacific marine
 2114 stratocumulus during VOCALS-REx, *Atmos. Chem. Phys.*, 12, 3045-3064,
 2115 10.5194/acp-12-3045-2012, 2012b.
- 2116 Saide, P. E., Carmichael, G. R., Liu, Z., Schwartz, C. S., Lin, H. C., da Silva, A. M., and
 2117 Hyer, E.: Aerosol optical depth assimilation for a size-resolved sectional model:
 2118 impacts of observationally constrained, multi-wavelength and fine mode retrievals on
 2119 regional scale analyses and forecasts, *Atmos. Chem. Phys.*, 13, 10425-10444,
 2120 10.5194/acp-13-10425-2013, 2013.
- 2121 Saide, P. E., Kim, J., Song, C. H., Choi, M., Cheng, Y., and Carmichael, G. R.: Assimilating
 2122 next generation geostationary aerosol optical depth retrievals can improve air quality
 2123 simulations, *Geophys. Res. Lett.*, 2014GL062089, 10.1002/2014gl062089, 2014.
- 2124 Saide, P. E., Spak, S. N., Pierce, R. B., Otkin, J. A., Schaack, T. K., Heidinger, A. K., da
 2125 Silva, A. M., Kacenelenbogen, M., Redemann, J., and Carmichael, G. R.: Central
 2126 American biomass burning smoke can increase tornado severity in the U.S, *Geophys.*
 2127 *Res. Lett.*, 2014GL062826, 10.1002/2014gl062826, 2015.
- 2128 Sartelet, K. N., Debry, E., Fahey, K. M., Roustan, Y., Tombette, M., and Sportisse, B.:
 2129 Simulation of aerosols and gas-phase species over Europe with the Polyphemus
 2130 system. Part I: model-to-data comparison for 2001, *Atmos. Environ.*, 29, 6116–6131,
 2131 2007.
- 2132 Schere, K., Flemming, J., Vautard, R., Chemel, C., Colette, A., Hogrefe, C., Bessagnet, B.,
 2133 Meleux, F., Mathur, R., Roselle, S., Hu, R.-M., Sokhi, R.S., Rao, S.T., and Galmarini,
 2134 S.: Trace gas/aerosol boundary concentrations and their impacts on continental-scale
 2135 AQMEII modeling domains, *Atmos. Env.*, 53, 38-50,
 2136 10.1016/j.atmosenv.2011.09.043, 2012.
- 2137 Schroedter-Homscheidt, M., Elbern, H., and Holzer-Popp, T.: Observation operator for the
 2138 assimilation of aerosol type resolving satellite measurements into a chemical transport
 2139 model, *Atmos. Chem. Phys.*, 10, 10435-10452, 10.5194/acp-10-10435-2010, 2010.
- 2140 Schubert, S. D., Rood, R. B., and Pfaendner, J.: An Assimilated dataset for Earth science
 2141 applications, *Bull. Amer. Meteor. Soc.*, 74, 2331–2342, 1993.
- 2142 Schutgens, N. A. J., Miyoshi, T., Takemura, T., and Nakajima, T.: Applying an ensemble
 2143 Kalman filter to the assimilation of AERONET observations in a global aerosol
 2144 transport model, *Atmos. Chem. Phys.*, 10, 2561–2576, doi:10.5194/acp-10-2561-
 2145 2010, 2010.
- 2146 Schwartz, C.S., Lu, Z., Liu, H.-C., and McKeen, S.A.: Simultaneous three-dimensional
 2147 variational assimilation of surface fine particulate matter and MODIS aerosol optical
 2148 depth, *J. Geophys. Res.*, 117, D13202, doi:10.1029/2011JD017383, 2012.
- 2149 Schwartz, C.S., Liu, Z., Lin, H.-C., and Cetola, J.D.: Assimilating aerosol observations with
 2150 a „hybrid“ variational-ensemble data assimilation system. *J. Geophys. Res. Atmos.*,
 2151 119, 4043-4069, doi:10.1002/2013JD020937, 2014.
- 2152 Schwinger, J. and Elbern, H.: Chemical state estimation for the middle atmosphere by four-
 2153 dimensional variational data assimilation: A posteriori validation of error statistics in
 2154 observation space, *J. Geophys. Res.* 115, D18307, 2010.

Mis en forme : Retrait :
 Avant : 0 cm, Suspendu :
 1,25 cm, Ne pas ajuster le
 retrait de droite quand la
 grille est définie, Ne pas
 ajuster l'espace entre le
 texte latin et asiatique, Ne
 pas ajuster l'espace entre le
 texte et les nombres
 asiatiques

Mis en forme :
 Police :(asiatique) Times
 New Roman, Anglais
 États-Unis

2155 SDS-WAS: Sand and dust storm warning advisory and assessment system (SDS-WAS).
2156 Science and implementation plan: 2015-2020, WMO Research Department.
2157 Atmospheric Research and Environment Branch, July 2014.

2158 Seinfeld, J.H. and Pandis, S.N.: Atmospheric Chemistry and Physics – from Air Pollution to
2159 Climate Change, Chapter 23: Atmospheric Chemical Transport Models, Wiley-
2160 Interscience, New York, NY, 2006.

2161 Semane, N., Peuch, V.-H., Pradier, S., Desroziers, G., El Amraoui, L., Brousseau, P.,
2162 Massart, S., Chapnik, B., Peuch A.: On the extraction of wind information from the
2163 assimilation of ozone profiles in Météo-France 4-D-Var operational NWP suite,
2164 Atmos. Chem. Phys., 9, 4855-4867, 2009.

2165 Shutts, G. J.: A kinetic energy backscatter algorithm for use in ensemble prediction systems,
2166 Q. J. R. Meteor. Soc. 139, 2117-2144, 2005.

2167 Singh, K. and Sandu, A.: Variational chemical data assimilation with approximate adjoints,
2168 Computers Geosci., 40, 10–18, 2012.

2169 Smit, H. G., Straeter, W., Johnson, B. J., Oltmans, S. J., Davies, J., Tarasick, D. W.,
2170 Hoegger, B., Stubi, R., Schmidlin, F.J., Northam, T., Thompson, A.M., Witte, J.C.,
2171 Boyd, I., and Posny, F.: Assessment of the performance of ECC-ozonesondes under
2172 quasi-flight conditions in the environmental simulation chamber: Insights from the
2173 Juelich Ozone Sonde Intercomparison Experiment (JOSIE). J. Geophysic. Res.,
2174 112(D19), 2007.

2175 Steinbacher, M., Zellweger, C., Schmarzenbach, B., Bugmann, S., Buchmann, B., Ordóñez,
2176 C., Prevot, A.S.H., and Hueglin, C.: Nitrogen oxide measurements at rural sites in
2177 Switzerland: Bias of conventional measurement techniques, J. Geophys.
2178 Res., **112**, 2007.

2179 Storch, R.B., Pimentel, L.C.G., and Orlando, H.R.B.: Identification of atmospheric boundary
2180 layer parameters by inverse problem. Atmospheric Environment 41: 1417–1425,
2181 2007.

2182 Streets, D. G., Canty, T., Carmichael, G.R., de Foy, B., Dickerson, R.R., Duncan, B.N.,
2183 Erwards, D.P., Haynes, J.A., Henze, D.K., Houyoux, M.R., Jacob, D.J., Krotkov,
2184 N.A., Lamsal, L.N., Liu, Y., Lu, Z., Martin, R.V., Pfister, G.G., Pinder, R.W.,
2185 Salawitch, R.J., and Wecht, K.J.: Emissions estimation from satellite retrievals: A
2186 review of current capability, Atmos. Environ., 77,
2187 doi:10.1016/j.atmosenv.2013.05.051, 2013.

2188 Sudo, K., Takahashi, M., and Akimoto, H.: CHASER: a global chemical model of the
2189 troposphere 2. Model results and evaluation, J. Geophys. Res., 107, 4586,
2190 doi:10.1029/2001JD001114, 2002. 16145, 2002.

2191 Takemura, T., Okamoto, H., Maruyama, Y., Numaguti, A., Higurashi, A., and Nakajima, T.:
2192 Global three-dimensional simulation of aerosol optical thickness distribution of
2193 various origins, J. Geophys. Res., 105, 17853–17873, 2000.

2194 Takemura, T., Nakajima, T., Dubovik, O., Holben, B., and Kinne, S.: Single-scattering
2195 albedo and radiative forcing of various aerosol species with a global three-
2196 dimensional model, J. Clim., 15, 333–352, 2002.

2197 Takemura, T., Nozawa, T., Emori, S., Nakajima, T., and Nakajima, T.: Simulation of climate
2198 response to aerosol direct and indirect effects with aerosol transport-radiation model,
2199 J. Geophys. Res., 110, D02202, doi:10.1029/2004JD005029, 2005.

2200 Talagrand, O. and Courtier, P.: Variational assimilation of meteorological observation with
2201 the adjoint vorticity equation. i: Theory. Q. J. R. Meteor. Soc. 113, 1311–1328, 1987.

2202 Talbot, R., Dibb, J., Scheuer, E., Seid, G., Russo, R., Sandholm, S., Tan, D., Singh, H.,
2203 Blake, D., Blake, N., Atlas, E., Sachse, G., Jordan, C., and Avery, M.: Reactive
2204 nitrogen in Asian continental outflow over the western Pacific: Results from the

2205 NASA Transport and Chemical Evolution over the Pacific (TRACE-P) airborne
 2206 mission, *J. Geophys. Res.*, 108(D20), 8803, doi:10.1029/2002JD003129, 2003.

2207 Tombette, M., Mallet, V., and Sportisse, B. : PM₁₀ data assimilation over Europe with the
 2208 optimal interpolation method, *Atmos. Chem. Phys.*, 9, 57-70, 2009, .

2209 Tørseth, K., Aas, W., Breivik, K., Fjæraa, A. M., Fiebig, M., Hjellbrekke, A. G., Lund
 2210 Myhre, C., Solberg, S., and Yttri, K. E.: Introduction to the European Monitoring and
 2211 Evaluation Programme (EMEP) and observed atmospheric composition change
 2212 during 1972–2009, *Atmos. Chem. Phys.*, 12, 5447-5481, doi:10.5194/acp-12-5447-
 2213 2012, 2012.

2214 Uppala, S.M., Kallberg, P.W., Simmons, A.J., Andrae, U., Da Costa Bechtold, V., Fiorino,
 2215 M., Gibson, J.K., Haseler, J., Hernandez, A., Kelly, G.A., Li, X., Onogi, K., Saarinen,
 2216 S., Sokka, N., Allan, R.P., Andersson, E., Arpe, K., Balmaseda, M.A., Beljaars,
 2217 A.C.M., Van De Berg, L., Bidlot, J., Bormann, N., Caires, S., Chevallier, F., Dethof,
 2218 A., Dragosavac, M., Fisher, M., Fuentes, M., Hagemann, S., Holm, E., Hoskins, B.J.,
 2219 Isaksen, I., Janssen, P.A.E.M., Jenne, R., McNally, A.P., Mahfouf, J.F., Morcrette,
 2220 J.-J., Rayner, N.A., Saunders, R.W., Simon, P., Sterl, A., Trenberth, K.E., Untch, A.,
 2221 Vasiljevic, D., Viterbo, P., and Woollen, J.: The ERA-40 re-analysis, *Q. J. R.*
 2222 *Meteorol. Soc.*, 131, 2961–3012, 2005..

2223 van Leeuwen, P. J.: Particle filtering in geophysical systems. *Mon. Wea. Rev.*, 137, 4089–
 2224 4114, 2009.

2225 Veefkind, J. P., Aben, I., McMullan, K., Förster, H., De Vries, J., Otter, G., Claas, J., Eskes,
 2226 H.J., de Haan, J.F., Kleipool, Q., van Weele, M., Hasekamp, O., Hoogeveen, R.,
 2227 Landgraf, J., Snel, R., Tol, P., Ingman, P., Voors, R., Kruizinga, B., Vink, R., Visser,
 2228 H., and Levelt, P. F.: TROPOMI on the ESA Sentinel-5 Precursor: A GMES mission
 2229 for global observations of the atmospheric composition for climate, air quality and
 2230 ozone layer applications. *Remote Sensing Environ.*, 120, 70-83, 2012.

2231 Verlaan, M. and Heemink, A. W.: Tidal flow forecasting using reduced rank square root
 2232 filters. *Stochastic Hydrology and Hydraulics* 11, 349–368, 1997.

2233 Vira, J. and Sofiev, M.: On variational data assimilation for estimating the model initial
 2234 conditions and emission fluxes for short-term forecasting of SO_x concentrations,
 2235 *Atmos. Environ.*, 46, 318-328, 2012.

2236 Vira, J and Sofiev, M.: Assimilation of surface NO₂ and O₃ observations into the SILAM
 2237 chemistry transport model. *Geosci. Model Dev.*, [8](#), 191-203, 2015..

2238 Wang, X., Hamill, T. M., and Bishop, C. H.: A comparison of hybrid ensemble transform
 2239 Kalman-optimum interpolation and ensemble square root filter analysis schemes,
 2240 *Mon. Wea. Rev.*, 135, 1055–1076, 2007.

2241 Wang, X., Mallet, V., Berroir, J.P., and Herlin, I.: Assimilation of OMI NO₂ retrievals into a
 2242 regional chemistry-transport model for improving air quality forecasts over Europe.
 2243 *Atmos. Environ.*, 45, 485-492, 2011.

2244 Wang, Y., Sartelet, K.N., Bocquet, M., and Chazette, P.: Assimilation of ground versus lidar
 2245 observations for PM10 forecasting, *Atmos. Chem. Phys.*, 13, 269–283, 2013.

2246 Wang, Y., Sartelet, K., Bocquet, M., Chazette, P., 2014a. Modelling and assimilation of lidar
 2247 signals over Greater Paris during the MEGAPOLI summer campaign. *Atmos. Chem.*
 2248 *Phys.*, 14, 3511-3532.

2249 Wang, Y., K. Sartelet, M. Bocquet et al. (2014b). Assimilation of lidar signals: application to
 2250 aerosol forecasting in the Mediterranean Basin, *Atmos. Chem. Phys.*, 14, 12031–
 2251 12053, 2014.

2252 Weaver, A. and Courtier, P. Correlation modelling on the sphere using a generalized
 2253 diffusion equation, *Q. J. R. Meteor. Soc.* 127, 1815–1846, 2001.

Supprimé : Discus.

Supprimé : 7

Supprimé : 5589-5621

Supprimé : 4

2254 Whitaker, J. S. and Hamill, T. M.: Ensemble data assimilation without perturbed
2255 observations, *Mon. Wea. Rev.*, 130, 1913–1924, 2002.

2256 Wiedinmyer, C., Akagi, S. K., Yokelson, R. J., Emmons, L. K., Al-Saadi, J. A., Orlando, J. J.,
2257 and A. J. Soja: The Fire INventory from NCAR (FINN): a high resolution global
2258 model to estimate the emissions from open burning, *Geosci. Model Dev.*, 4, 625–641,
2259 doi:10.5194/gmd-4-625-2011, 2011.

2260 Williams E.J., Fehsenfeld, F. C., Jobson, B. T., Kuster, W. C., Goldan, P. D., Stutz, J., and
2261 McClenny, W. A.: Comparison of Ultraviolet Absorbance, Chemiluminescence, and
2262 DOAS Instruments for Ambient Ozone Monitoring, *Environ. Sci. Technol.*, 40,
2263 5755–5762, doi: 10.1021/es0523542, 2006.

2264 Winker, D. M., Pelon, J., and McCormick, M. P.: The CALIPSO mission: Spaceborne lidar
2265 for observation of aerosols and clouds, *Proc. SPIE Int. Soc. Opt. Eng.*, 4893, 1–11,
2266 2003.

2267 Wu, L., Mallet, V., Bocquet, M., Sportisse, B.: A comparison study of data assimilation
2268 algorithms for ozone forecasts, *J. Geophys. Res.*, 113, D20310, 2008..

2269 Wu, L., Bocquet, M., and Chevallier, M.: Optimal Reduction of the Ozone Monitoring
2270 Network over France, *Atmos. Env.*, 44, 3071–3083, 2010.

2271 Wu, L. and Bocquet, M. Optimal Redistribution of the Background Ozone Monitoring
2272 Stations over France, *Atmos. Env.*, 45, 772–783, 2011.

2273 Wu, W.-S., Purser, J., and Parrish, D.: Three-dimensional variational analysis with spatially
2274 inhomogeneous covariances, *Mon. Wea. Rev.*, 130, 2905–2916, 2002.

2275 Yu, H., Dickinson, R. E., Chin, M., Kaufman, Y. J., Holben, B. N., Geogdzhayev, I. V., and
2276 Mishchenko, M. I.: Annual cycle of global distributions of aerosol optical depth from
2277 integration of MODIS retrievals and GOCART model simulations, *J. Geophysic.
2278 Res.*, 108, 4128, 10.1029/2002jd002717, 2003.

2279 Yumimoto, K., Uno, I., Sugimoto, N., Shimizu, A., Hara, Y., and Takemura, T.: Size-
2280 resolved adjoint inversion of Asian dust, *Geophys. Res. Lett.*, 39,
2281 doi:10.1029/2012GL053890, 2012.

2282 Yumimoto, K. and Takemura, T.: The SPRINTARS version 3.80/4D-Var data assimilation
2283 system: development and inversion experiments based on the observing system
2284 simulation experiment framework. *Geosci. Model Dev.*, 6, 2005–2022, 2013.

2285 Zaveri, R. A., Easter, R. C., Fast, J. D., and Peters, L. K.: Model for simulating aerosol
2286 interactions and chemistry (MOSAIC), *J. Geophys. Res.*, 113, D13204, 2008.

2287 Zhang, Y.: Online coupled meteorology and chemistry models: History, current status, and
2288 outlook, *Atmos. Chem. Phys.*, 8, 2895–2932, 2008.

2289 Zhang, Y., Bocquet, M., Mallet, V., Seigneur, C., and Baklanov, A.: Real-time air quality
2290 forecasting, Part I: History, techniques, and current status, *Atmos. Environ.*, 60, 632–
2291 655, 2012a.

2292 Zhang, Y., Bocquet, M., Mallet, V., Seigneur, C., and Baklanov, A.: Real-time air quality
2293 forecasting, Part II: State of the science, current research needs, and future prospects,
2294 *Atmos. Environ.*, 60, 656–676, 2012b.

2295 Zyryanov, D., Foret, G., Eremenko, M., Beekmann, M., Cammas, J.-P., D'Isidoro, M.,
2296 Elbern, H., Flemming, J., Friese, E., Kioutsioutkis, I., Maurizi, A., Melas, D., Meleux,
2297 F., Menut, L., Moinat, P., Peuch, V.-H., Poupkou, A., Razinger, M., Schultz, M.,
2298 Stein, O., Suttie, A. M., Valdebenito, A., Zerefos, C., Dufour, G., Bergametti, G., and
2299 Flaud, J.-M.: 3-D evaluation of tropospheric ozone simulations by an ensemble of
2300 regional Chemistry Transport Model, *Atmos. Chem. Phys.*, 12, 3219–3240,
2301 doi:10.5194/acp-12-3219-2012, 2012.

2302 Table 1: Summary of major satellite instruments for the period 2003 to the near future, and
 2303 the atmospheric composition species detected by these instruments. The focus is on
 2304 tropospheric composition.
 2305

Sensor (Satellite)	Measurement Period	Species	Reference
SCIAMACHY (ENVISAT)	2002-2012	NO ₂ , SO ₂ , HCHO, CO, CH ₄ , CO ₂ , AOD, O ₃ , CHOCHO	Bovensmann et al., 1999
OMI (EOS-Aura)	2004-	NO ₂ , SO ₂ , HCHO, AOD, O ₃ , CHOCHO	Levelt et al., 2006
GOME-2 (METOP-A) GOME-2 (METOP-B)	2006-2012-	NO ₂ , SO ₂ , HCHO, AOD, O ₃ , CHOCHO	Callies et al., 2000
AIRS (EOS-Aqua)	2002-	O ₃ , SO ₂ , CO, CH ₄ , CO ₂	Aumann et al., 2003
MOPITT (EOS-Terra)	2000-	CO, CH ₄	Drummond and Mand, 1996
TES (EOS-Aura)	2004-	O ₃ , CO, CH ₄ , NH ₃ , CO ₂	Beer et al., 2001
IASI (METOP-A) IASI (METOP-B)	2006-2012-	O ₃ , SO ₂ , CO, CH ₄ , NH ₃ , NMVOC, NH ₃ , CO ₂	Clerbaux et al., 2009
MISR (EOS-Terra)	2000-	AOD	Diner et al., 2001
MODIS (EOS-Terra) MODIS (EOS-Aqua)	2000-2002-	AOD, fires	Barnes et al., 1998
VIIRS (Suomi-NPP)	2011-	AOD, fires	GSFC (2011)
POLDER (PARASOL)	2004-2013	AOD, aerosol properties	Lier and Bach, 2008
CALIOP (CALIPSO)	2006-	Aerosol backscatter profiles	Winkler et al., 2003
<u>GOCI (COMS)</u>	<u>2010-</u>	<u>AOD</u>	<u>Lee et al., 2010</u>
TANSO-FTS (GOSAT)	2009-	CH ₄ , CO ₂	Kuze et al., 2009

2306

2307 Table 2: Selected list of acronyms
 2308

AIRS	Atmospheric Infrared Sounder
AVHRR	Advanced Very High-Resolution Radiometer
CALIOP	Cloud-Aerosol Lidar with Orthogonal Polarization
CALIPSO	Cloud-Aerosol Lidar and Infrared Pathfinder Satellite Observations
<u>COMS</u>	<u>Communication, Ocean, and Meteorology Satellite</u>
<u>GOCI</u>	<u>Geostationary Ocean Color Imager</u>
IASI	Infrared Atmospheric Sounding Interferometer
MISR	Multiangle Imaging SpectroRadiometer
MODIS	Moderate Resolution Imaging Spectroradiometer
MOPITT	Measurements Of Pollution In The Troposphere
NPP	National Polar-orbiting Partnership
OMI	Ozone Monitoring Instrument
PARASOL	Polarization & Anisotropy of Reflectances for Atmospheric Sciences coupled with Observations from a Lidar
SCIAMACHY	SCanning Imaging Absorption SpectroMeter for Atmospheric CHartographY
TES	Tropospheric Emission Spectrometer
VIIRS	Visible Infrared Imaging Radiometer Suite

2309

2310 Table 3. Bias and correlation coefficient for comparison with independent satellite
2311 observations of AATSR for the considered regions

	Correlation, a priori	Correlation, a posteriori	Bias, a priori	Bias, a posteriori
Africa	0.44	0.47	-0.02	-0.01
Asia	0.41	0.50	-0.07	-0.04
Europe	0.23	0.30	-0.01	-0.005

2312

2314 **Figure captions**

2315 | **Figure 1.** Measurements of the tropospheric NO₂ column over Europe from the Ozone
2316 Monitoring Instrument (OMI) on EOS-Aura (Boersma et al., 2011). Top panel: yearly-mean
2317 observation for 2005. Bottom panel: A sum of all observations available for assimilation on
2318 one day with little cloud cover (30 August 2005), showing the pixel size (13x24 km at nadir)
2319 and the overlap between orbits at high latitude. The retrieved cloud fraction is used to fade out
2320 the measurements (white indicates 100% cloud cover).

2322 | **Figure 2:** Cross section at 180 E of the average zonal CO flux (kg/(m²s)) in the 2003-2012
2323 period calculated from the CO, U and density fields of the MACC re-analysis (top). Time
2324 series of monthly mean CO (kg/s) transported over the Northern Pacific through a pane at 180
2325 E (30N-70N, up 300 hPa) (bottom).

2327 | **Figure 3.** 24-hour average PM_{2.5} concentrations (µg/m³) for June 29 (left) and July 05, 2012
2328 (right).

2330 | **Figure 4.** Bias (µg/m³) (top) and temporal correlation (bottom) of forecasts for NoDA (left)
2331 and EnKF (right) simulations against AIRnow observations for the period 28 June – 6 July
2332 2012. Black dots denote negative correlations.

2334 | **Figure 5.** Diurnal cycle of bias (µg/m³) (left) and spatial correlation (right) of PM_{2.5} forecasts
2335 for the NoDA (blue) and EnKF (red) simulations against AIRnow observations for the period
2336 28 June – 6 July 2012. The black vertical lines are plotted at assimilation times.

2338 | **Figure 6.** Results when assimilating satellite retrieved AOD over the SW US for the first 10
2339 days of May 2010. Top-left panel shows time series of model and observed mean PM_{2.5} over
2340 AQS sites in California and Nevada. Top-right panel shows mean PM_{2.5} as a function of
2341 forecast hour for the same sites. Bottom panels shows AOD time series at two sites for
2342 AERONET data (500 nm), operational MODIS (550 nm), NASA NNR (550 nm), the non-
2343 assimilated forecast and the two assimilation forecasts (500 nm). Modified from Saide et al.
2344 (2013).

2346 | **Figure 7.** Fractional error reductions for 550 nm AOD and 550–870 nm Ångström exponent
2347 (rows) from non-assimilated to assimilation of Terra retrievals computed using Aqua
2348 retrievals (e.g., errors for a ~3 hour forecast). Figures in the left column assimilate only
2349 MODIS 550 nm AOD while the ones in the right column assimilate MODIS 550, 660, 870,
2350 and 1240 nm over ocean and only 550 nm over land. Modified from Saide et al. (2013).

2352 | **Figure 8.** Results when assimilating cloud retrievals to improve below-cloud aerosol state.
2353 Top panels show observed and model maps of cloud droplet number [N_d, #/cm³] for the
2354 southeastern Pacific. The bottom panel shows time series of GOES and N_d forecasts after
2355 assimilation of the MODIS retrieval on the top panels. The time series are presented as box
2356 and whisker plots computed over the rectangle on the top-left panel; center solid lines indicate
2357 the median, circles represent the mean, boxes indicate upper and lower quartiles, and whiskers
2358 show the upper and lower deciles. Time series are shown during day time for 2 days after
2359 assimilation.

2361 | **Figure 9.** SILAM a priori (top), MODIS observations (middle) and SILAM a posteriori
2362 (bottom) AOD, mean over 2008, model output fully collocated with MODIS.

Supprimé : Figure 1.
Assimilation of SCIAMACHY
data in the CMAQ CTM for a
simulation of O₃
concentrations over the Madrid
Region, Spain. Top (a): O₃
data from SCIAMACHY on
01/08/2007. Middle (b):
Monthly-average O₃
concentrations simulated with
MM5-CMAQ prior to data
assimilation, August 2007.
Bottom (c): Linear regression
between simulated and
measured O₃ concentrations
averaged over all Madrid
monitoring stations for the
week of 1 to 8 August 2007.
Model simulation results were
obtained with assimilation of
SCIAMACHY data. The
correlation coefficient is 0.754.

Supprimé : 2

Supprimé : 3

Supprimé : 4

Supprimé : 5

Supprimé : 6

Supprimé : B

Supprimé : 7

Supprimé : 8

Supprimé : 9

Supprimé : 1

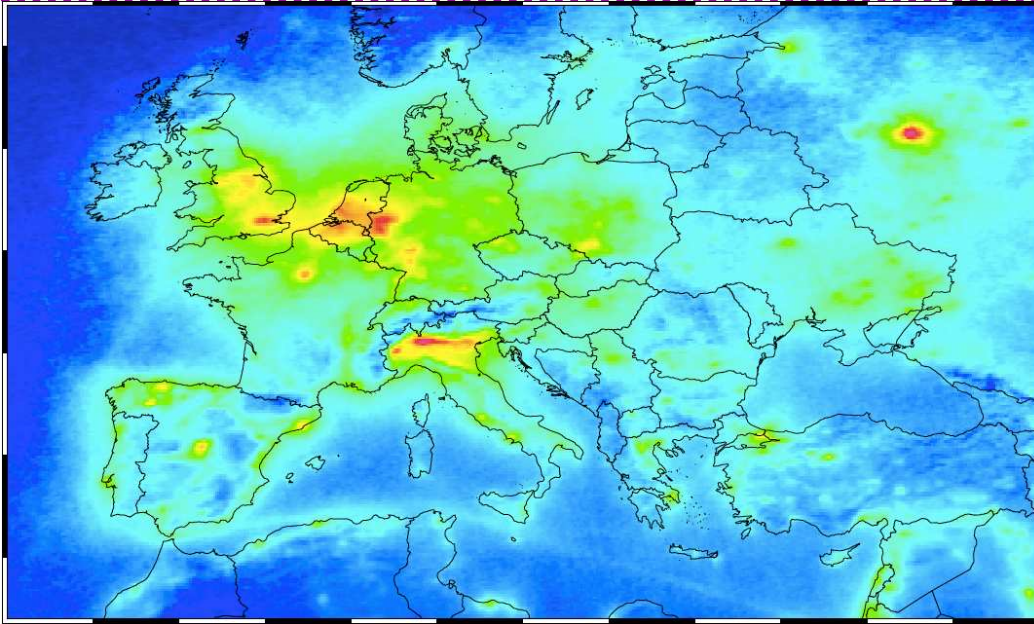
Supprimé : 0

2363

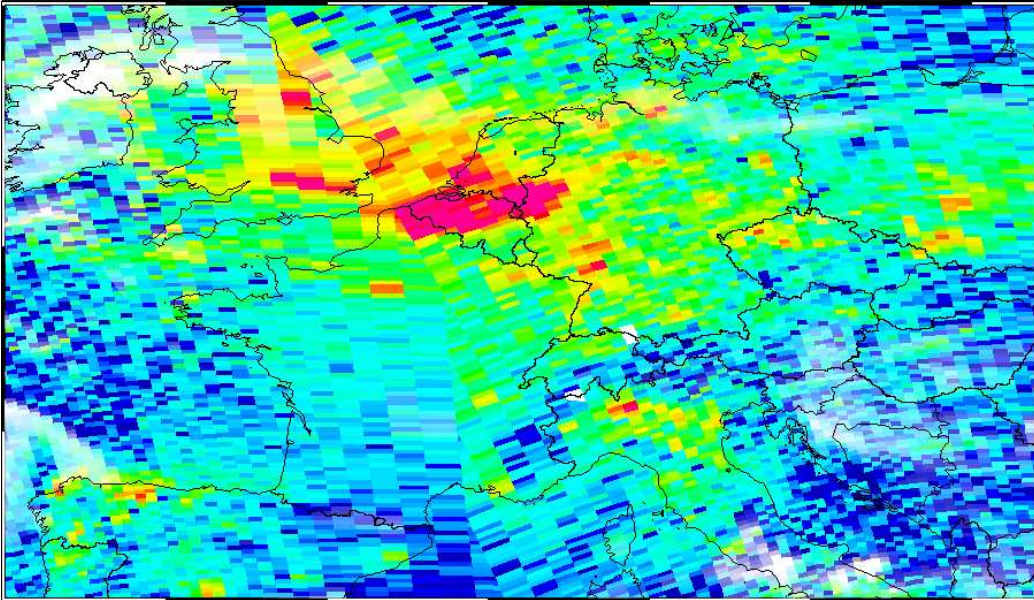
2364 | Figure 10. Monthly emissions of OC in Asia, total 2008, unit = Mt PM month⁻¹.

Supprimé : !

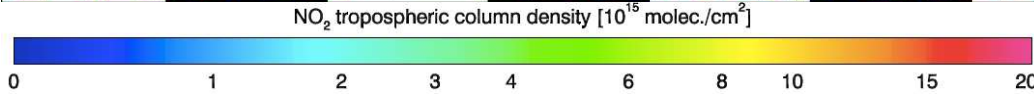
2365



2366



2367



2368

2369

2370

2371

2372

2373

2374

2375

Figure 1. Measurements of the tropospheric NO₂ column over Europe from the Ozone Monitoring Instrument (OMI) on EOS-Aura (Boersma et al., 2011). Top panel: yearly-mean observation for 2005. Bottom panel: A sum of all observations available for assimilation on one day with little cloud cover (30 August 2005), showing the pixel size (13x24 km at nadir) and the overlap between orbits at high latitude. The retrieved cloud fraction is used to fade out the measurements (white indicates 100% cloud cover).

Supprimé : ¶

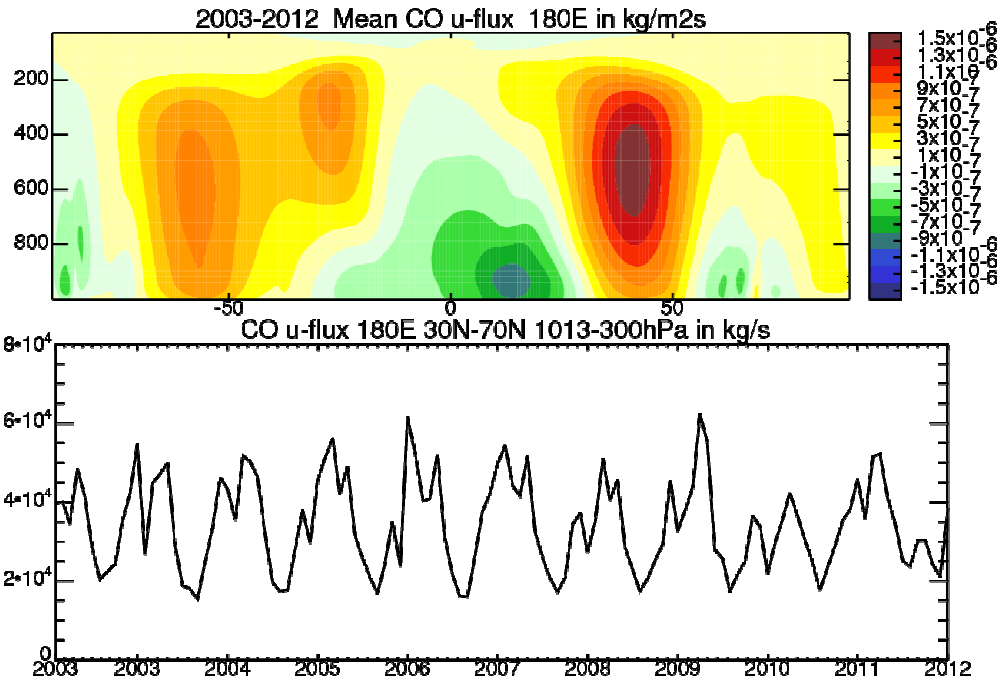
<sp> . . (a)¶

<sp> . . (b)¶

<sp> . . (c)¶

Figure 1. Assimilation of SCIAMACHY data in the CMAQ CTM for a simulation of O₃ concentrations over the Madrid Region, Spain. Top (a): O₃ data from SCIAMACHY on 01/08/2007. Middle (b): Monthly-average O₃ concentrations simulated with MM5-CMAQ prior to data assimilation, August 2007. Bottom (c): Linear regression between simulated and measured O₃ concentrations averaged over all Madrid monitoring stations for the week of 1 to 8 August 2007. Model simulation results were obtained with assimilation of SCIAMACHY data. The correlation coefficient is 0.754.¶

Supprimé : 2



2376
2377

2378 | Figure 2: Cross section at 180 E of the average zonal CO flux ($\text{kg}/(\text{m}^2\text{s})$) in the 2003-2012
 2379 period calculated from the CO, U and density fields of the MACC re-analysis (top). Time
 2380 series of monthly mean CO (kg/s) transported over the Northern Pacific through a pane at
 2381 180 E (30N-70N, up 300 hPa) (bottom).

Supprimé : 3

2382

2383

2384

2385

2386

2387

2388

2389

2390

2391

2392

2393

2394

2395

2396

2397

2398

2399

2400

2401

2402

2403

2404

2405

2406

2407

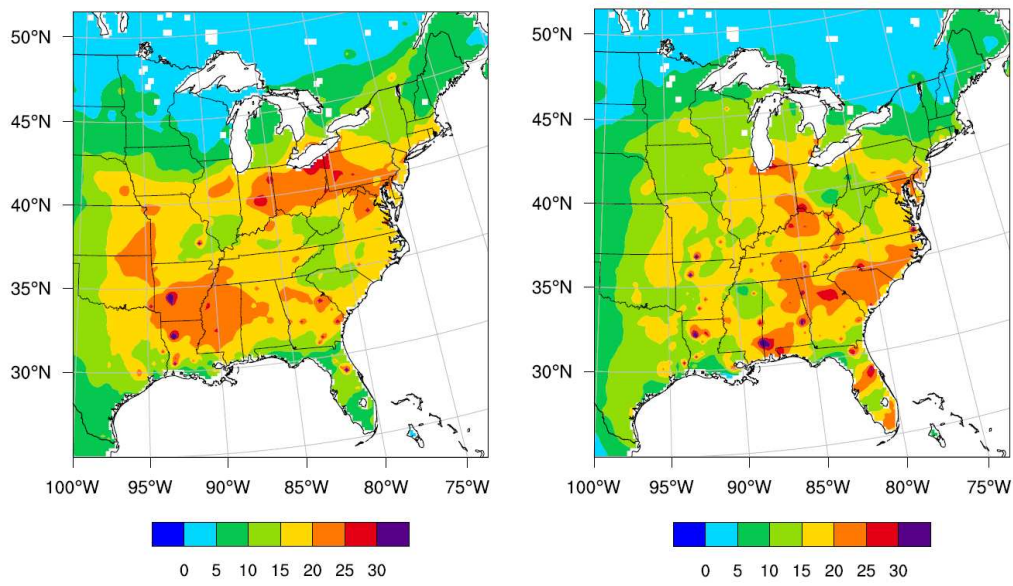


Figure 3. 24-hour average PM_{2.5} concentrations (µg/m³) for June 29 (left) and July 05, 2012 (right).

Supprimé : 4

2408

2409

2410

2411

2412

2413

2414

2415

2416

2417

2418

2419

2420

2421

2422

2423

2424

2425

2426

2427

2428

2429

2430

2431

2432

2433

2434

2435

2436

2437

2438

2439

2440

2441

2442

2443

2444

2445

2446

2447

2448

2449

2450

2451

2452

2453

2454

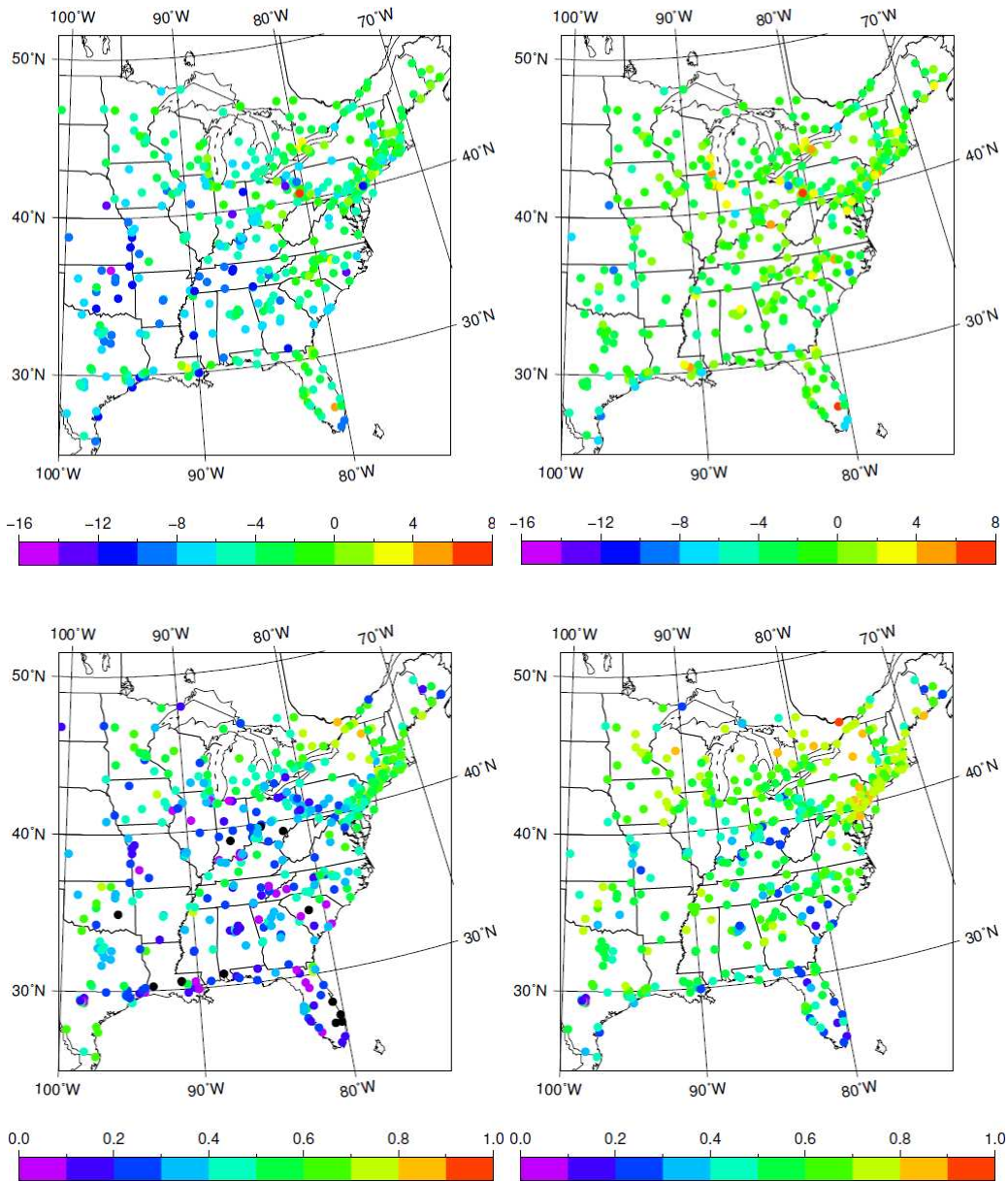


Figure 4. Bias ($\mu\text{g}/\text{m}^3$) (top) and temporal correlation (bottom) of forecasts for NoDA (left) and EnKF (right) simulations against AIRnow observations for the period 28 June – 6 July 2012. Black dots denote negative correlations.

Supprimé : 5

2455

2456

2457

2458

2459

2460

2461

2462

2463

2464

2465

2466

2467

2468

2469

2470

2471

2472

2473

2474

2475

2476

2477

2478

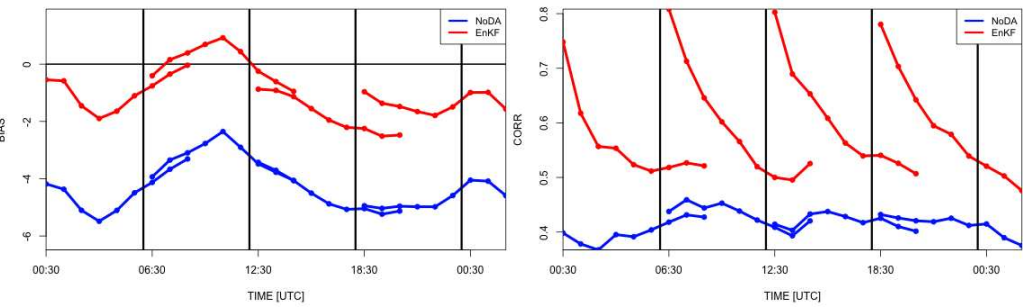


Figure 5. Diurnal cycle of bias ($\mu\text{g}/\text{m}^3$) (left) and spatial correlation (right) of $\text{PM}_{2.5}$ forecasts for the NoDA (blue) and EnKF (red) simulations against AIRnow observations for the period 28 June – 6 July 2012. The black vertical lines are plotted at assimilation times.

Supprimé : 6

Supprimé : B

2479

2480

2481

2482

2483

2484

2485

2486

2487

2488

2489

2490

2491

2492

2493

2494

2495

2496

2497

2498

2499

2500

2501

2502

2503

2504

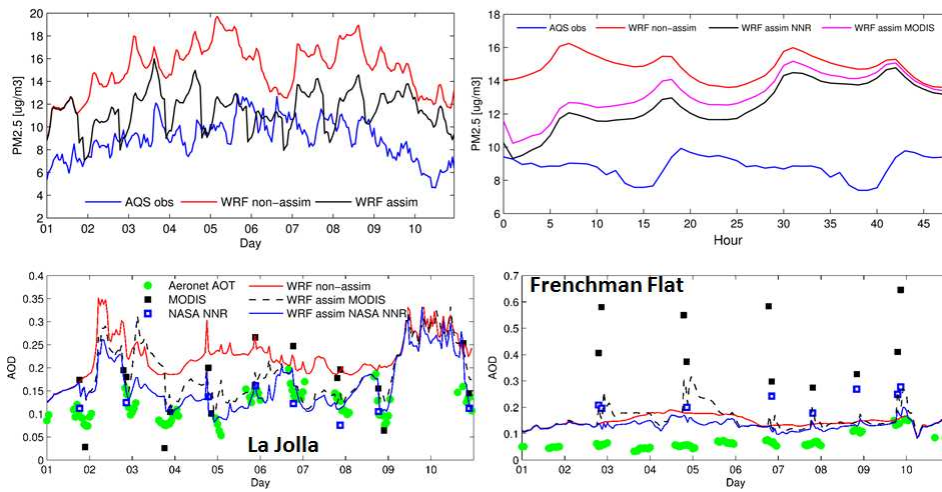


Figure 6. Results when assimilating satellite retrieved AOD over the SW US for the first 10 days of May 2010. Top-left panel shows time series of model and observed mean $PM_{2.5}$ over AQS sites in California and Nevada. Top-right panel shows mean $PM_{2.5}$ as a function of forecast hour for the same sites. Bottom panels shows AOD time series at two sites for AERONET data (500 nm), operational MODIS (550 nm), NASA NNR (550 nm), the non-assimilated forecast and the two assimilation forecasts (500 nm). Modified from Saide et al. (2013).

Supprimé : 7

2505

2506

2507

2508

2509

2510

2511

2512

2513

2514

2515

2516

2517

2518

2519

2520

2521

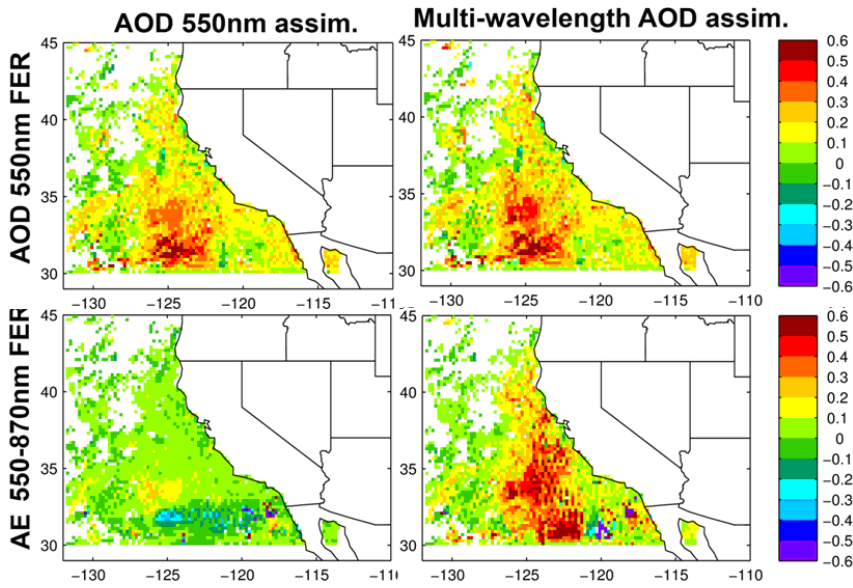
2522

2523

2524

2525

2526



2527 | Figure 7. Fractional error reductions for 550 nm AOD and 550–870 nm Ångström exponent
 2528 (rows) from non-assimilated to assimilation of Terra retrievals computed using Aqua
 2529 retrievals (e.g., errors for a ~3 hour forecast). Figures in the left column assimilate only
 2530 MODIS 550 nm AOD while the ones in the right column assimilate MODIS 550, 660, 870,
 2531 and 1240 nm over ocean and only 550 nm over land. Modified from Saide et al. (2013).

Supprimé : 8

2532

2533

2534

2535

2536

2537

2538

2539

2540

2541

2542

2543

2544

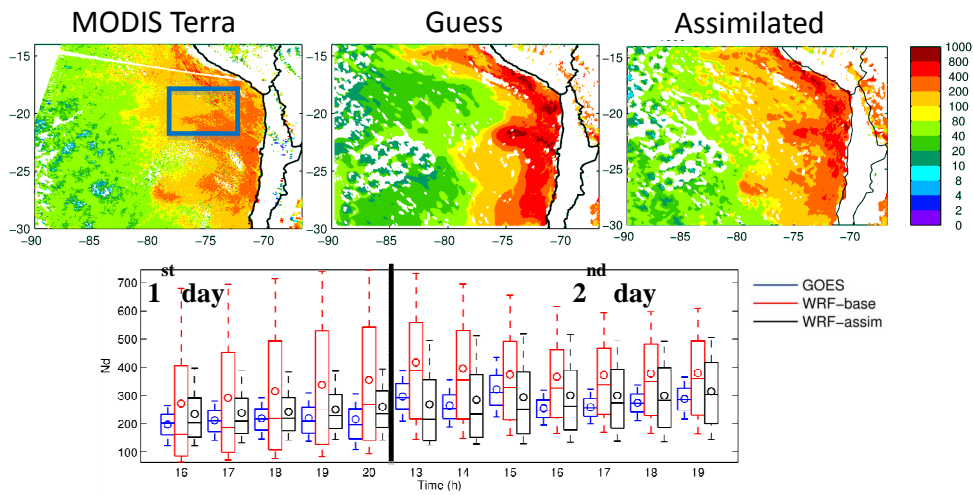
2545

2546

2547

2548

2549



2550 | Figure 8. Results when assimilating cloud retrievals to improve below-cloud aerosol state.
 2551 Top panels show observed and model maps of cloud droplet number [N_d , $\#/cm^3$] for the
 2552 southeastern Pacific. The bottom panel shows time series of GOES and N_d forecasts after
 2553 assimilation of the MODIS retrieval on the top panels. The time series are presented as box
 2554 and whisker plots computed over the rectangle on the top-left panel; center solid lines
 2555 indicate the median, circles represent the mean, boxes indicate upper and lower quartiles, and
 2556 whiskers show the upper and lower deciles. Time series are shown during day time for 2 days
 2557 after assimilation.

Supprimé : 9

2558

2559

2560

2561

2562

2563

2564

2565

2566

2567

2568

2569

2570

2571

2572

2573

2574

2575

2576

2577

2578

2579

2580

2581

2582

2583

2584

2585

2586

2587

2588

2589

2590

2591

2592

2593

2594

2595

2596

2597

2598

2599

2600

2601

2602

2603

2604

2605

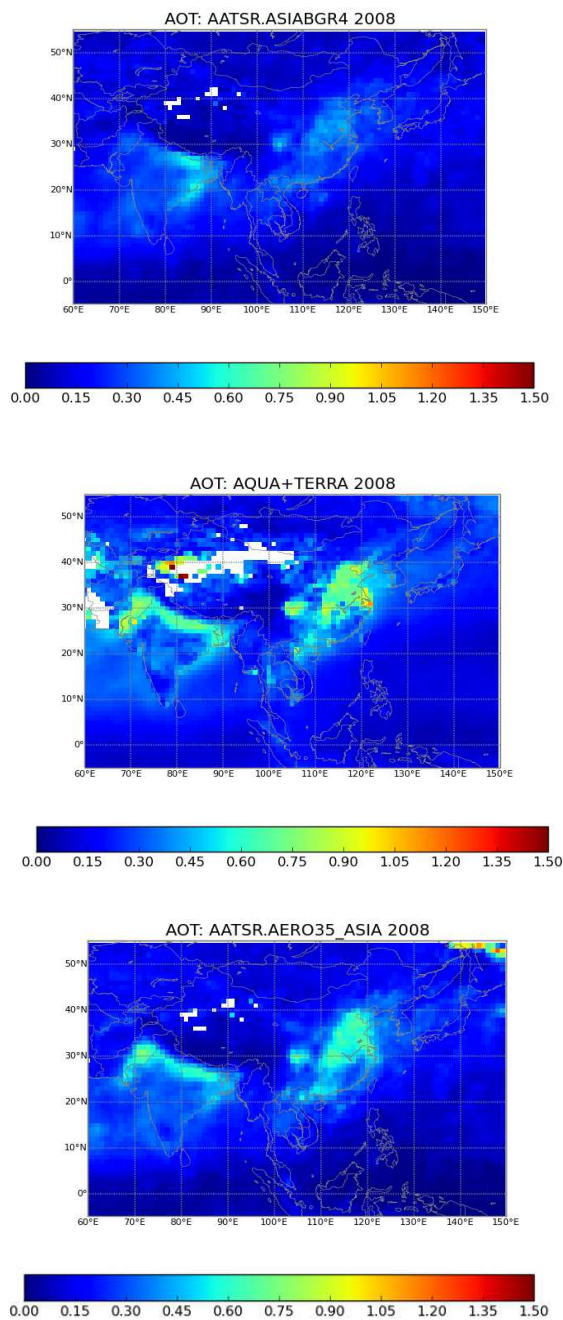
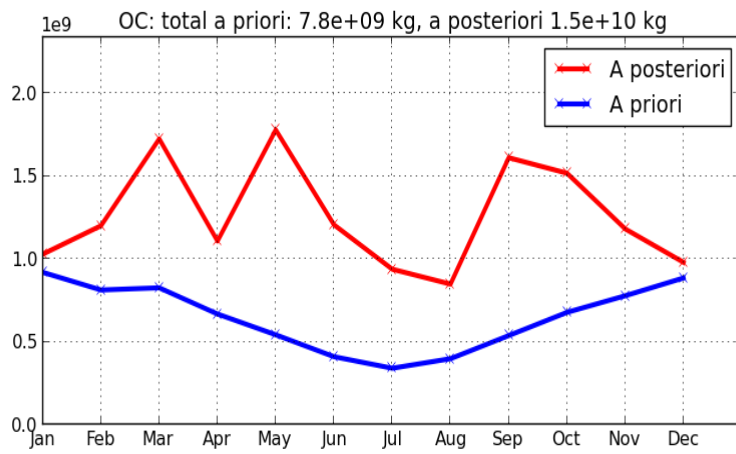


Figure 9. SILAM a priori (top), MODIS observations (middle) and SILAM a posteriori (bottom) AOD, mean over 2008, model output fully collocated with MODIS.

Supprimé : 10

2606



2607

2608 | Figure 10. Monthly emissions of OC in Asia, total 2008, unit = Mt PM month⁻¹.

2609

Supprimé : 1

2610

2611

San Jose and Pérez Carmaño of the Technical University of Madrid (UPM) also performed a multi-species data assimilation with a CTM. In their work, NO₂ and O₃ data from SCanning Imaging Absorption SpectroMeter for Atmospheric CHartographY (SCIAMACHY) were assimilated into a simulation conducted with the Community Multiscale Air Quality CTM (CMAQ) of the U.S. Environmental Protection Agency. SCIAMACHY makes measurements in both nadir and limb modes, which allows the subtraction of stratospheric O₃ from the total O₃ column measurements to obtain tropospheric O₃ column estimates. Figure 1a shows an example of O₃ SCIAMACHY data for 01/08/2007. CMAQ was used here in combination with MM5 for the meteorological fields and applied to two domains covering the Iberian Peninsula with a grid spacing of 27 km and the central region of Spain including the Madrid metropolitan area with a grid spacing of 9 km. A vertical resolution with 23 layers was used in both MM5 and CMAQ. Results are presented here for the episode of 1 to 8 August 2007 (see Figure 1b).

The vertical profiles of NO₂ and O₃ were assimilated into the CMAQ simulation for each grid cell using the Cressman (1959) method. A comparison of model simulation results with and without data assimilation showed a slight improvement from 0.751 to 0.754 in the correlation between the hourly model simulation results and O₃ concentrations available from the surface monitoring network. The results show important differences in the Madrid region with the most important ones (up to 22 µg/m³) being located over downtown Madrid and typically decreasing away from the city. A scatter diagram of the simulated and measured O₃ concentrations averaged over the 22 monitoring stations of the Madrid area is shown in Figure 1c.